UNIVERSITY OF CALIFORNIA, SAN DIEGO

Mechanism of Gene Regulation by the NF-kappaB p52 Homodimer and Bcl3

A dissertation submitted in partial satisfaction of the

requirements for the degree Doctor of Philosophy

in

Chemistry

by

Ya-Fan Wang

Committee in charge:

Professor Gourisankar Ghosh, Chair
Professor Christopher Glass
Professor Alexander Hoffmann
Professor Yitzhak Tor
Professor Leor Weinberger

2011

The Dissertation of Ya-Fan Wang is approved, and it is acceptable in quality and form for publication on microfilm and electronically:

_____

_____

_____

_____

_____

Chair

University of California, San Diego

2011

DEDICATION

I would like to thank and dedicate this thesis to my be loved parents, Zeng-Yang Wang and Jin-Mei Gu, for their endless love, caring, and understanding throughout my life. Thank you both for giving me strength to reach my dreams; without your support and encouragement, I might have never found the mental strength or endurance to complete what I have achieved in my life so far.

TABLE OF CONTENTS

LIST OF ABBREVIATIONS

ARD	ankyrin repeats domain
ATCC	American Type Culture Collection
BMDM	Bone marrow-derived macrophages
βME	β-mercaptoethanol
cDNA	coding DNA
CE	cytoplasmic extract
ChIP	chromatin immunoprecipitation
CHX	cycloheximide
DTT	dithiothreitol
EMSA	electrophoretic mobility shift assay
Flag	peptide with sequence D-Y-K-D-D-D-D-K
GFP	green fluorescent protein
GRR	glycin rich repeat
IκB	inhibitor of NF-κB
IKK	inhibitor of NF-κB kinase
IP	immunoprecipitation
IPTG	isopropylthiogalactoside
kDa	kiloDalton
LPS	lipopolysaccharide

LTβR	lymphotoxin beta receptor
MEF	mouse embryonic fibroblast
NE	nuclear extract
NIK	NF-κB inducing kinase
NF-κB	nuclear factor kappa B
NLS	nuclear localization sequence
PAGE	polyacrylamide gel electrophoresis
RHR	Rel homology region
SDS	sodium dodecyl sulfate
TLR	Toll-like receptor
TNFα	Tumor necrosis factor-alpha
WB	Western blotting
YFP	yellow fluorescent protein

LIST OF FIGURES

LIST OF TABLES

ACKNOWLEDGEMENTS

First and foremost, I would like to sincerely thank my advisor, Dr. Gourisankar Ghosh, for providing me the opportunity to study in his lab, being a wise and wonderful mentor, being patient with me and have confidence on me all the time, and giving me all the guidance, support, and encouragement to succeed as a graduate student. His truly scientist intuition, enthusiasm and passion in science exceptionally inspired and enriched my growth as a graduate student, a researcher, and a scientist.

I would like to thank past members of the G.Ghosh lab, Dr. Olga Savinova and Dr. Anu K. Moorthy, for showing me all the experiments when I first joined the lab, and guided me to become an independent researcher.

I would like to thank present lab member, Dr. Yidan Li, for giving me advises in many aspects of the project, and working together with me when I have to work with Lentivirus for the first time. This project would not have been finished without her suggestions and critical discussions.

I would like to thank Professor Jacky Chi-Ki Ngo, for all his suggestions, helps, and tremendous encouragements. And also thanks for sharing all the laughs, funs, and joys through out all these years.

I would like to thank my friend, Don Vu, for his enormous support and listening to my constant complaints, and walking with me for coffee every morning.

I would like to thank other past and present lab members of G.Ghosh lab, Dr. Sutapa Chakrabarti, Dr. Amanda Fusco, Dr. Suhyung Cho, Dr. Jessica

Ho, Dr. Sulakshana Mukherjee, Dr. Zhihua Tao, and Dr. De-Bin Huang, for providing invaluable support and intellectual contributions.

I would like to thank the rest of the G.Ghosh lab members and people in the neighboring P.Ghosh lab and the A.Hoffmann lab, for their friendship and making the lab a fun place to work in.

I would like to thank member of my committee, Dr. Christopher Glass, and his lab members, Dr. Wendy Huang, Dr. Nathan Spann, and Jesse Fox, for helping me with the RNAi, ChIP and mRNA-RTqPCR experiments in RAW 264.7 cells and primary macrophages.

I would like to thank member of my committee, Dr. Alexander Hoffmann, for taking time and interest in my project, and providing me with all the knockout cells. And Dr. Soumen Basak, Dr. Christine S. Cheng, and Dr. Vincent Feng-Sheng Shih from the Hoffmann lab for all their valuable input in the project in the form of the scientific discussion, experimental advice.

I would like to thank Dr. Majid Ghassemian at the UCSD Biomolecular and Proteomics Mass Spectrometry Facility for performing the phosphopeptide enrichment and LC-MS/MS analysis; and for all his help with interpreting the data.

I would like to thank professor Dr. Susan Taylor, for providing the fluorescence plate reader in the past five years.

I gratefully thank my friends, Polly Wong, Aki Tse, Nikki Cheung, and Anita Wong, for their friendship and being tremendously supportive, caring, and helpful in many aspects of my life throughout these years. Especially

those late nights, staying beside me, listening to my complaints, and taking care of me when I was extremely stressed out and depressed.

Last but not least, I offer my regards and blessings to all of those who supported me in any aspect during the completion of the project.

This project is supported by grant NIH-GM-085490 and NIH-AI-064326 from the National Institutes of Health to Dr. Gourisankar Ghosh.

Chapter II is currently being prepared for submission for publication. Wang, Vivien Y.; and Ghosh, Gourisankar. “The central base pair of κB DNA sequences is a key regulator of the NF-κB dimer transcriptional specificity”. The dissertation author was the primary investigator and author of this paper.

Chapter III is currently being prepared for submission for publication. Fusco, Amanda J.; Wang, Vivien Y.; Basak, Soumen; Tao, Zhihua; Savinova, Olga V.; Hoffmann, Alexander; and Ghosh, Gourisankar. “RelB plays a critical role in regulating both processing and stabilization of NF-κB2/p100”. The dissertation author was the co-primary investigator and author of this paper.

VITA AND PUBLICATIONS

2005	Bachelor of Science, University of California, San Diego
2008	Master of Science, University of California, San Diego
2011	Doctor of Philosophy, University of California, San Diego

Wang, V.Y., and Ghosh, G. (2011) The central base pair of κB DNA sequences is a key regulator of the NF-κB dimer transcriptional specificity. (Manuscript in preparation)

Fusco, A.J., Wang, V.Y., Basak, S., Tao, Z., Savinova, O.V., Ware, C., Hoffmann, A., and Ghosh, G. (2011) RelB plays a critical role in regulating both processing and stabilization of NF-κB2/p100. (Manuscript in preparation)

Fusco, A.J., Huang, D-B., Miller, D., Wang, V.Y., Vu, D., and Ghosh, G. (2009) NF-kappaB p52:RelB heterodimer recognizes two classes of kappaB sites with two distinct modes. *EMBO Rep*. **10**, 152-159.

Moorthy, A.K., Huang, D-B., Wang, V.Y., Vu, D., and Ghosh, G. (2007) X-ray structure of a NF-kappaB p50/RelB/DNA complex reveals assembly of multiple dimers on tandem kappaB sites. *J Mol Biol.* **373**, 723-734.

Moorthy, A.K., Savinova, O.V., Ho, J.Q., Wang, V.Y., Vu, D., and Ghosh, G. (2006) The 20S proteasome processes NF-kappaB1 p105 into p50 in a translation-independent manner. *EMBO J*. **25**, 1945-1956.

ABSTRACT OF THE DISSERTATION

Mechanism of Gene Regulation by the NF-kappaB p52 Homodimer and Bcl3

by

Ya-Fan Wang

Doctor of Philosophy in Chemistry

University of California, San Diego, 2011

Professor Gourisankar Ghosh, Chair

The mammalian Rel/NF-κB family of transcription factors plays a central role in the immune system by regulating various processes involving in both innate and adaptive immunity, inflammation, lymphocyte differentiation, and lymphoid malignancies. A wide variety of signals activate NF-κB driven gene expression through different NF-κB signaling pathways in a stimulus- and cell type-dependent manner. Due to the diverse regulatory mechanism acting on NF-κB signaling, the signal dependent activation of NF-κB remains a

challenging area of research. This thesis describes the mechanism of gene regulation by the NF-κB p52 homodimer with its specific transcriptional co-regulator Bcl3. Chapter I introduces the NF-κB family transcription factors together with its regulation through the IκB family, NF-κB signaling pathways, and its DNA recognition in gene transcription initiation. Chapter II describes the promoter specificity by NF-κB p52 homodimers. Our results show that a single nucleotide change in the central base pair of κB DNA discriminates between classical RelA containing NF-κB dimers versus the p52:Bcl3 complex. Chapter III studies the degradation, re-synthesis, and processing of NF-κB2/p100 and the generation of p52 in non-canonical NF-κB signaling pathway as well as inhibitory function of NF-κB2/p100 referred as IκBδ. Our results showed that LTβ-mediated non-canonical signaling is a NIK-dependent biphasic event, which induces both the activation and suppression of NF-κB activity. Chapter IV studies the phosphorylation state of Bcl3 and its function in terms of p52:Bcl3 gene activation. Two new Bcl3 phosphorylation sites were identified and biochemical analysis showed that these two phosphorylations enhance the protein-protein interaction between p52 and Bcl3, which in turn enhance their specific gene activation. Chapter V employed a combination of X-ray crystallography and biochemical technique to investigate the molecular basis of p52:Bcl3 complex formation. Stable p52:Bcl3 core complex was identified and crystallized.

Chapter I: Introduction

A. Eukaryotic Activator-dependent Transcription Initiation

Transcription is the key step in the regulation of gene expression and it is a highly regulated complex process, which involves several distinct steps. The core promoter structure contains sequences that serve to anchor a set of protein complexes generally referred as the transcription factors. The binding of transcription factors to the specific DNA sequences in the promoter (close to the transcription start site) or enhancer (thousands of base pairs upstream or downstream from the initiation site) region initiates a cascade of events; recruitment of histone modifying enzymes to clear nucleosomes, recruitment of co-activators and finally, recruitment of the general transcription complex including the RNA polymerase at the transcription initiation site. Therefore, the recruitment of transcription factors at the promoter/enhancer sites is a critical step in transcription initiation.

In eukaryotes, RNA polymerases encounter chromatinized DNA templates to initiate transcription. The main constituent of chromatin is the nucleosome in which 147 base pair DNA duplex is wrapped around the octameric histone proteins. One of the essential features of transcription is chromatin decondensation. A large number of protein factors assemble together in a coordinated fashion to initiate transcription (Kadonaga, 2004). The nucleosome remodeling complexes aided by the histone acetylases remove or transiently displace the nuclesomes at the regions which got transcribed by RNA polymerase II (RNA Pol II). General transcriptional machinery along with the polymerase is loaded onto the nucleosome free

promoter and the initiation region (Boeger et al., 2005). Transcription factors play a critical role in both acetylase and general transcription machinery recruitment (Figure 1.1). Recruitment of the basal machinery by the transcription factors also requires co-activators and mediator complexes (Roeder, 2005; Rosenfeld et al., 2006).

Decades of *in vitro* studies had led to the dogma that transcription factors interact with their specific DNA response elements in the promoter or enhancer region of the target genes in a stable manner, persisting on a time scale of hours. Transcription factors together with co-activators and mediators form a stable complex known as the enhanceosome (Agalioti et al., 2000; Kim and Maniatis, 1997; Maniatis et al., 1998; Panne et al., 2007). However, several recent reports challenge this enhanceosome hypothesis. It was a surprise to find that the binding of sequence-specific transcription factors, such as the glucocorticoid receptor (GR), the progesterone receptor, and NF-κB family proteins, to the array of their cognate binding sites was highly transient when analyzed by fluorescence recovery after photobleaching (FRAP) analysis (Bosisio et al., 2006; McNally et al., 2000; Rayasam et al., 2005). Quantitative FRAP analysis estimated that the residence time of transcription factors on chromatin range from a few milliseconds to around hundred seconds. These estimations can vary by several order of magnitude depending on the details in the FRAP model (Mueller et al., 2008; Phair et al., 2004; Sprague et al., 2004).

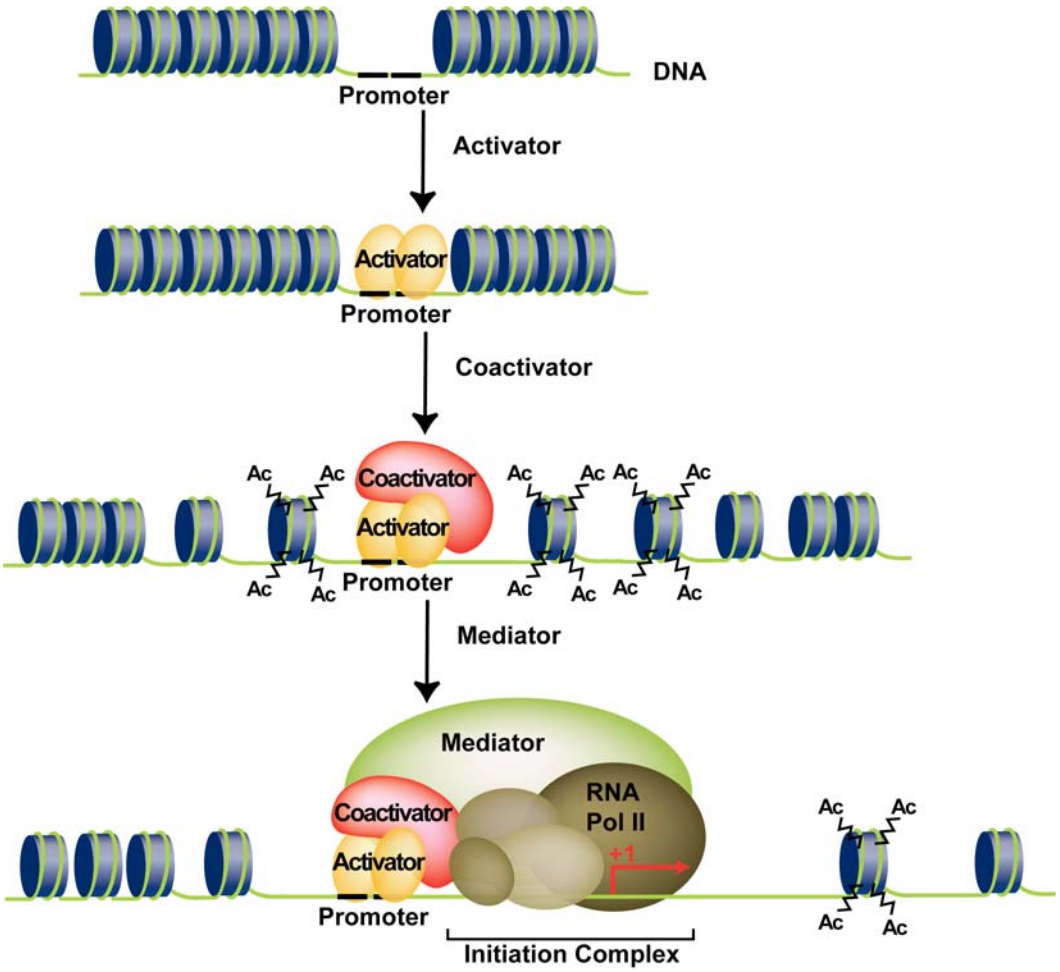

Figure 1.1 A Schematic Model of Eukaryotic Transcription Initiation Complex Assembly.

B. NF-κB Protein Family

NF-kappaB (NF-κB) was first identified about twenty years ago as a transcription factor that binds to the intronic enhancer of the kappa light chain gene in B cells (Sen and Baltimore, 1986a, b). NF-κB family proteins control the expression of genes that play important roles in several physiological events including immune responses, inflammation, growth, proliferation, and apoptosis (Baldwin, 1996; Ghosh et al., 1998). NF-κB family refers to a group of homo- and hetero-dimers that are formed in a combinatorial manner from five subunits: RelA (p65), RelB, c-Rel, p50, and p52 (Figure 1.2). NF-κB subunits share a highly homologous sequence near their N-termini, referred to as the rel homology region (RHR). The RHR region mediates the dimerization, DNA binding, and nuclear localization of NF-κB proteins (Baldwin, 1996; Ghosh et al., 1998). NF-κB subunits can be divided into two classes. The p50 and p52 subunits belong to class I by virtue of not having a C-terminal transcription activation domain (TAD), thus categorizing them as transcriptional repressors. The p50 and p52 subunits are synthesized from their precursor proteins p105 and p100, respectively (Bours et al., 1990; Ghosh et al., 1990; Kieran et al., 1990; Schmid et al., 1991). The other three subunits, RelA, c-Rel and RelB, constitute class II which contains a TAD at their C-termini. Homo- and hetero-dimers with at least one class II subunit have transcription activation potential. NF-κB dimers regulate expression of hundreds of genes by binding to specific DNA sequences, collectively known

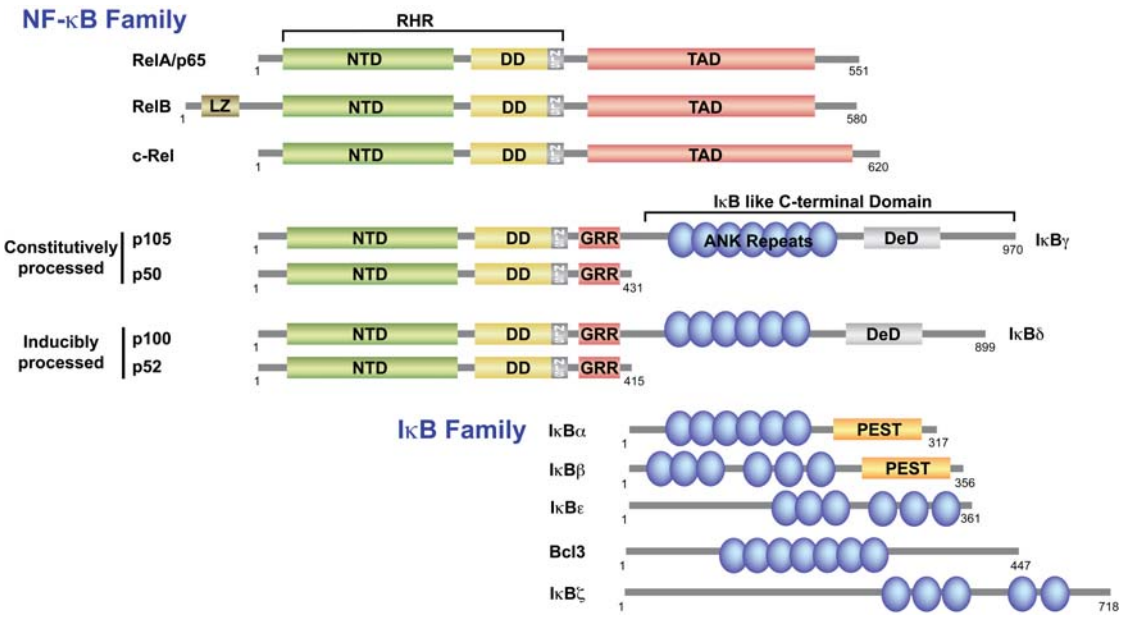

Figure 1.2 A schematic representation of members of the NF-κB and IκB protein families. Domains are designed as filled rectangles and circles and labeled. NF-κB family members are characterized by the presence of the rel homology region (RHR) which is responsible for dimerization, DNA binding, and nuclear localization of the proteins. NF-κB subunits are classified into two classed based on the presence or absence of a C-terminal transcription activation domain (TAD). Note that p50 and p52 are generated from their precursor proteins, p105 and p100, respectively. IkB proteins are characterized by the presence of ankyrin repeat domain (ARD). Due to the C-terminal ARD, both p105 and p100 also classified as members of the IκB protein family.

as κB DNA, located within the promoter/enhancer region of target genes (Baldwin, 1996; Ghosh et al., 1998).

C. IκB Protein Family

Inhibitor of NF-κB protein (IκB) is a physiological regulator of the activities of the NF-κB transcription factors. IκB proteins regulate NF-κB activity in at least two ways: IκB can anchor NF-κB dimers in the cytoplasm in resting cells by blocking the nuclear localization signals (NLS); it can also inhibit NF-κB binding to its consensus κB DNA. The central region of IκB proteins contains multiple ankyrin repeats which folds into a single domain referred to as ankyrin repeat domain (ARD) (Baldwin, 1996; Ghosh et al., 1998). The ARD of IκBs and the RHR of NF-κB dimers are primarily responsible for the IκB:NF-κB complex formation (Huxford et al., 1998; Jacobs and Harrison, 1998; Malek et al., 2003). The IκB proteins also contain other functional motifs: the signal response region (SRR) at the N-terminus and the PEST region (regions containing proline (P), glutamate (E), serine (S), and threonine (T) bordered by positively charged residues) at the C-terminus. The SRR contains serine residues which undergo phosphorylation in a signal dependent manner. These serines are preceded by lysine residues which undergo signal dependent ubiquitination. The PEST sequence, in IκBα particularly, has been shown to modulate its half-life in stimulated cells.

There are two distinct classes of IκB proteins in cells (Figure 1.2). IκBα, IκBβ and IκBε constitute the first class. These inhibitors bind primarily to RelA and c-Rel containing NF-κB dimers. The NF-κB precursor proteins p100 (NF-κB2) and p105 (NF-κB1), which also function as inhibitors of NF-κB, comprise the second class of IκB proteins. The IκB-like C-termini of p105 (called IκBγ) and p100 (called IκBδ) use their ARD to inhibit NF-κB (Dobrzanski et al., 1995; Liou et al., 1992). The mechanism of how they inhibit NF-κB is not entirely clear. These two proteins also contain SRR in their C-terminus, which contains serine residues that undergo stimulus dependent phosphorylations.

Although the IκBs are similar in structure, they each have their own binding preferences and are subjected to differential transcriptional regulation by the NF-κB family. The most extensively studied IκB protein, IκBα, preferentially regulates the p50/RelA heterodimers and retain them in the cytoplasm in resting cells. In response to inflammatory stimuli such as tumor necrosis factor-alpha (TNFα) and lipopolysaccharide (LPS), IκBα is degraded rapidly through the proteasomal pathway and then re-synthesized in an NF-κB dependent manner to constitute a negative feedback loop in which the newly synthesized IκBα associate with p50/RelA heterodimer in the nucleus and shuttle them back to the cytoplasm (Arenzana-Seisdedos et al., 1997). Signal dependent degradation and re-synthesis of IκBβ and IκBε occur at a much slower kinetics (Hoffmann et al., 2002). Therefore, the temporal differences in

different IκB degradation and re-synthesis play a major role in determining their functional characteristics in the regulation of NF-κB activity.

In addition to the classical IκBs, there are atypical IκB-like proteins, which include Bcl3 and IκBζ. They are subjected to differential regulation and serve different functions compare to the classical IκBs. Bcl3 and IκBζ preferentially regulate NF-κB p52 and p50 homodimers, and can function as transcriptional co-factors to regulate their specific target gene transcription (Kashatus et al., 2006; Park et al., 2006; Westerheide et al., 2001; Yamamoto et al., 2004).

D. NF-κB Activation Pathways

Physiological NF-κB dimers with demonstrated transcription activation function *in vivo* are p50/RelA, p52/RelA, RelA/RelA, c-Rel/c-Rel, p50/c-Rel, p52/RelB and p50/RelB. The most ubiquitously expressed and predominant NF-κB dimer in cells is the p50/RelA heterodimer. These dimers regulate expression of hundreds of genes by binding to specific DNA sequences, collectively known as κB sites, located within the promoter or enhancer elements (Baldwin, 1996; Ghosh et al., 1998). There are two NF-κB signaling pathways, the canonical and the non-canonical signaling pathway. These signaling pathways differ in respect of the activating stimuli, kinases, and specific IκB and NF-κB molecules involved. The canonical NF-κB pathway activates RelA and c-Rel containing homo- and hetero-dimers in response to

inflammatory cytokines, pathogen associated molecules, such as TNFα and LPS. In unstimulated cells, NF-κB dimers with transcription activation potential are maintained inactive through stable protein-protein association with IκB protein. Upon stimulation, inhibitor of NF-κB kinase (IKK) complex that consists of two protein kinases, IKK1 and IKK2, and a regulatory particle, NF-κB essential modulator (NEMO), gets activated. The IKK2 activity is required for the activation of the canonical signaling pathway. Phosphorylation of IκB protein by IKK2 leads to the ubiquitination and proteasomal degradation of IκB and the release of the NF-κB dimers which in turn translocate into nucleus and activate the target genes (Karin and Ben-Neriah, 2000) (Figure 1.3, left panel). Another set of stimuli including LTβ, CD40, and BAFF, initiate the non-canonical NF-κB activation pathway, which leads to the processing of p100 to p52. The activation of the non-canonical pathway requires the catalytic activities of NF-κB inducing kinase (NIK) and IKK1. NIK is an unstable protein which undergoes constitutive degradation in unstimulated cells. NIK ligand-receptor binding leads to the stabilization of NIK. NIK and IKK1 phosphorylate the serine residues at p100 C-terminus which leads to the processing of p100 and the generation of p52 through a yet unknown mechanism. In cells, most p52 heterodimerize with RelB and regulate the target gene expression (Figure 1.3, right panel). p52 homodimer has been shown to regulate a limited numbers of genes. However, the mechanism of p52 homodimer activated gene regulation is not clear.

Genes activated by the canonical pathway are activated rapidly and are mostly involved in inflammation, whereas the genes activated by the non-canonical pathway are mostly involved in developmental programs (Ghosh and Karin, 2002; Perkins and Gilmore, 2006). However, these pathways are not linear but converge at many points and influence each other (Basak et al., 2007). Aberrant NF-κB activity is a hallmark feature of several inflammatory diseases and cancers. The ability of NF-κB to induce cell proliferation and survival makes it a perfect regulator of cancerous cell growth (Karin, 2006). Inhibition of NF-κB activity has been a major strategy adapted by the pharmaceutical industry to combat these diseases (Courtois and Gilmore, 2006; Gilmore and Herscovitch, 2006; Kim et al., 2006).

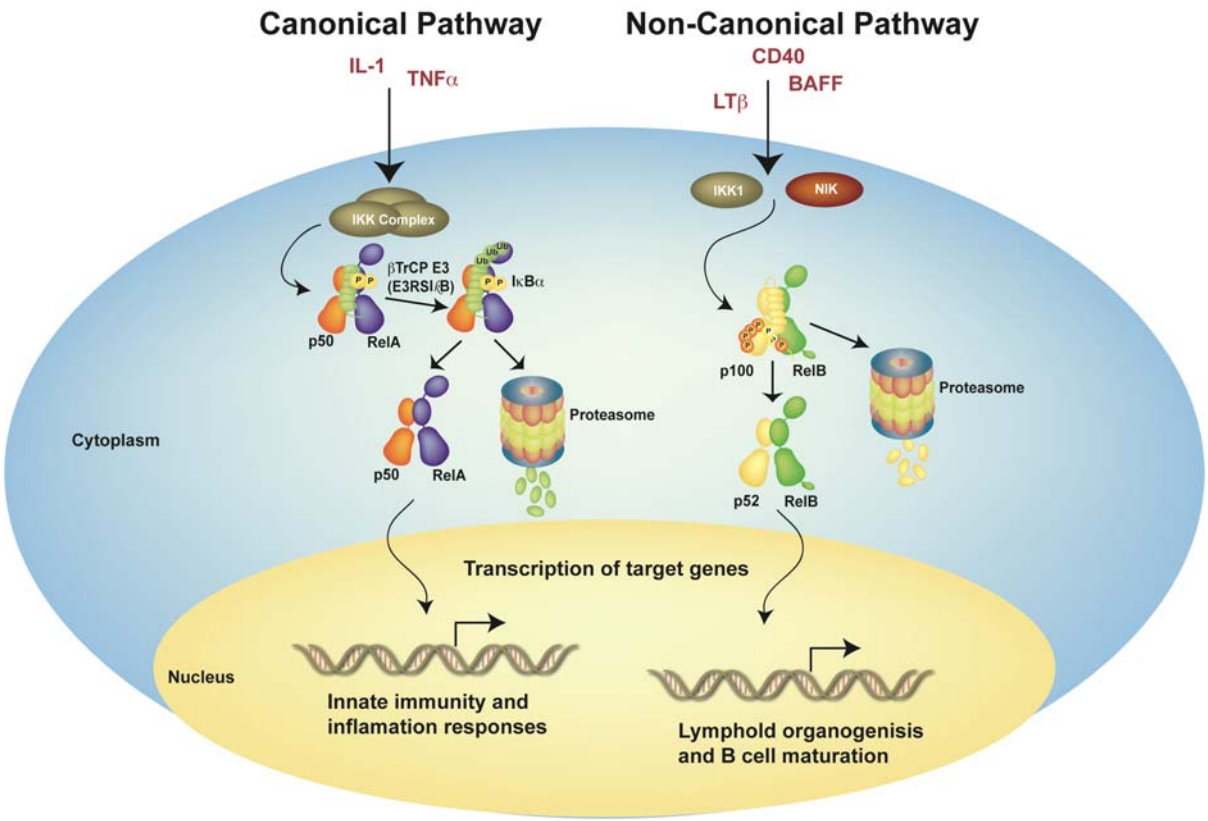

Figure 1.3 NF-κB Activation Pathways. For canonical pathway, it involves RelA or c-Rel containing NF-κB dimers. p50/RelA heterodimer is the most abundant NF-κB dimers in cells. In the resting stage, p50/RelA dimers are retained in the cytoplasm through the binding with IκBα. Upon stimulation and the activation of IKK complex, IκBα is phosphorylated, ubiquitinated, and degraded by the proteasomal pathway, which in turn lead to the translocation of p50/RelA into nucleus and activate its target genes. The Non-canonical pathway involves the p100 processing into p52. A distinct class of stimuli activates the non-canonical pathway, in which the kinase activity of NIK and IKK1 is required to phosphorylate the p100 C-terminal IκB like domain. p100 is then processed to p52; most p52 heterodimerizes with RelB in cells and activate its target genes.

E. Mechanism of NF-κB Dimer Formation

X-ray structures of several DNA-bound NF-κB dimers have been solved in our lab. All the three-dimentional structures of DNA-bound NF-κB complexes resemble a butterfly with the protein domains as wings connected to a cylindrical body of DNA double helixes. And these structures reveal that the NF-κB RHR region is folded into two domains; the N-terminal domain (NTD) and the dimerization domain (DD). The dimerization domain, containing a core β-sandwish structure with similarities to immunoglobulin (Ig) domains, is responsible for NF-κB dimer formation (Chen et al., 1998a; Chen et al., 1998b; Ghosh et al., 1995; Muller et al., 1995). Structures of dimerization domains and NF-κB:DNA complexes show that the dimerization interface remains fairly conserved in the free and DNA bound forms (Huang et al., 1997). All structures solved to date, with the exception of the RelB dimerization domain, show similar overall features wherein each monomer assumes an independent Ig-fold that packs against each other to form a dimer interface; and the dimer interface is formed by the face of a three-stranded β-sheet packing against the same sheet in the opposite subunit. The variable specificities may then be based primarily on amino acid substitutions within the dimerization domain. In addition, amino acid differences at sites distal to the subunit interface may also play roles in determining dimerization strengths. RelB dimerization domain forms a domain swapped homodimer, most likely due to the lack of folding stability of the core domain feature.

F. DNA Recognition by NF-κB Dimers

The NF-κB specific DNA target sites are collectively referred to as the κB DNA or κB site. The κB DNA initially discovered and characterized seemed to be 10 base pairs (bp) in length with the consensus sequence of 5' -GGGRN W YYCC-3' (where R is an unspecific purine, N is any nucleotide, W is an adenine or thymine, and Y is an unspecific pyrimidine) (Baldwin, 1996; Ghosh et al., 1998; Kunsch et al., 1992). The p50 and p52 subunits prefer 5 bp half sites (5' –G(-5)G(-4)G(-3)R(-2)N(-1)-3'), whereas the RelA and c-Rel subunits prefer 4 bp half sites (5'-Y(+1)Y(+2)C(+3)C(+4)-3') (Figure 1.4). A set of highly conserved residues contacts the first four base pairs in both half sites. A histidine from p50 or p52 contacts the guanine at position -5 (the outermost residue). This histidine is not conserved in RelA, c-Rel and RelB, which explains why they recognize 4 bp DNA half site. This rule of κB DNA binding also predicted that RelA and c-Rel homodimers would preferentially bind to a 9 bp consensus DNA sequences whereas p50 and p52 homodimers would bind to a 11 bp DNA. Figure 1.4 summarizes the base-specific interaction between NF-κB dimers and a κB DNA. The G/C rich sequences in the flanking region are contacted by a set of invariant amino acids in NF-κB monomers. The central base pair, W, fall in the pseudo dyad axis does not contact any protein subunits and hence its role in NF-κB dimer recruitment remained clear.

Another important feature of NF-κB:DNA complexes is the ability of NF-κB dimers to recognize DNA with high affinity even when a κB site deviates significantly from the consensus. Analysis of a large number of physiological κB DNAs suggests that there are a large number of NF-κB binding sites that show only loose consensus. Some of the extreme binding sequences retain only one recognizable half site. It has been previously showed that the unique modular domain architecture allow NF-κB to form complexes with such DNA sites (Chen et al., 1998b). In these complexes, only one subunit makes base-specific contacts whereas the other makes sequence non-specific contacts. The mode of NF-κB DNA binding is very different than other well characterized DNA binding transcription factors such as nuclear hormone receptors where the target sites are more strictly defined following proper rules (Khorasanizadeh and Rastinejad, 2001).

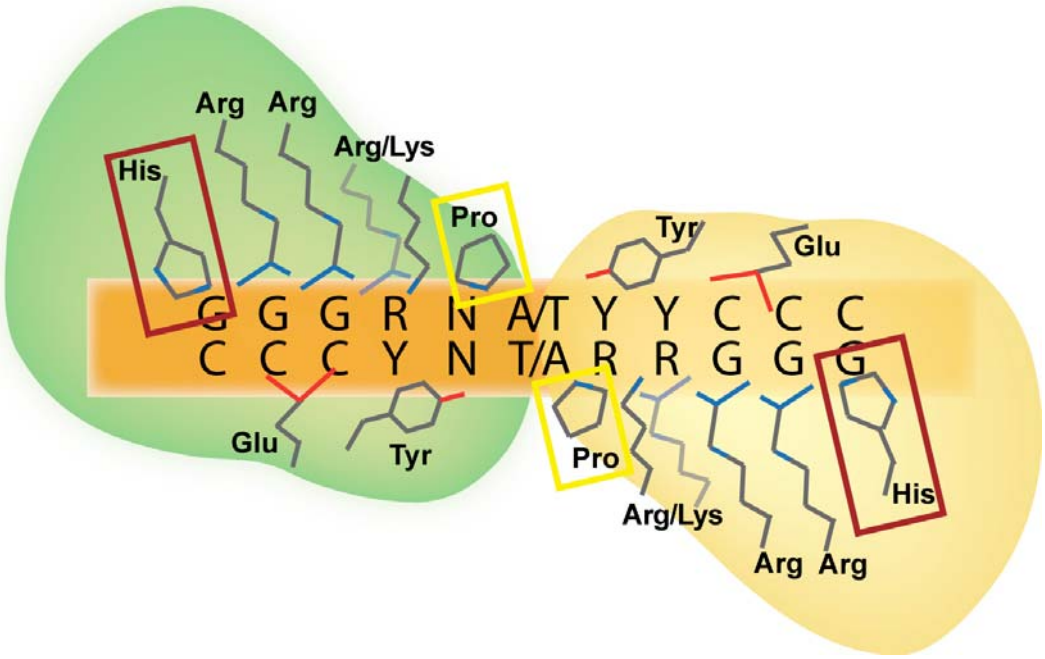

Figure 1.4 Base-specific contacts between an NF-κB dimer and a κB DNA. This model represents a consensus mode of DNA binding by the NF-κB dimer. Histidine residues in the box are present only in p50 and p52 subunits.

G. NF-κB, Co-activators, and Co-repressors

It is well known that like other transcription activators, NF-κB requires global co-activators and co-repressors for activation and repression of target genes respectively (Parker et al., 1996; Perkins et al., 1997; Sheridan et al., 1995). By definition, transcriptional co-activators do not bind DNA directly. However, they assist the assembly of transcription factors at the promoter/enhancer regions of target genes and play a critical role in the recruitment of the basal transcription machinery (Rosenfeld et al., 2006). CBP/p300 is one of the general co-activators that have been extensively studied both *in vitro* and *in vivo*. It is known that CBP/p300 is recruited to the promoter by the transcription factors where it plays two roles. First, using the histone acetylase activity, CBP/p300 acetylates the histones in the nucleosome to promote nucleosome disassembly and sliding. The second role of CBP/p300 is the assembly role, where CBP/p300 interacts with multiple transcription factors in the promoters as well as with the general transcription machinery. NF-κB subunits RelA and c-Rel have been shown to directly interact with CBP/p300 both in phosphorylation dependent and independent manner. It has been shown that NF-κB also interacts with co-repressor such as histone deacetylase (HDAC1, 3) as well as other co-repressor such as nuclear receptor co-repressor (NCoR) and the related silencing mediator of retinoic acid and thyroid hormone receptors (SMRT).

H. Transcriptional Co-activator Functions of IκB Proteins

Bcl3 and IκBζ have been shown to function as co-regulators of p52 and p50 homodimers. There are several recent reports suggesting that p50:IκBζ complex induces gene activation at some promoters. Similar functions of Bcl3 have also been proposed and in some cases *in vivo* experiments have confirmed this. These two IκB proteins have not been shown to be a target of IKK; other kinases might be able to phosphorylate Bcl3. However, these phosphorylation events have not yet been linked to gene activation. The p50:Bcl3 complex has also been shown to repress certain gene activation such as IL-23, IL-12, and IL-1β. How the same complex elicits both gene activation and repression has reminded unclear. As for the activation function, it has been shown that the p52:Bcl3 complex also recruits a histone acetylase, known as Tip60, to the promoter of the target gene (Dechend et al., 1999).

A recent report has also shown that IκBβ can activate gene expression through the interaction with RelA/c-Rel heterodimer on the TNFα promoter (Rao et al.). The IκBβ which binds to the RelA/c-Rel:DNA complex is in the hypophosphorylated stage.

I. Focus of Study

As mentioned earlier, the NF-κB p52 homodimer cannot activate its target gene transcription by itself since the lack of the C-terminal TAD. In order to function as transcription activator, p52 homodimer has to function together

with its specific transcriptional co-activator, Bcl3. Mice deficient in both *nfκb2* and *bcl3* genes, but not either one alone, led to a profound breakdown in central tolerance resulting in rapid and fatal multiorgan inflammation (Zhang. et al., 2007). Thus, demonstrating that p52 and Bcl3 functions together to regulate genes at the transcriptional level which is important for immune tolerance. However, only a limited number of genes are known to be regulated by the p52:Bcl3 complex which includes P-Selectin, cyclin D1 and IP-10 (Cogswell et al., 2000; Leung et al., 2004; Pan and McEver, 1995). The promoter analysis revealed that the κB sites in the promoter region of these genes are specifically regulated by the p52:Bcl3 complex. It is not clear why this promoter is not regulated by the classical NF-κB dimers such as RelA homodimer or p50/RelA heterodimer. The focus of the study is to understand how NF-κB p52 subunit activates target genes in association with its specific transcriptional co-factor Bcl3. In this regard, one of the thesis goals is to understand if NF-κB p52 homodimer activate transcription by binding to a distinct subset of κB sites and if these κB sites are discriminated by other NF-κB subunits such as RelA. The role of Bcl3 in κB site recognition by p52 homodimer has remained unclear. Therefore, transcriptional regulation will be tested in the presence or absence of Bcl3.

p52 is generated from its precursor protein, p100. Mechanistic understanding of how p52 is generated and form two distinct dimers, p52/RelB heterodimer and p52/p52 homodimer, by specific stimuli has remained

unclear. Another goal of the thesis is to investigate how p52 is generated from p100 and how the processed p52 form specific dimers by binding with either itself or with other NF-κB subunits such as RelB.

Finally, this work also aims to understand if and how Bcl3 is regulated by stimulus which also generates p52, and as a result both p52 and Bcl3 gets load onto a promoter in a synchronized manner if both proteins are necessary to regulate a target gene.

Chapter II: The Central Base Pair of κB DNA Sequences is A Key Regulator of The NF-κB dimer Transcriptional Specificity

A. Introduction

The NF-kappaB (NF-κB) family of dimeric transcription factors plays decisive roles in diverse physiological programs including inflammation and immune responses, survival and death, development and differentiation, and proliferation and growth. NF-κB dimers exert their effect by orchestrating transcriptional regulation of large number of downstream effector genes whose coordinated function results in signal responsive cellular outcomes (Hoffmann et al., 2006). These effector genes contain NF-κB binding sites, known as κB sites (or κB DNA), which recruit NF-κB dimers to activate or repress their transcription. There are five NF-κB family monomers (p50, p52, RelA/p65, cRel and RelB), which form combinatorial dimers. NF-κB family is defined by a ~300 amino acids homologous region, referred to as the rel homology region (RHR), located at their N-terminus. This region contains both the dimerization domain and sequence-specific κB DNA binding domain.

Initial discovery of just few physiological κB sites established the pseudo-symmetric consensus κB site as 5'-GGGRN W YYCC-3' (R= purines and Y= pyrimidine, N= any nucleotide). The X-ray crystal structures of several NF-κB dimers bound to different κB DNAs are known to date (Huxford et al.). These structures have revealed the general theme of how NF-κB dimers recognize consensus κB site using an apparently conserved mode: The GGGRN half site is recognized by p50 or p52 subunit whereas the YYCC half site is recognized by RelA, cRel and RelB subunits. Thus the p50 (or p52)

heterodimers with RelA (or cRel or RelB) preferentially recognize 10 bp κB sites. RelA and cRel homodimers bind these 10 bp sites as the 9 bp recognition sites of RelA or cRel homodimers are contained within the 10 bp sites. The (G)GG/CC core sequences in the flanking region are contacted by a set of invariant amino acids in NF-κB monomers. The inner variable base pairs make semi-invariant contacts (Figure 1.4). The central base pair, falls in the pseudo dyad axis remain mostly uncontacted through specific hydrogen bonds, and is the main source of asymmetric DNA contacts by the NF-κB dimers. Within the confinement of conserved binding modes the greatest variations in protein-DNA contacts found to occur at positions ±1 positions of DNA. In addition to κB sites that in general follow the consensus, there are a large number of NF-κB binding sites that show only loose consensus. Some of the extreme binding sequences retain only one recognizable half site. These κB-like sites also bind NF-κB dimers. For instance, a subset of IRE contains half site specificity for p50 homodimer binding and it has been recently reported that p50 homodimer represses expression of IFNβ-responsive genes that contain these sites now called G-IRE sites (Cheng et al.).

Although some NF-κB regulated genes are known to be regulated by a specific or a sub-set of NF- κB dimers, so far no clear rule dictating dimer-specific gene activation to the nucleotide sequence of κB sites (Hoffmann et al., 2003; Natoli et al., 2005; Ogawa et al., 2005). Therefore, we would like to investigate whether dimer selectivity of accomplished at the level of both

nucleotide sequences. In our studies, we used cultured macrophage cell line, RAW 264.7, and primary macrophages, bone marrow-derived macrophages (BMDM), as our model system; and used bacterial lipopolysaccharide (LPS) to activate NF-κB pathways in macrophages. It is known that LPS activates both canonical and non-canonical NF-κB signaling pathways through Toll-like receptor 4 (TLR4) (Kawai and Akira, 2007). In addition, TLR4 activates several other signal transduction pathways (Figure 2.1).

In this chapter, in combination of both *in vitro* and cellular approaches, we show a strong correlation between the sequence identity of the central base pair (bp) of κB sites and the transcriptional activity of NF-κB dimers. We found that whereas the RelA homodimer prefers an A/T at the central position (A/T-centric), the p52 homodimer prefers a G/C-centric κB site for transcriptional activation. However, although the p52 homodimer is responsible for bp selectivity, being devoid of a transcriptional activation domain it requires Bcl3 for the transcriptional activation. The affinity of the NF-κB:DNA complexes is not an indicator of transcriptional specificity as the p52:Bcl3 complex prefers A/T-centric κB sites over G/C-centric for stable binding; however, it represses transcription from the A/T-centric κB sites. Our results thus reveal how a specific set of NF-κB dimers activated by a single stimulus can establish a biological program by activating a set of genes while repressing another set of genes through a single bp switch in the κB DNA response element. The fact that multiple dimers can induce expression of a

gene is due to the presence of multiple κB sites in the promoters which all can be independently regulated by a single or a specific set of dimers through stimulus, temporal and/or cell type-specific manner.

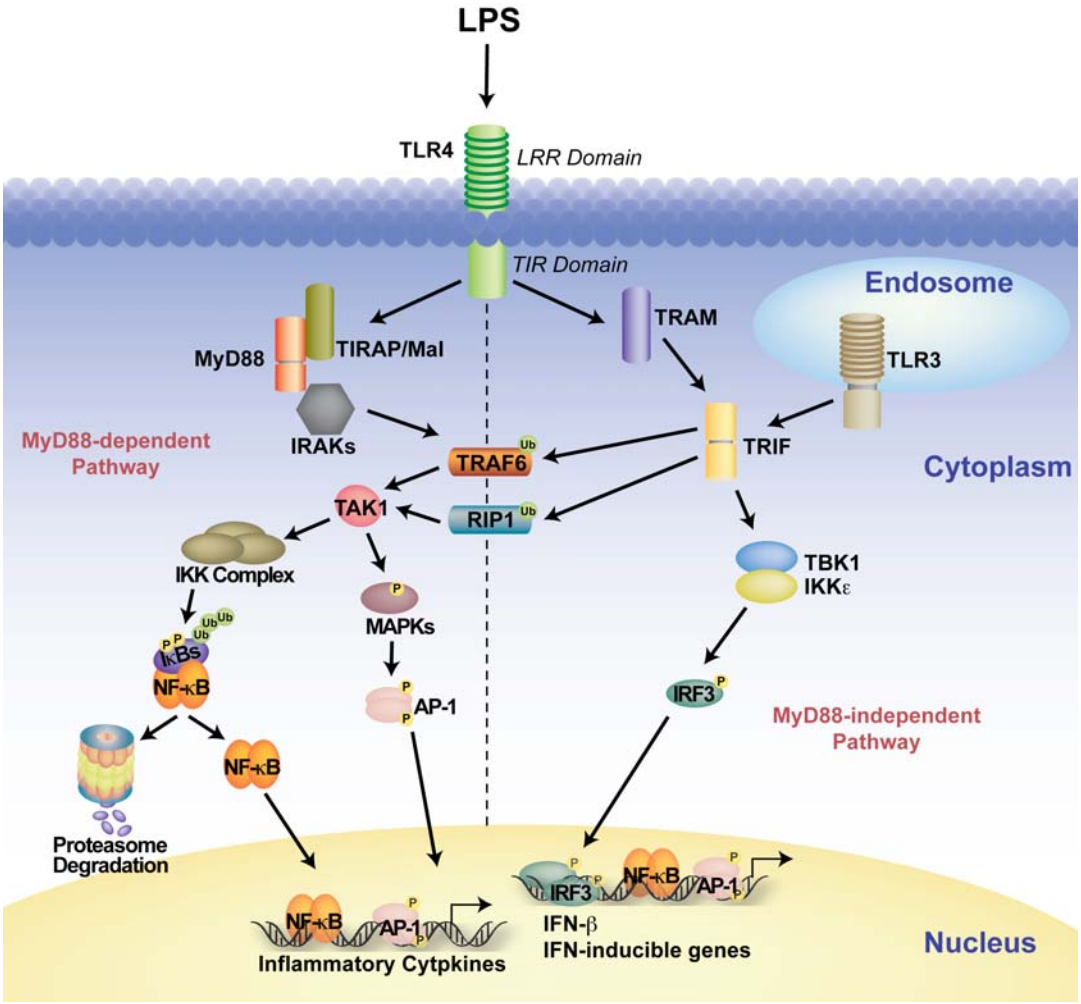

Figure 2.1 LPS activates signal transduction pathways through TLR4.

B. Materials and methods

1. Antibodies and Reagents

The RelA (sc-372), αTubulin (sc-5286), RNA Pol II (sc-900), normal rabbit IgG, and all the secondary HRP-conjugated antibodies were purchased from Santa Cruz Biotecnology. Flag (M2) (F3165) antibody and LPS (L6529) were from Sigma. p100/p52 (#1494 for ChIP assays and #1495 for Western Blot and EMSA super-shift) and Bcl3 (#1348) rabbit antisera were a kindly gift from Dr. Nancy (NIH, Bethesda, MD).

2. Mammalian Cell Culture and Transfection

Bone marrow-derived macrophages (BMDM) were obtained from 5-7-week-old C57BL/6 mice as decribed (Sawka-Verhelle et al., 2004). In brief, macrophages were cultured in RPMI 1640 medium (Invitrogen) supplemented with 25% fetal bovine serum and 25% L cell-conditioned medium as a source of M-CSF. RAW 264.7 cells and HeLa cells were grown in Dulbecco's modified Eagle's medium (CellGro) supplemented with 10% fetal bovine serum, 2 mM glutamine and antibiotics.

For RNAi experiments, scramble control or smart-pool siRNAs (Dharmacon) against Bcl3 were transfected into BMDM using Lipofectamine 2000 (Invitrogen) as described (Ghisletti et al., 2009). Cells were used for experiments after 48 hours incubation and target gene knockdown efficiency was validated by qPCR.

3. Mammalian Expression Vector Modification

pEYFP-C1-YFP+NT-Flag: Original pEYFP-C1 (Clonetech) vector was double digested with Nhe I and Bgl II (NEB) to remove the enhanced YFP. N-Terminal Flag-tag was cloned using Nhe I and Bgl II sites. Primers contain N-terminal Nhe I and C-terminal Bgl II restriction site and Flag peptide sequence with Asp-Tyr-Lys-Asp-Asp-Asp-Asp-Lys: NheI_Flag_BglIIt: 5'-CG CTA GCG GAT TAC AAG GAT GAC GAC GAT AAG AGA TCT CGA-3'

NheI_Flag_BglIIb: 5'-TCG AGA TCT CTT ATC GTC GTC ATC CTT GTA ATC CGC TAG CG-3'

Top and bottom primers were annealed, double digested with Nhe I and Bgl II restriction enzyme (NEB), and then ligated in pEYFP-C1-YFP vector at the corresponding cut sites.

pEYFP-C1-YFP+NT-Flag+CT-His8: C-Terminal His8-tag was cloned to pEYFP-C1-YFP+NT-Flag vector using Sac II and BamH I sites, in which EcoRV site (in frame) was added in front of His8-tag, stop codon was introduced after His8-tag and before BamH I restriction site. Both top and bottom primers contain N-terminal Sac II and C-terminal BamH I restriction site: SacII_His8_StBamHIt: 5'-GT ACC GCG GGC CCG GGA GAT ATC CAC CAC CAC CAC CAC CAC CAC CAC TAG GGA TCC A-3'

SacII_His8_StBamHIb: 5'- T GGA TCC CTA GTG GTG GTG GTG GTG GTG GTG GTG GAT ATC TCC CGG GCC CGC GGT AC-3'

Top and bottom primers were annealed, double digested with Sac II and BamH I restriction enzyme (NEB), and then ligated in pEYFP-C1-YFP+NT-Flag vector at the corresponding cut sites.

4. Protein Expression Plasmids

Flag-RelA(1-551): Flag-tagged human RelA(1-551) in pEYFP-C1-YFP+NT-Flag+CT-His8 (Kan) vector was generated by PCR reaction using human HA-RelA(1-551) as a template, N-terminal primer containing Hind III restriction site: hp65_Hind III_1F: 5'- CC CAA GCT TCG ATG GAC GAA CTG TTC CCC-3'

C-terminal primer containing EcoR V restriction site:

hmp65_sEcoRV_550/551R: 5'- TC GAT ATC TTA GGA GCT GAT CTG ACT C-3'

The PCR reaction product was first gel purified, then double digested with Hind III and EcoR V restriction enzymes (NEB), and gel purified again. The DNA fragment was then ligated in pEYFP-C1-YFP+NT-Flag+CT-His8 vector at the corresponding cut sites.

Flag-p52(1-415): Flag-tagged human p52(1-415) in pEYFP-C1-YFP+NT-Flag (Kan) vector was generated by PCR reaction using human pHis8-p100(1-899) as a template, N-terminal primer containing EcoR I restriction site: p100_EcoRI_1F: 5'-CG AAT TCT ATG GAG AGT TGC TAC AAC C-3'

C-terminal primer containing BamH I restriction site: p100_BamHI_415R: 5'-CG GGA TCC GTC CCT GCT GGG CAC C-3'

The PCR reaction product was first gel purified, then double digested with EcoR I and BamH I restriction enzymes (NEB), and gel purified again. The DNA fragment was then ligated in pEYFP-C1-YFP+NT-Flag vector at the corresponding cut sites.

Flag-Bcl3(1-447): Flag-tagged human Bcl3(1-447) in pEYFP-C1-YFP+NT-Flag+CT-His8 (Kan) vector was generated by PCR reaction using human pHis8-p100(1-899) as a template, N-terminal primer containing EcoRI restriction site: Bcl3_EcoRI_1F(pEYFPC1): 5'-CG AAT TCT ATG GAC GAG GGG CCC G-3'

C-terminal primer containing BamHI restriction site:

Bcl3_sBamHI_447R(pEYFPC1): 5'- CG GGA TCC TCA GCT GCC TCC TGG AGC TGG-3'

The PCR reaction product was first gel purified, then double digested with EcoRI and BamHI restriction enzymes (NEB), and gel purified again. The DNA fragment was then ligated in pEYFP-C1-YFP+NT-Flag+CT-His8 vector at the corresponding cut sites.

5. Protein Purifications

Recombinant mouse RelA(19-304) protein was provided by Dr. Sulakshana Mukherjee.

Non-tagged human p52(1-408) in pET11a (Novagen) was transformed in *E.coli* BL21(DE3) cells and were grow in 2L culture of LB/Ampicillin (100ug/mL) broth to an $O.D._{600}$ of 0.6 at 37°C and induced with 0.4mM IPTG for overnight at 37°C. Cells were harvested by centrifugation. Cell pellets of pET11a-p52(1-408) were resuspended in 150mL of lysis buffer containing 20mM Tris pH7.5, 100mM NaCl, 5% glycerol, 2mM EDTA, 0.5mM PMSF, 10mM βME, 100μL of Sigma Protease Inhibitor Cocktail (Sigma). The resuspended cells were lysed at 4°C by sonication five times at 1 minute burst intervals. The lysed cells were then centrifuged to remove insoluble fraction. The soluble fraction was loaded onto a tandem fast flow Q- and S-sepharose column at 4°C. The S-sephorose column was washed and eluted with 100mM to 1M NaCl gradient. The pooled peak fractions were concentrated using Centriprep YM-30 (Amicon) at room temperature, diluted 5-fold with 100mM NaCl lysis buffer, and then loaded onto a 5mL HiTrap-SP column (GE Healthcare) pre-equilibrated with 20mM Tris pH 7.5, 100mM NaCl, 5% glycerol, 2mM EDTA, 0.5mM PMSF, 2mM DTT. The column was washed and eluted with 100mM to 600mM NaCl gradient. The peak fractions containing p52(1-408) were concentrated and loaded onto a Superdex-200 gel filtration column (GE Healthcare) which was pre-equalibrated with 350mM NaCl, 20mM Tris pH7.5, 2mM EDTA, 5% glycerol, 0.5mM PMSF, 1mM DTT. Pooled peak

fractions were concentrated to ~14mg/mL, aliquoted, flash frozen by liquid nitrogen and stored at -80°C.

Flag-Bcl3(1-447) was transfected into HEK 293T cells using Lipofectamine 2000 reagent (Invitrogen) following the manufacturer's protocol. Cells were collected 48 hours after transfection and lysed with RIPA buffer (20mM Tris pH 8.0, 200mM NaCl , 1% Triton-X100, 2mM DTT, 5mM 4-nitrophenyl phosphate di(Tris)Salt, 2mM Na_2VO_4, and 1mM PMSF) supplemented with proteases inhibitor cocktail. Lysed cells were sonicated three times at 15 seconds burst intervals, centrifuged to remove DNA debris and then incubate with 400μL Anti-Flag M2 Affinity resin (Sigma A2220) overnight at 4°C. Bound protein was washed three times with ice-cold 1xTBS buffer (25mM Tris pH 7.5, 140mM NaCl,), and then eluted three times with 500μL 100μg/mL Flag-peptide (Sigma F3290). Three elutions were combined and concentrated using Microcon YM-30 (Millipore), aliquoted, and flash frozen by liquid nitrogen and stored at -80°C.

6. Luciferase Reporter Assays

HeLa cells were transciently transfected with Flag-RelA(1-551), or Flag-p52(1-415) together with Flag-Bcl3(1-447) expression vectors or empty Flag-vector, and the luciferase reporter DNA with specific κB DNA promoters. The total amount of plasmid DNA was kept constant for all assays. Transient

transfections were carried out using Lipofectamine 2000 reagent (Invitrogen) following the manufacturer's protocol. Renilla luciferase expression plasmid was co-transfected as an internal control. Cells were collected 48 hours after transfection. Luciferase activity assays were performed using Dual-Luciferase Reporter Assay System (Promega) following the manufacturer's protocol. Data are represented as mean ± standard deviations (SD) of three independent experiments in triplicates.

All luciferase reporters containing specific κB DNA promoter were cloned in CMXTK-Luciferase reporter (Amp) (a kindly gift from Dr. D. Chakravarti from Northwestern University Feinberg School of Medicine) using SalI and BamHI restriction enzymes (NEB). Sequences of oligonucleotides containing N-terminal SalI restriction site, C-terminal BamHI restriction site, and specific κB site used for reporter cloning are listed in Table 2.3.

7. Chromatin Immunoprecipitation (ChIP) Assays

ChIP assays were performed in RAW 264.7 cells. After LPS (100ng/mL) stimulation at various time points, cells were cross-linked by adding formaldehyde directly to the medium to a final concentration of 1% at room temperature for 10 minutes. Fixation was stopped by directly adding glycine to the medium to a final concentration of 0.1M at room temperature for 10 minutes. Then cells were washed three times with ice-cold PBS and

scraped. Cells were collected by centrifugation and then lysed in Lysis buffer (50mM Tris-HCl pH8.0, 10mM EDTA, and 1% SDS) supplemented with proteases inhibitor cocktail (Sigma). Chromatin was sheared by sonication (Bio-ruptor UCD-200 ultrasound sonicator from Diagenode), resulting in DNA fragments between 200 and 500 bp in size. After centrifugation to remove cell debris, 10% of the sample was kept as INPUT and then diluted 10 times in dilution buffer (50mM Tris pH8.0, 0.5% Triton-X100, 0.1M NaCl, 2mM EDTA) supplemented with proteases inhibitor cocktail. Extracts were pre-cleared for 1 hour at 4°C using 50μL of salmon sperm DNA/Protein A Agarose (Millipore). Immunoprecipitations were carried out overnight at 4°C with indicated antibodies. Immune complexes were collected with 50μL of salmon sperm DNA/Protein A Agarose and washed three times (5 minute each time) at room temperature using washing buffer with increasing salt concentration from 150mM NaCl, 250mM NaCl, to 250mM LiCl (20mM Tris-HCl pH 7.5, 0.1% SDS, 1% Triton-X100, 2mM EDTA) and two times with TE buffer. Immune complexes were extracted with 1% SDS (v/v), 0.1M $NaHCO_3$, and heated overnight at 65°C to reverse the cross-linking. After proteinase K digestion (100μg, 2 hours at 50°C), DNA fragments were purified on QIAquick Spin columns (Qiagen) in 50μL of elution buffer and 1μL of each sample was used in each qPCR. Sequences of promoter-specific primers are listed in Table 2.1. Data are presented as enrichment of the precipitated target sequences as compared to input DNA.

8. RNA Isolation and Real-time qPCR

Total RNA (isolated by RNeasy kit, Qiagen) was prepared from RAW 264.7 cells treated with LPS (100ng/mL) as indicated. 0.1μg of total RNA was used for cDNA synthesis (using Invitrogen SuperScriptIII First-Strand Synthesis System) and 1μL of cDNA was used for real-time qPCR analysis. Values are normalized with GAPDH content (Livak and Schmittgen, 2001). Data are represented as mean ± standard deviations (SD) of three independent experiments in duplicates. Primer sequences are listed in Table 2.2.

9. Electrophoretic Mobility Shift Assays (EMSA)

The oligonucleotides containing κB sites from different genes used for EMSA were PAGE purified, end radiolabeled with ^{32}P using T4-polynucleotide kinase (NEB) and [γ-^{32}P] ATP, and annealed to the complementary strands. Binding reaction mixtures contained recombinant RelA(19-304), or p52(1-408), and Flag-Bcl3(1-447) at different concentrations, binding buffer (10mM Tris-HCl pH 7.5, 50mM NaCl, 10% (v/v) glycerol, 1% (v/v) NP-40, 1mM EDTA, 0.1mg/mL poly(dI-dC)), and ~10000cpm of ^{32}P-labeled DNA. Reaction mixtures were incubated at room temperature for 20 minutes and analyzed by electrophoresis on a 5% (w/v) non-denatured polyacrylamide gel at 200V for 1 hour in 25mM Tris, 190mM glycine, and 1mM EDTA. The gels were then

dried, exposed to a phosphorimager, and scanned by Typhoon scanner 9400 (Amershan Bioscience). Gels were quantified by using ImageQuant version5.2 (Molecular Dynamics). Sequences of κB DNAs used in EMSA are listed in Table 2.3.

Table 2.1 Sequences of promoter-specific primers in ChIP assays

Target Promoter	Name	Sequence (5' → 3')
IP10(*CXCL10*)	mIP10_F(ChIP) mIP10_R(ChIP)	GGGAGAGGGAAATTCCA TTTCCCTCCCTGAGTCC
IL10	mIL10_F(ChIP) mIL10_R(ChIP)	GAAGAGGGAGGAGGAGCCT GGCTTTGGTAGTGCAAGAGC
Skp2	mSkp2_F(ChIP) mSkp2_R(ChIP)	TCCTCCTTCAATCCCGCCCG CCCCGTTGCCTGCTGGGAATTG
IL23p19 proximal	mIL23p19p_F(ChIP) mIL23p19p_R(ChIP)	CCCGACCTAGGCCTCTAG GCCCGCCCTTCACACTA
IL23p19 distal	mIL23p19d_F(ChIP) mIL23p19d_R(ChIP)	GGGTCATCATCGCTGTACTTT CCATCGGTTCTGCGGG
MCP-1(*CCL2*)	mCCL2_F(ChIP) mCCL2_R(ChIP)	CTGGAGCTCACATTCCAGC GGATGTTCTTCCCAGCG

Table 2.2 Primer Sequences of mRNA RT-qPCR

Target mRNA	Name	Sequence (5' → 3')
IP10	mIP10_F(mRNA) mIP10_R(mRNA)	CGGGCCAGTGAGAATGAGGGC CGTGGCAATGATCTCAACACGTGG
IL10	mIL10_F(mRNA) mIL10_R(mRNA)	GGCTGAGGCGCTGTCATCGATT ATCACTCTTCACCTGCTCCACTGC
Skp2	mSkp2_F(mRNA) mSkp2_R(mRNA)	TGGTACCGCCTCTCGCTCGA CGGGAGAGCAAGCGCACAGT
IL23p19	mIL23p19_F(mRNA) mIL23p19_R(mRNA)	GCCAACTCCTCCAGCCAGAGGATC TCTTGGAACGGAGAAGGGGGCG
MCP-1	mMCP1_F(mRNA) mMCP1_R(mRNA)	CAGCCAGATGCAGTTAACGCCCC AGCTCTCCAGCCTACTCATTGGGA
CD95Fas	mFAS_F(mRNA) mFAS_R(mRNA)	CCCATGCACAGAAGGGAAGGAGTAC CCTCTAAACCATGCTCTTCATCGCA
CD40	mCD40_F(mRNA) mCD40_R(mRNA)	GGGCTGCTTGTTGACAGCGGT CAGTCGGCTTCCTGGCTGGC
PSMA2	mPSMA2_F(mRNA) mPSMA2_R(mRNA)	CACGCAGTCAGGTGGTGTTCGT TGGTCGTCCCTCATTCCACCCA
TGFβ1	mTGFb1_F(mRNA) mTGFb1_R(mRNA)	ACAGGGCTTTCGATTCAGCGC ACGTTTGGGGCTGATCCCGTTG
TNFα	mTNFa_F(mRNA) mTNFa_R(mRNA)	CCAGACCCTCACACTCAGATC CACTTGGTGGTTTGCTACGAC
Bcl3	mBcl3_F(mRNA) mBcl3_R(mRNA)	TATGAAGGGCTCACTGCCCTGCA ACTGCATCGATGTCCGCGCC
nfkb1/p105	mnfkb1_F(mRNA) mnfkb1_R(mRNA)	GGAGACCGGCAACTCACAGACAG ATGAGGCGCACCACGCTCAG
nfkb2/p100	mnfkb2_F(mRNA) mnfkb2_R(mRNA)	CATCCATGACAGCAAGTCTC TCCTCATAGAACCGAACCTC
RelA	mRelA_F(mRNA) mRelA_R(mRNA)	GAATGTCGTCAGGATCTGC TGGTGGACTTCTTGTCGTAG
RelB	mRelB_F(mRNA) mRelB_R(mRNA)	GCAGTATCCATAGCTTCCAG TGCTCCTCTATAGGAACGTG
36B4	m36B4_F(mRNA) m36B4_R(mRNA)	AGGGCGACCTGGAAGTCC CCCACAATGAAGCATTTTGGA
GAPDH	mGAPDH_F(mRNA) mGAPDH_R(mRNA)	AATGTGTCCGTCGTGGATCT CATCGAAGGTGGAAGAGTGG

Table 2.3 Sequences of κB DNAs used in cloning of luciferase reporters and EMSAs. κB binding sites are bolded and underlined, mutations are indicated in red, restriction sites are indicated in blue.

κB Promoter	Name	Sequence
IL10	SalI_IL10_BamHIt	5′-TCGACTGCCAGGAAGGCCCCACTGAG-3′
	SalI_IL10_BamHIb	3′-GACGGTCCTTCCGGGGTGACTCCTAG-5′
IL10(A/T)	SalI_IL10(AT)_BamHIt	5′-TCGACTGCCAGGAATGCCCCACTGAG-3′
	SalI_IL10(AT)_BamHIb	3′-GACGGTCCTTACGGGGTGACTCCTAG-5′
P-selectin	SalI_P-Selectin_BamHIt	5′-TCGACGGAAGGGGGTGACCCCTTGGG-3′
	SalI_P-Selectin_BamHIb	3′-GCCTTCCCCCACTGGGGAACCCCTAG-5′
P-selectin(A/T)	SalI_P-Selectin(AT)_BamHIt	5′-TCGACGGAAGGGGGTAACCCCTTGGG-3′
	SalI_P-Selectin(AT)_BamHIt	3′-GCCTTCCCCCATTGGGGAACCCCTAG-5′
Skp2	SalI_Skp2_BamHIt	5′-TCGACCATCTGGAACTCCCCCCAAGG-3′
	SalI_Skp2_BamHIb	3′-GGTAGACCTTGAGGGGGGTTCCCTAG-5′
Skp2(A/T)	SalI_Skp2(AT)_BamHIt	5′-TCGACCATCTGGAATTCCCCCCAAGG-3′
	SalI_Skp2(AT)_BamHIb	3′-GGTAGACCTTAAGGGGGGTTCCCTAG-5′
Cyclin D1	SalI_CyclinD1_BamHIt	5′-TCGACCTACAGGGGACTTTTGTTGAG-3′
	SalI_CyclinD1_BamHIb	3′-GGATGTCCCCTGAAAACAACTCCTAG-5′
Cyclin D1(A/T)	SalI_CyclinD1(AT)_BamHIt	5′-TCGACCTACAGGGGAATTTTGTTGAG-3′
	SalI_CyclinD1(AT)_BamHIb	3′-GGATGTCCCCTTAAAACAACTCCTAG-5′
CD95Fas	SalI_CD95Fas(295)_BamHIt	5′-TCGACAACCCGGGCGTTCCCCAGCGG-3′
	SalI_CD95Fas(295)_BamHIb	3′-GTTGGGCCCGCAAGGGGTCGCCCTAG-5′
CD95Fas(A/T)	SalI_CD95Fas(295)AT_BamHIt	5′-TCGACAACCCGGGCATTCCCCAGCGG-3′
	SalI_CD95Fas(295)AT_BamHIb	3′-GTTGGGCCCGTAAGGGGTCGCCCTAG-5′
CD40	SalI_CD40(468)_BamHIt	5′-TCGACGTGGGGGGAACTTCCTCAGGG-3′
	SalI_CD40(468)_BamHIb	3′-GCACCCCCCTTGAAGGTGTCCCCTAG-5′
CD40(A/T)	SalI_CD40(468)AT_BamHIt	5′-TCGACGTGGGGGGAAATTCCTCAGGG-3′
	SalI_CD40(468)AT_BamHIb	3′-GCACCCCCCTTTAAGGTGTCCCCTAG-5′

Table 2.3: Sequences of κB DNAs used in cloning of luciferase reporters and EMSAs, Continued.

κB Promoter	Name	Sequence
Proteasome α2 subunit	SalI_alpha2(304)_BamHIt SalI_alpha2(304)_BamHIb	5′-TCGACTCTGC**GGAAGCTTCC**GTAGCG-3′ 3′- GAGACG**CCTTCGAAGG**CATCGCCTAG-5′
Proteasome α2 subunit(A/T)	SalI_alpha2(304)AT_BamHIt SalI_alpha2(304)AT_BamHIb	5′-TCGACTCTGC**GGAAATTTCC**GTAGCG-3′ 3′- GAGACG**CCTTTAAAGG**CATCGCCTAG-5′
HIV	SalI_HIV4Mut_BamHIt SalI_HIV4Mut_BamHIb	5′-TCGAC**GGGACTTTCC**GCTGGCCACTTTAAG-3′ 3′- G**CCCTGAAAGG**CGACCGGTGAAATTCCTAG-5′
HIV(G/C)	SalI_HIV4Mut(GC)_BamHIt SalI_HIV4Mut(GC)_BamHIt	5′-TCGAC**GGGACGTTCC**GCTGGCCACTTTAAG-3′ 3′- G**CCCTGCAAGG**CGACCGGTGAAATTCCTAG-5′
MHC	SalI_MHC_BamHIt SalI_MHC_BamHIb	5′-TCGACGGGCT**GGGGATTCCCC**ATCTCG-3′ 3′- GCCCGA**CCCCTAAGGGG**TAGAGCCTAG-5′
MHC(G/C)	SalI_MHC(GC)_BamHIt SalI_MHC(GC)_BamHIb	5′-TCGACGGGCT**GGGGAGTCCCC**ATCTCG-3′ 3′- GCCCGA**CCCCTCAGGGG**TAGAGCCTAG-5′
IL23p19 proximal	SalI_IL23p19p_BamHIt SalI_IL23p19p_BamHIb	5′-TCGACAGGGA**GGGGAATCCC**ACCTGG-3′ 3′- GTCCCT**CCCCTTAGGG**TGGACCCTAG-5′
IL23p19 proximal(G/C)	SalI_IL23p19p(GC)_BamHIt SalI_IL23p19p(GC)_BamHIb	5′-TCGACAGGGA**GGGGAGTCCC**ACCTGG-3′ 3′- GTCCCT**CCCCTCAGGG**TGGACCCTAG-5′
IP10 proximal	SalI_MutIP10_BamHIt SalI_MutIP10_BamHIb	5′- TCGACAAGGAGACACAAATTGCAAGTTCATGGGTCACAATAAACACAAGCAATGCCCTCGGTTTAC AG**GGGACTTCCC**TCGGGTTG-3′ 3′- GTTCCTCTGTGTTTAACGTTCAAGTACCCAGTGTTATTTGTGTTCGTTACGGGAGCCAAATGTC**CC** **CTGAAGGG**AGCCCAACCTAG-5′
IP10 proximal (A/T)	SalI_IP10II(AT)_BamHIt SalI_IP10II(AT)_BamHIb	5′- TCGACAAGGAGACACAAATTGCAAGTTCATGGGTCACAATAAACACAAGCAATGCCCTCGGTTTAC AG**GGGAATTCCC**TCGGGTTG-3′ 3′- GTTCCTCTGTGTTTAACGTTCAAGTACCCAGTGTTATTTGTGTTCGTTACGGGAGCCAAATGTC**CC** **CTTAAGGG**AGCCCAACCTAG-5′

C. Results

1. The Central Base Pair of κB DNA Sequences Play a Key Role in Providing Transcription Activity of NF-κB Dimers

Although genetic experiments have shown examples of dimer-specific gene activation, neither *in vitro* nor *in vivo* experiments found a clear correlation between κB site and specific NF-κB dimer binding and transcriptional activation (Hoffmann et al., 2003; Natoli et al., 2005; Ogawa et al., 2005). The promoter region of most target genes contains multiple non-identical κB sites and they function non-cooperatively (Giorgetti et al.). Although each κB site may impose dimer restriction, most promoters are primarily bound and activated by dimers containing the RelA subunit (also known as p65) and to a lesser extent c-Rel subunits. RelA homodimer (or p50/RelA heteordimer) is ubiquitous and is responsible for the activation of large fraction of NF-κB regulated genes. Therefore, the mechanistic involvement of other NF-κB subunits in gene regulation has remained unclear except that most of the subunits can form heterodimers with RelA or c-Rel. The role of sequence variations among κB DNA sequences has remained largely unclear either. Since most promoters contain multiple non-identical κB sites, and most stimuli could activate most NF-κB dimers, the task to determine which dimer binds what κB DNA sequence poses enormous challenge.

We wanted to investigate if dimer selectivity is accomplished at the level of nucleotide sequence using *in vitro* and cellular approaches. To this cause, we chose to investigate two dimers that are functionally distinct; the p52 and RelA homodimers. p52 homodimer has more restricted gene regulatory activity and it acts in association with the specific transcriptional co-factor, Bcl3 (Cogswell et al., 2000; Nolan et al., 1993). Two well studied promoters that are shown previously to be regulated by the p52:Bcl3 complex are P-selectin, and cyclin D1 (Guttridge et al., 1999; Pan and McEver, 1995). p52 and Bcl3 were also shown to be involved in the regulation of Skp2, IP-10 and IL-10 genes (Barre and Perkins, 2007; Leung et al., 2004; Muhlbauer et al., 2008); however, no κB site has been clearly identified and linked to their gene regulation. Although κB DNA sequences are different in these cases, they all contain at least one G/C-centric κB site in their promoters (Figure 2.2). Because most known κB sites contain A/T bp at the central position, we wanted to investigate if this single nucleotide switch might be responsible for RelA to p52:Bcl3 specificity switch. To examine the role of the central bp, we have generated reporter constructs with natural (G/C-centric) and mutant (A/T-centric) for all five of these κB sites. As shown in Figure 2.3, p52 or Bcl3 alone did not induce the luciferase activity; however, when coexpressed, p52:Bcl3 complex strongly enhanced the luciferase activity than the reporter alone control. And we found that in all cases G/C-centric κB sites are clearly selective for the p52:Bcl3 complex, although the extent of selectivity differed

(Figure 2.4) We also found that in all cases G/C at the central position strongly discriminated RelA. To further investigate the presence of G/C-centric κB sites and their relationship with NF-κB dimers, we looked at the promoters of NF-κB target genes from published literature and the rel/NFkappaB target genes website (http://bioinfo.lifl.fr/NF-KB/) which has compiled promoters over 100 mouse/human genes that are activated by NF-κB dimers. We identified several more G/C-centric κB sites and tested three of them (CD95Fas(*FAS*), TNFSF5(*CD40*), MCP-1(*CCL2*), and proteasome sunubit α2(*PSMA2*)). The G/C-centric κB sites of MCP-1 and CD40 are identical in sequences (Figure 2.2) We tested three of them; CD95Fas, CD40, and PSMA2. Our analysis showed a strong correlation between G/C-centric κB site and their activation by the p52:Bcl3 complex; in addition, RelA activated the mutated A/T-centric κB sites (Figure 2.5). However, mutation of G/C to A/T central bp did not significantly reduced p52:Bcl3 transcriptional activity in these cases. This suggests that other bps in κB DNAs also contribute to the p52:Bcl3 mediated gene expression. To further establish the significance of the central bp in NF-κB dimer recruitment, we tested two of the well characterized κB sites, HIV and MHC-κB sites. It is known the HIV-κB site is strongly activated by the p50/RelA heterodimer and RelA homodimer; and the MHC-κB site is regulated by the p50 homodimer. As shown in Figure 2.6b, RelA activates wt HIV-κB site (A/T) but not the mutated G/C-centric HIV-κB site. And the p52: Bcl3 complex showed the opposite trend in the promoter activity. Similar effects were

observed on the MHC-κB site (Figure 2.6a). We further found that p50:Bcl3 complex activate the G/C-centric P-Selectin κB site to a lesser degree than p52:Bcl3 complex suggesting that transcriptional activation specificity of G/C-centric κB sites are tied to the p52:Bcl3 complex (Figure 2.7).

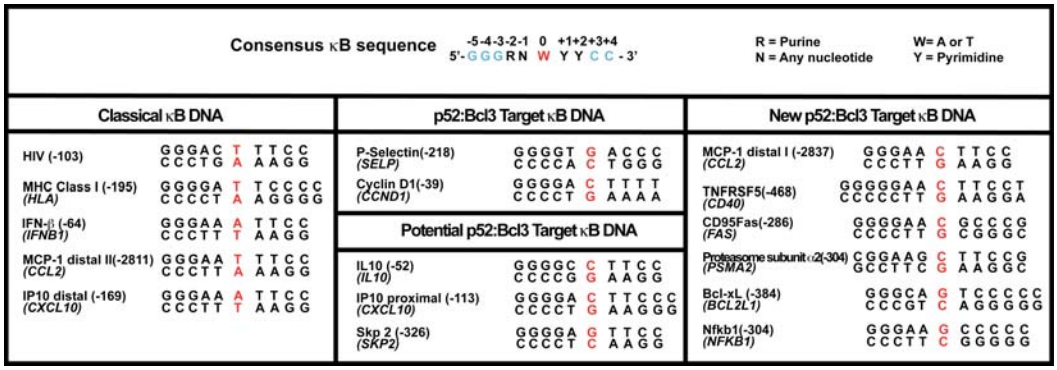

Figure 2.2 Sequences of κB DNAs. Left column, classical κB DNAs with A/T central base pair; middle column, p52:Bcl3 target κB DNAs with G/C central base pair; right column, newly identified κB DNAs with G/C central base pairs.

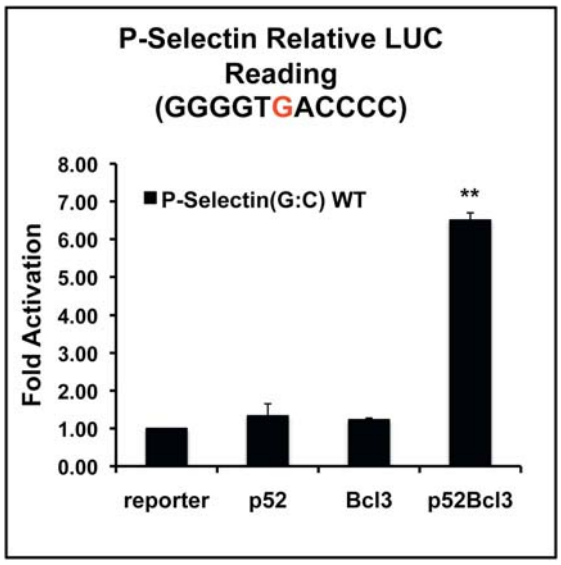

Figure 2.3 p52:Bcl3 complex activates P-Selectin luciferase reporter. Either p52 or Bcl3 alone did not activated P-Selectin reporter in HeLa cells. Co-expression of p52 and Bcl3 strongly activated P-Selectin reporter. **p < 0.01 versus reporter only control. Error bars represent standard deviation (SD).

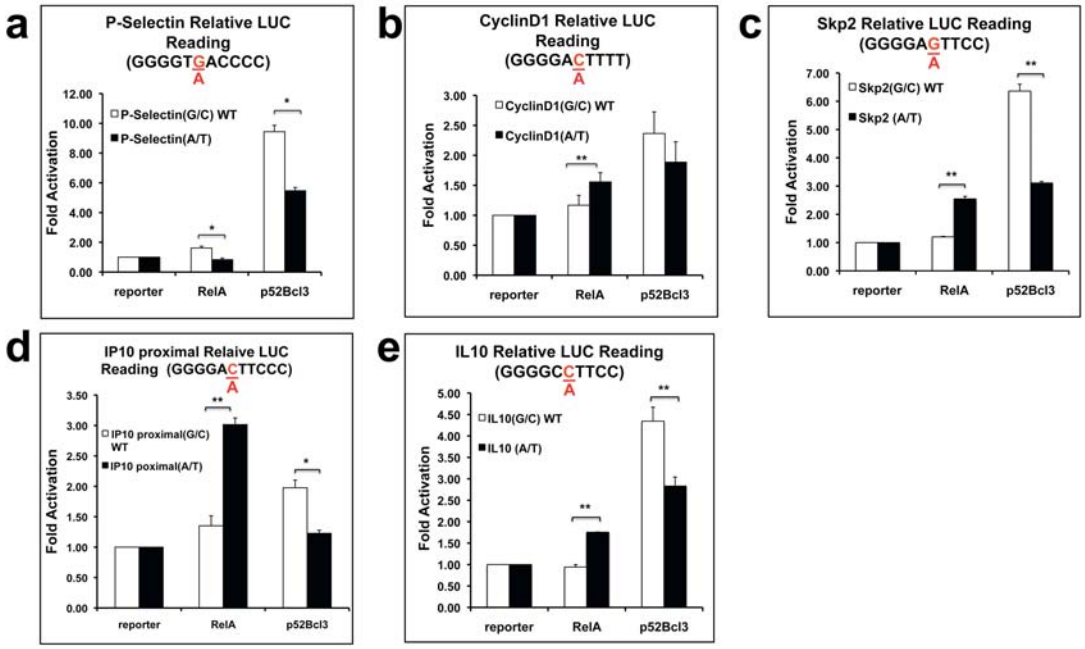

Figure 2.4 p52:Bcl3 complex activates reporters with G/C-centric κB sites. a) P-Selectin, b) Cyclin D1, c) Skp2, d) IP-10, and e) IL-10 wt luciferase reporters with G/C-centric κB sites were activates by p52:Bcl3 complex, but not RelA. A/T mutant reporters decreased p52:Bcl3 activities and switched the activity toward RelA. *$p < 0.05$, **$p < 0.01$. Error bars represent SD.

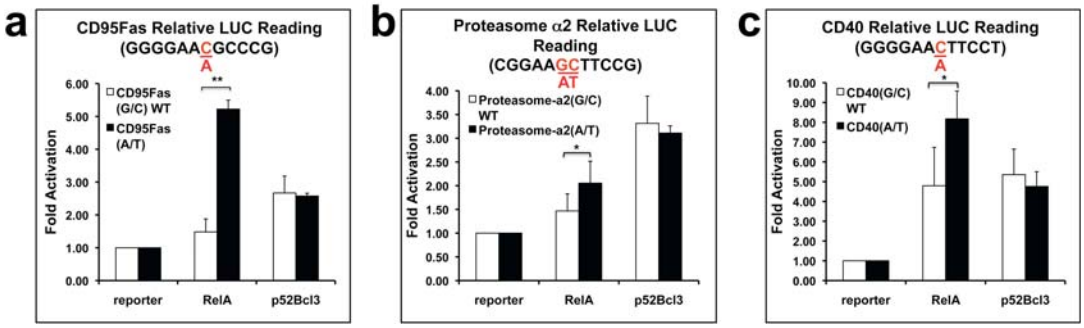

Figure 2.5 p52:Bcl3 complex activates reporters with newly identified G/C-centric κB sites. a) CD95Fas, b) Proteasome subunit α2, and c) CD40 wt luciferase reporters with G/C-centric κB sites were activates by p52:Bcl3 complex, but not RelA. A/T mutant reporters switched the activity toward RelA. *p < 0.05, **p < 0.01. Error bars represent SD.

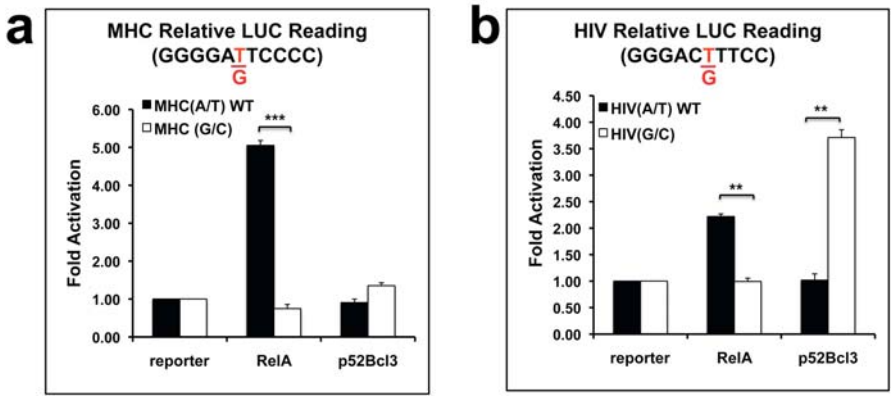

Figure 2.6 Single nucleotide change can switch classical RelA κB DNA to p52:Bcl3 targeted κB DNA. a) MHC and b) HIV wt luciferase reporters with A/T-centric κB sites were activates by RelA. G/C mutant reporters abolished RelA activity, and HIV G/C reporter was activated by p52:Bcl3. **p < 0.01, ***p < 0.001. Error bars represent SD.

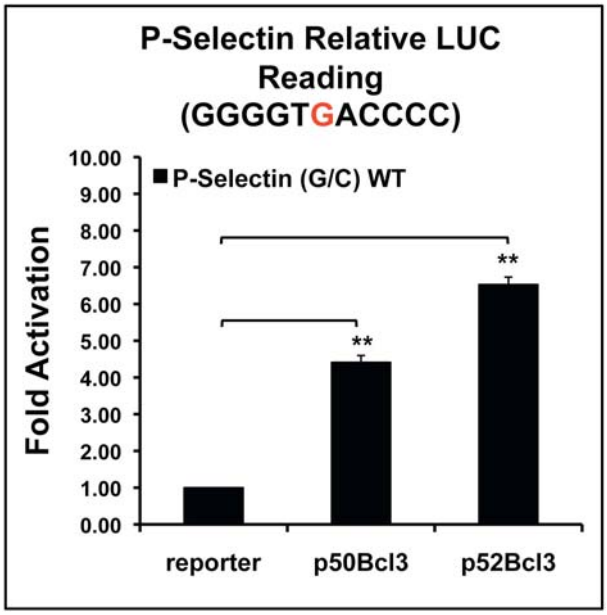

Figure 2.7 p50:Bcl3 activates P-Selectin reporter to a less degree than p52:Bcl3. **p < 0.01 versus reporter only control. Error bars represent SD.

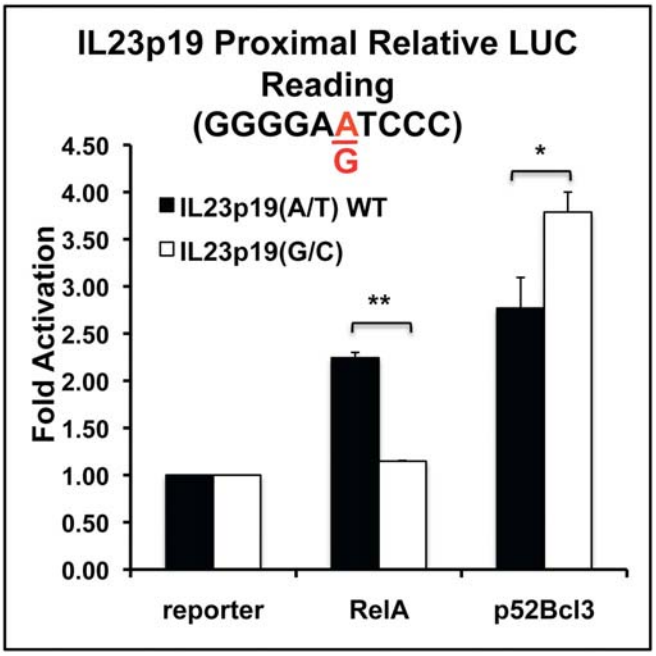

Figure 2.8 G/C mutant switches the IL23p19 proximal κB reporter activity from RelA to p52:Bcl3. *p < 0.05, **p < 0.01. Error bars represent SD.

2. The p52:Bcl3 Complex is Recruited to Both G/C- and A/T-centric κB Sites upon LPS Stimulation

To further investigate if the target gene promoters are similarly regulated in the endogenous context as depicted in the transfection system, we used RAW 264.7 macrophage cell line as a model system. This cell line has been extensively investigated for its LPS responsive gene regulation program by NF-κB (Lee et al., 2006; Ogawa et al., 2005; Wessells et al., 2004). It is also known that both p52 and Bcl3 are activated by LPS in macrophages. Indeed, we also found nuclear accumulation of Bcl3 and p52 at around 8 to 12 hours upon LPS stimulation (Figure 2.9). In contrast, peak of nuclear RelA accumulation is at 1 to 2 hours and at 12 hours RelA levels were significantly diminished. Chromatin immunoprecipitation (ChIP) revealed that both p52 and Bcl3 were bound to IL-10, IP-10, MCP-1, and Skp2 promoters at 12 hours of LPS induction; however, no RelA recruitment was observed at this time point (Figure 2.10a-d). In contrast, RelA bound to IP-10 and MCP-1 promoters at 2 hours. NF-κB dimer binding pattern is consistent with the promoter architecture of these genes. IL-10 and Skp2 do not contain an A/T-centric κB site in their promoters. IP-10 and MCP-1 contain two non-identical κB sites with one A/T- and one G/C-centric. And the A/T-centric IP-10-κB site results in RelA recruitment at early time of LPS stimulation; the other G/C-centric κB site results in the p52:Bcl3 recruitment at late time of stimulation. Using luciferase reporter assay, we showed the A/T-centric, but not the G/C-

centric IP-10 κB site is activated by RelA homodimer (Figure 2.12). IL-10 is a proinflammatory cytokine, which is known to repress transcription of the p19 subunit of anti-inflammatory cytokine IL-23. It has been speculated that IL-23p19 transcription is inhibited by p50 and Bcl3. To test if the p19 promoter is bound by p52 and Bcl3, we carried out ChIP assay. Our result clearly showed that both p52 and Bcl3 occupied the IL-23p19 promoter at 12 hours upon LPS stimulation (Figure 2.10e).

We next tested if the kinetics of gene expression correlates with the recruitment of the NF-κB complexes (Figure 2.10). Consistent with previous reports, RT-qPCR assay revealed that all tested genes are expressed in RAW 264.7 cells upon LPS stimulation with the exception of IL-23p19 and Skp2. However, the kinetics of expression are different for different genes. Upon LPS stimulation, IP-10 mRNA level showed prolonged induction from 2 to 12 hours with peak at 2 hours, suggesting a continuous transcription from early to late time of induction. The early massive IP-10 induction is probably due to its RelA recruitment whereas the late induction results from the p52:Bcl3 recruitment. MCP-1 showed an opposite pattern. MCP-1 mRNA expression level at early time (2 hours) was low compared to the enhanced expression level at late time (8 to 12 hours). IL-10 mRNA expression level followed the similar pattern with highest levels at 8 to 12 hours. We also found that the expression of IL-23p19 was completely blocked during the entire course of LPS stimulation even though ChIP assay showed the recruitment of both p52

and Bcl3 at IL-23p19 promoter. Promoter search revealed that IL-23p19 contains two A/T-centric κB sites, but no G/C-centric κB site. To further confirm the endogenous promoter binding and gene expression, we carried out IL-23p19 reporter assay. Changing the IL-23p19 proximal G/C-centric κB reporter to A/T-centric κB site increased p52:Bcl3 activity (Figure 2.8).

Therefore, there is a positive correlation between the gene expression pattern and promoter occupancy of different NF-κB dimers. Our results also suggest that in the early times RelA activates these genes upon binding to the A/T-centric κB DNA targets and at late times the p52:Bcl3 complex takes over and continue activation by engaging the G/C-centric κB sites. The levels of mRNA rely both on synthesis and degradation rates. Some of the genes mRNAs are very stable whereas others are unstable. To test if the levels of IP-10 at late times can be accounted from its half-life, we measured its half-life. As reported by the Baltimore group (Hao and Baltimore, 2009), we also found the half-life IP-10 mRNA upon LPS stimulation is ~2 hours (Figure 2.11). Based on this, calculated that levels of IP-10 mRNA at 12 hours require more synthesis at late times. MCP-1 mRNA half-life on the other hand is transient at late induction. This suggests that promoter must be active for the late transcription. Taken together, these results prompted us to propose an intriguing hypothesis which is that the co-occupancy of p52 and Bcl3 to A/T-centric κB sites results in repression of transcription whereas the activate

transcription by binding to G/C-centric κB sites. This is consistent with the repression role of p52 as demonstrated previously.

Although, p52 and Bcl3 bound to Skp2 promoter and RNA Pol II was also recruited to the transcription initiation site, suggesting that the promoter is active, Skp2 mRNA level was immeasurable. The extremely low Skp2 mRNA level might be due to extreme sensitivity of mRNA or due to a defect in the transcriptional elongation step. Since macrophage cells are terminally differentiated, mRNA level of Skp2, a cell cycle regulator, might undergo rapid degradation.

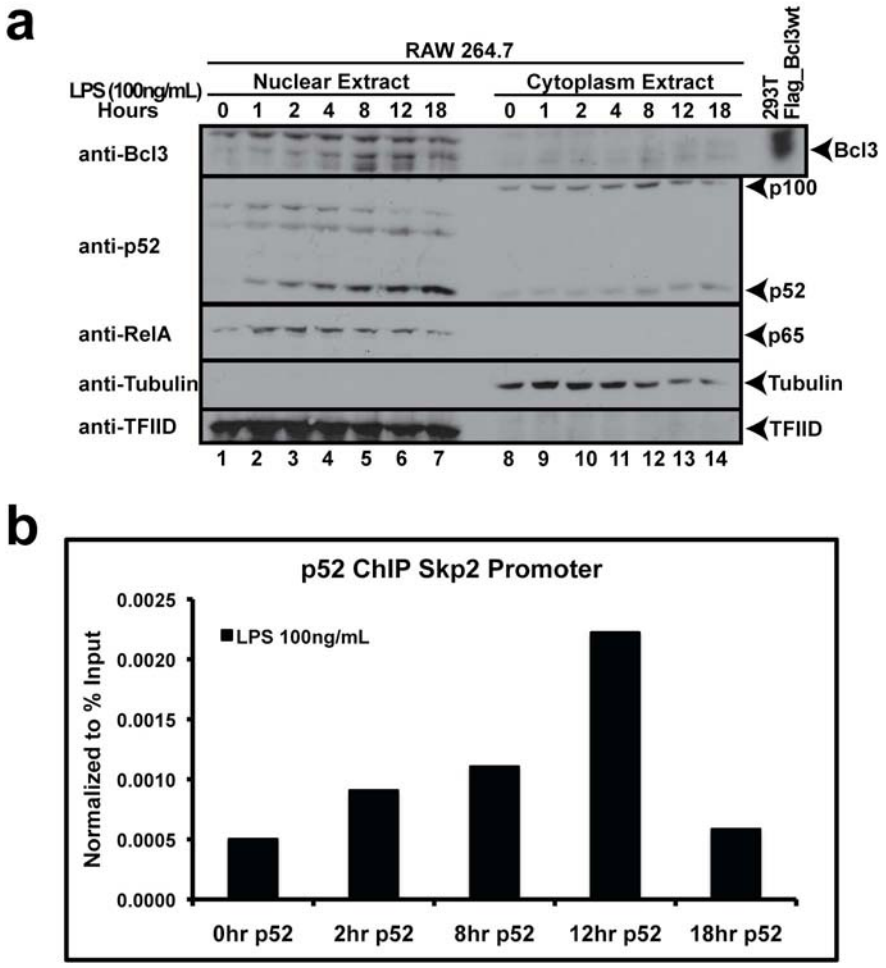

Figure 2.9 p52 and Bcl3 activation by LPS stimulation in RAW 264.7 cells. a) nuclear and cytoplasmic extracts of RAW 264.7 cells upon LPS stimulation showing RelA accumulated into the nucleus upon 1 to 2 hours of LPS stimulation; Bcl3 and p52 accumulated into the nucleus at later time points, peaked at 8 to 12 hours of LPS stimulation. b) ChIP assay for p52 in RAW 264.7 cells treated with LPS for the indicated time.

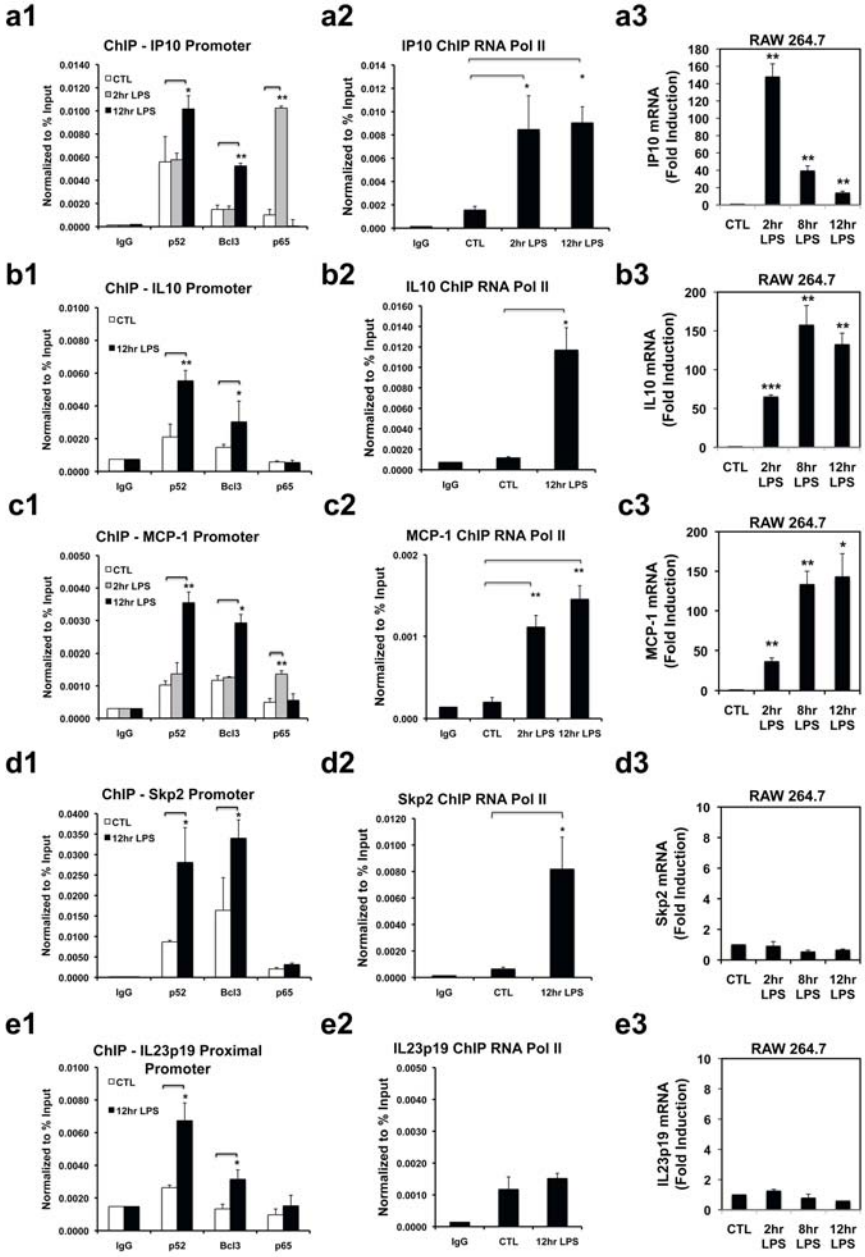

Figure 2.10 p52 and Bcl3 binding to endogenous promoters and the gene activation in RAW 264.7 cells upon LPS stimulation. Column 1, ChIP assays for p52, Bcl3, and RelA in RAW 264.7 cells treated with LPS for the indicated time. Column 2, ChIP assays for RNA Pol II in RAW 264.7 cells treated with LPS for the indicated time. *$p < 0.05$, **$p < 0.01$. Column 3, gene expressions by LPS stimulation in RAW 264.7 for the indicated time. **$p < 0.01$, ***$p < 0.001$ versus nontreated controls. Error bars represent SD.

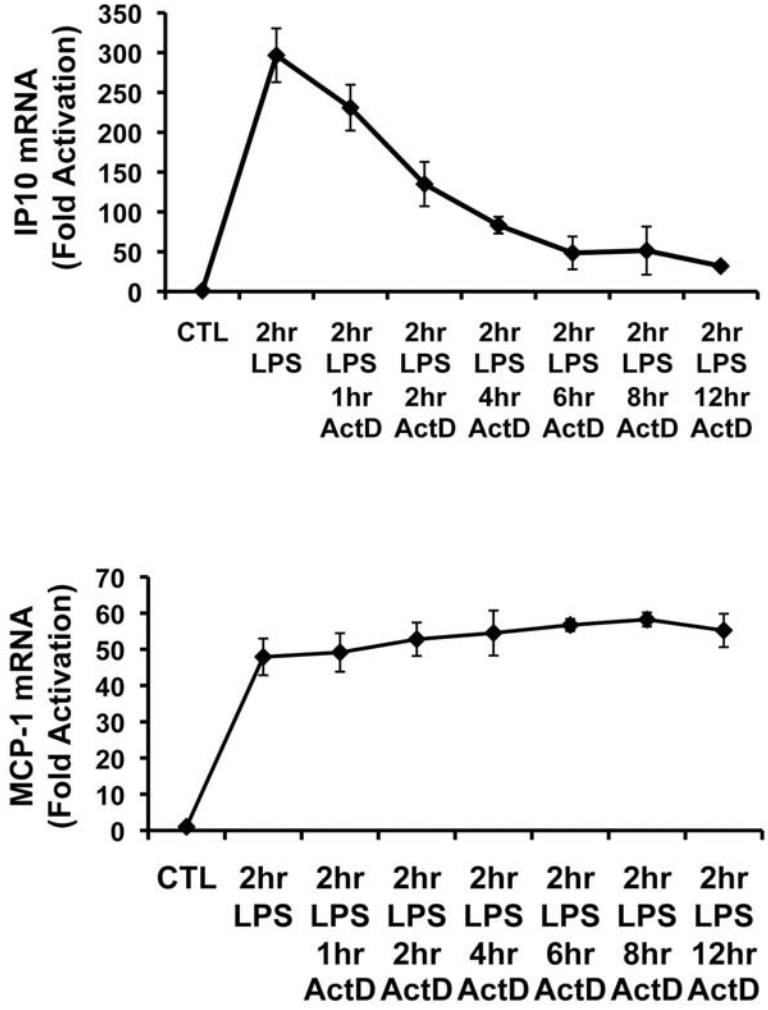

Figure 2.11 Stability of IP10 and MCP-1 mRNA. Quantitative RT-qPCR analysis of mRNA transcripts upon 2 hours of LPS stimulation followed by the addition of actinomycin D (ActD) for indicated time to RAW 264.7 cells, normalized to results obtained for GAPDH and presented relative to the baseline value measured before LPS stimulation. $p < 0.01$ versus nontreated controls. Error bars represent SD of three independent experiments.

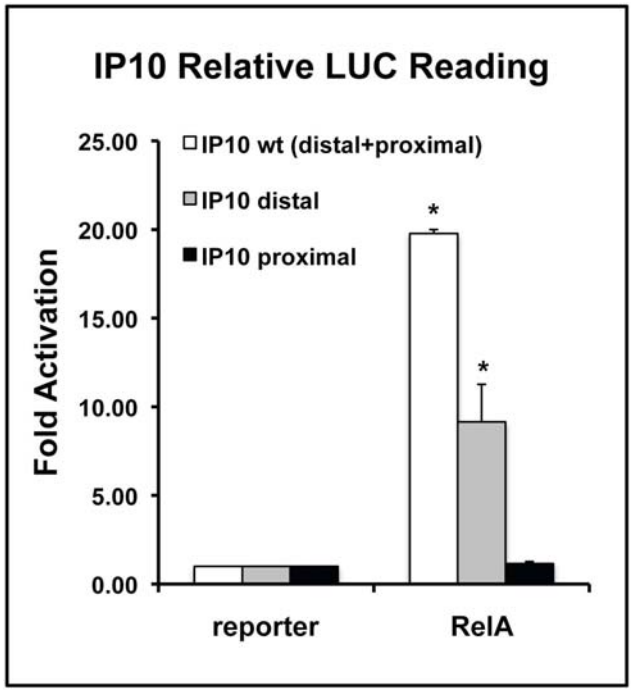

Figure 2.12 RelA activity on IP-10 κB luciferase reporter. The distal IP-10 κB site was activated by RelA. *p < 0.05 versus reporter only control. Error bars represent SD.

3. Bcl3 is Essential for p52 Homodimer-mediated Transcriptional Regulation

To further confirm the role of the p52:Bcl3 complex both in gene activation and repression, we carried out Bcl3 knockdown experiments in BMDM using siRNA against Bcl3 and tested the how it affect gene expression. We first tested if the genes tested above follow a similar trend in expression in wt BMDM cells. We found that all of the NF-κB target genes expressed in RAW 264.7 cells also expressed in BMDM although amplitude and kinetics differed (Figure 2.14). For instance, Bcl3 mRNA levels were highest at 8 hours and most target genes showed highest levels at 8 hours in BMDM instead of 12 hours in RAW 264.7 cells upon LPS stimulation. We were able to obtain ~70% knockdown of Bcl3 mRNA by siBcl3 (Figure 2.13). mRNA levels of target genes tested above were measured both in control siCTL (mouse scrambled siRNA) and siBcl3 treated cells. We found that all target genes responded to Bcl3 knockdown compared to the control knockdown: levels of some genes enhanced whereas others were repressed. IL-10 and MCP-1 mRNA levels increased whereas IP-10, CD40, CD95Fas and NF-κB2/p100 levels were enhanced (Figure 2.14). Indeed, expression of most genes was enhanced suggesting a dominant repression function of Bcl3. These results strongly suggest that the p52:Bcl3 complex not only activates gene transcription by binding to the G/C-centric κB sites of a promoter, it also represses the A/T-centric κB site of the same promoter and thereby controls

the levels of mRNA. It might even have a role in repressing genes that contain only A/T-centric κB site. Profoundly high level of IP-10 mRNA in Bcl3 knockdown cells may suggest that the repression function the p52:Bcl3 complex from the A/T-centric κB site is dominant over it its activation function from the G/C-centric κB site. Activity of this complex for the MCP-1 promoter might just be opposite.

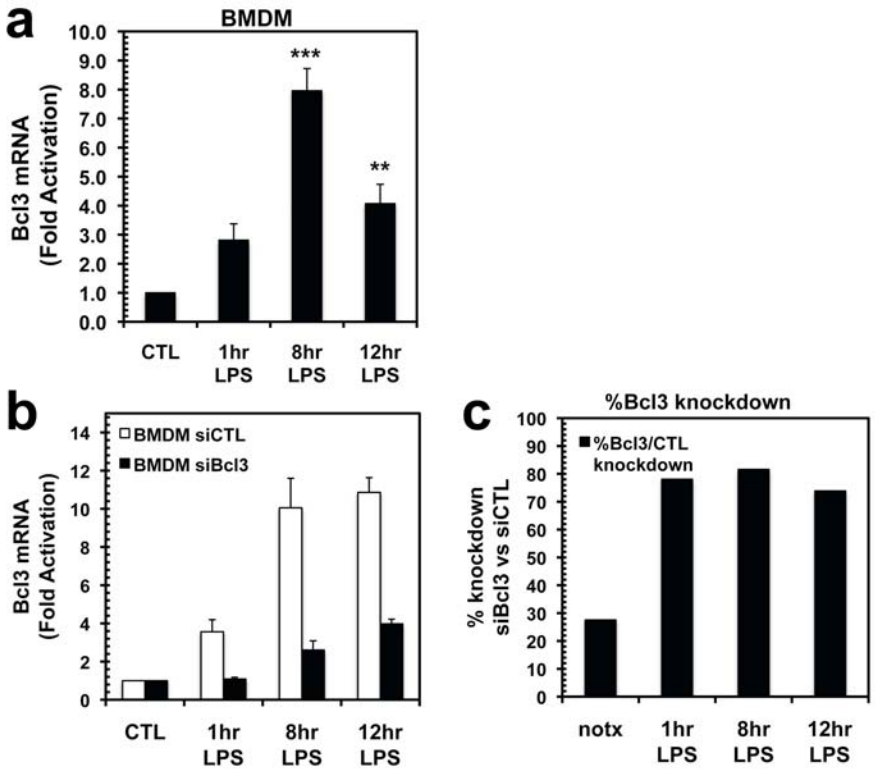

Figure 2.13 Bcl3 mRNA levels in primary macrophages. a) Bcl3 mRNA expressions in wt BMDM upon LPS stimulation. b) Bcl3 mRNA levels upon LPS stimulation in BMDM transfected with siRNA against Bcl3 vs scramble control siRNA. c) Bcl3 knockdown efficiency compared to control siRNA. **$p < 0.01$, ***$p < 0.001$ versus nontreated control. Error bars represent SD.

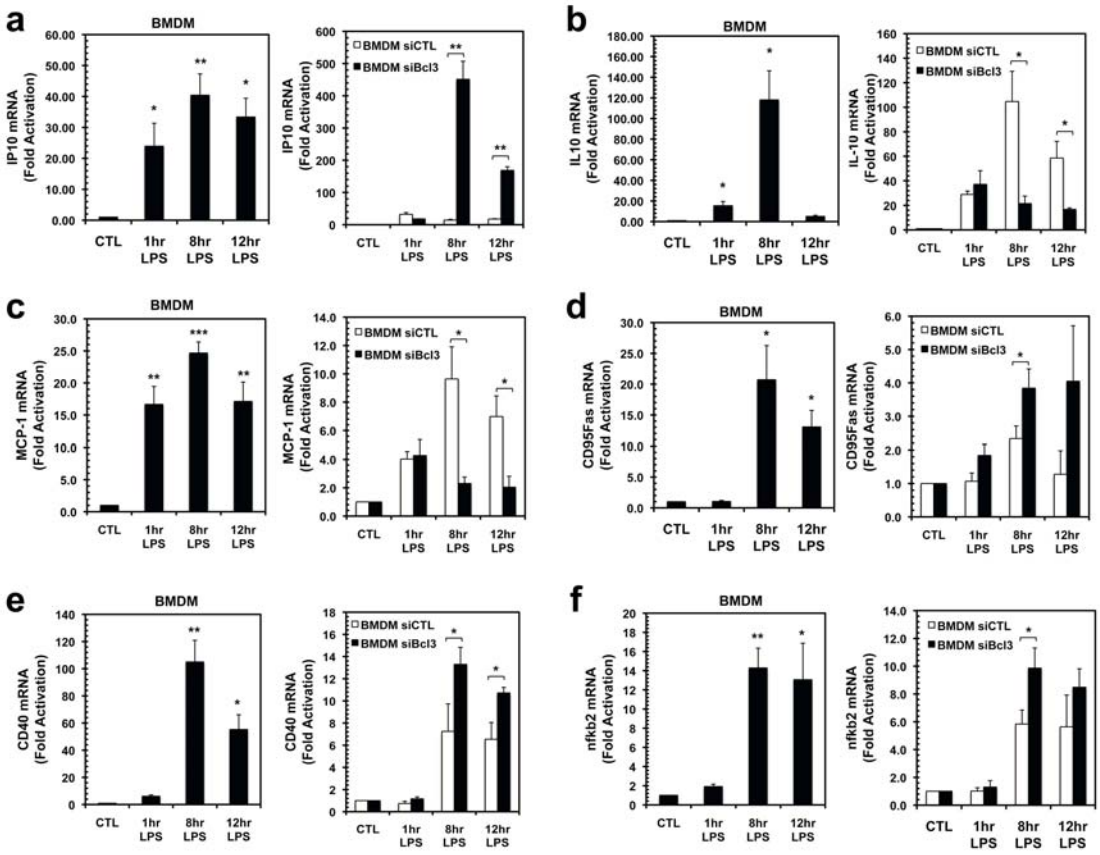

Figure 2.14 Bcl3 is essential for target gene expressions. Target gene mRNA levels upon LPS stimulation in wt BMDM (left) and Bcl3 knockdown compared to control siRNA (right). a) IP10, b) IL-10, c) MCP-1, d) CD95Fas, e) CD40, and f) nfkb2/p100. *$p < 0.05$, **$p < 0.01$, ***$p < 0.001$ versus nontreated control or as indicated. Error bars represent SD.

4. NF-κB Dimers Bind to G/C and A/T-centric κB DNAs with Different Affinities

To determine if p52 and/or p52:Bcl3 bind the G/C-centric κB sites with higher affinity than the A/T-centric κB sites, we have carried out EMSA experiments. To our surprise we found that p52 homodimer bound to A/T-centric κB sites with higher affinity than the G/C-centric sites. To test if Bcl3 reverses this effect, we examined ternary complex formation on the G/C- and A/T-centric sites. We used both Bcl3-transfected nuclear extracts or affinity purified Flag-tagged Bcl3 from HEK 293T cells and tested the binding of the p52:Bcl3 complex to four wt (G/C) and corresponding mutant (A/T) κB sites; P-selectin, Skp2, IP10-proximal, Cyclin D1, and IL-10 (Figure 2.15-2.19). We also tested three wt (A/T) and the corresponding mutant (G/C) κB sites; HIV, IL23p19, and MHC (Figure 2.20-2.22). Contrary to our expectation we found that with increasing concentration of Bcl3, the p52:(G/C)-centric κB DNA complex disappeared with no visible ternary complex in the gel. This behavior is a reminiscent of IκBα-mediated inhibition of DNA binding by RelA or p50/RelA heterodimer. It has been showed recently that IκBα actively dissociate RelA: κB DNA complex forming the IκBα:RelA complex liberating free DNA. In our case, however, we found no enhancement of free P-selectin κB probe with increasing amount of Bcl3 suggesting lack of dissociation of the p52/DNA complex (Figure 2.15a light exposure, lane 22-25). Antibody super-shift identified distinct slow mobility complexes in the presence of antibodies

against both anti-Bcl3 and anti-p52 (Figure 2.15a. Anti-Bcl3 super-shifted band is indicated by (*) in Figure 2.15a, lane 32, 35, and 38; this Bcl3 super-shifted band is absent when mock HEK 293T cells NE were used, lane 41 and 44). This suggested that although no ternary complex was visible in the gel, both proteins were bound to the probe simultaneously. In contrast, association between A/T-centric κB DNA with p52 and Bcl3 was detected clearly as a distinct slow mobility complex (Figure 2.15b). Presence of both proteins in the complex was confirmed by antibody super-shift. We also noted that CyclinD1 κB site was the only exception where both G/C- and A/T-centric probes revealed similar behavior with no visible ternary complex in the gel (Figure 2.18). However, in both cases antibody super-shift confirmed the presence of both proteins. CyclinD1-κB site differs significantly from most other κB sites. The presence of one T-riched half site in CyclinD1-κB DNA, therefore, is likely to influence the p52:Bcl3: κB DNA complex stability. The overall binding affinity was very low in case of IL-10-κB DNA; however, it followed the same trend as the other κB DNAs have been tested (Figure 2.19). Also, mutating the wt (A/T) to the corresponding (G/C) κB sites of HIV, IL23p19, and MHC showed the same results as expected (Figure 2.20-2.22). In all, these experiments suggest that the p52:Bcl3 complex binds to two distinct classes of κB sites with distinct consequences. Perhaps, the conformational differences and/or the kinetic stability of the p52:Bcl3:κB DNA complex recruits distinct

cofactors to the promoters, such as a co-repressor to the A/T-centric sites and a co-activator to the G/C-centric sites.

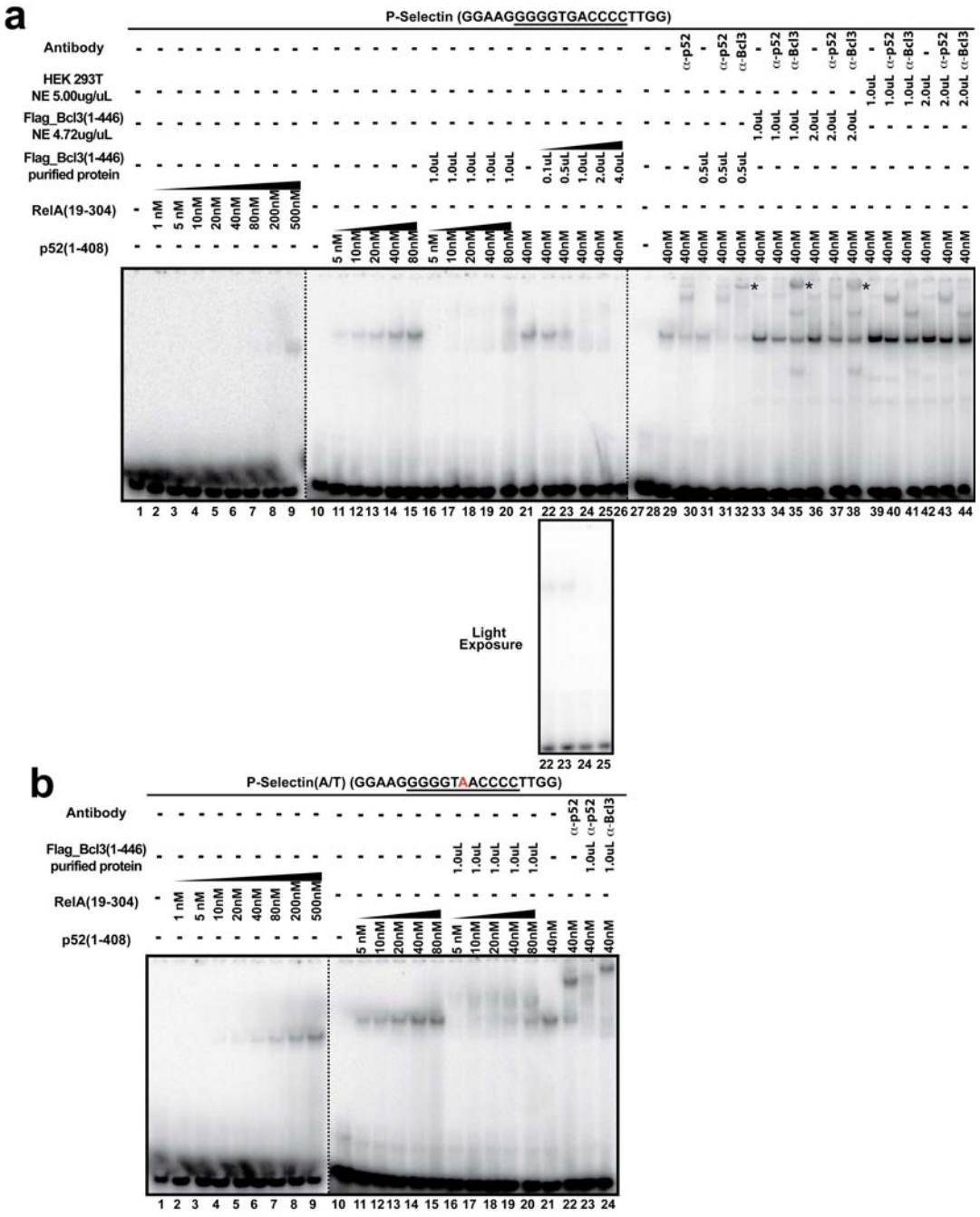

Figure 2.15 EMSA of p52, Bcl3, and RelA on P-Selectin κB DNAs. a) Recombinant p52, RelA, Flag-tagged Bcl3 protein and Bcl3 NE binding to wt (G/C)-centric P-Selectin κB DNA. (*) indicated the super-shifted band of p52:Bcl3/DNA ternary complex. b) Recombinant p52, RelA, Flag-tagged Bcl3 protein binding to mutant (A/T)-centric P-Selectin κB DNA.

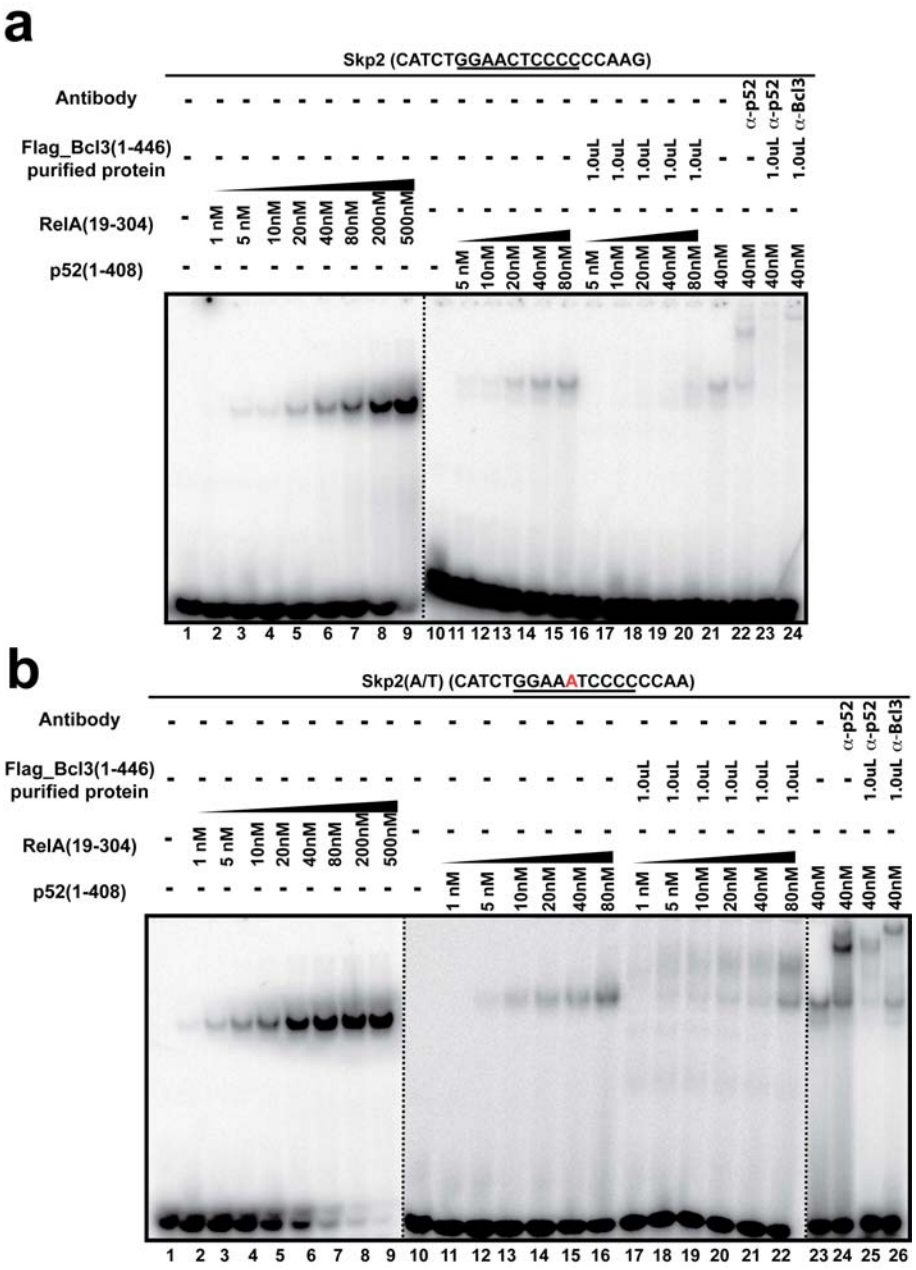

Figure 2.16 EMSA of p52, Bcl3, and RelA on Skp2 κB DNAs. Recombinant p52, RelA, Flag-tagged Bcl3 protein binding to a) wt (G/C)-centric, b) mutant (A/T)-centric Skp2 κB DNA.

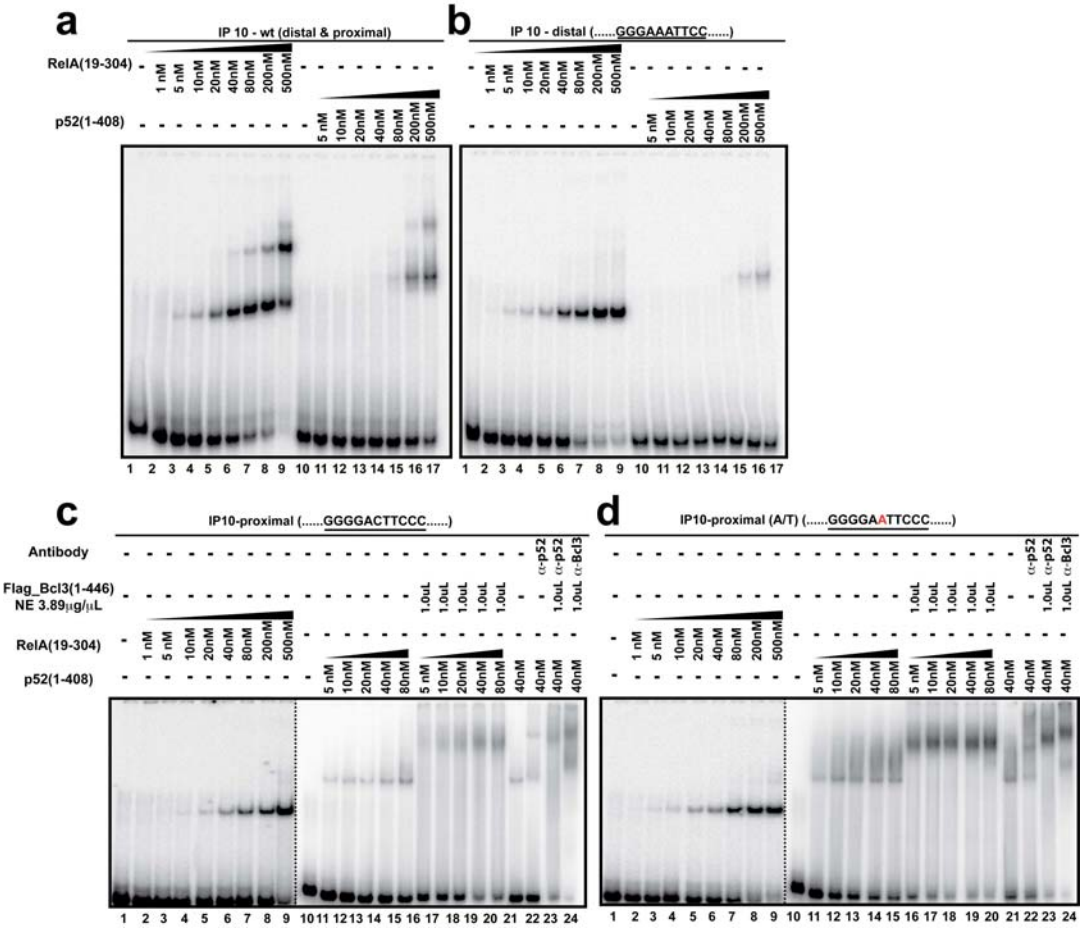

Figure 2.17 EMSA of p52, Bcl3, and RelA on IP-10 κB DNAs. Recombinant p52, RelA binding to a) wt IP-10 (distal + proximal), b) distal κB DNA. Recombinant p52, RelA, Flag-tagged Bcl3 NE c) (G/C)-centric, d) mutant (A/T)-centric proximal IP-10 κB DNA.

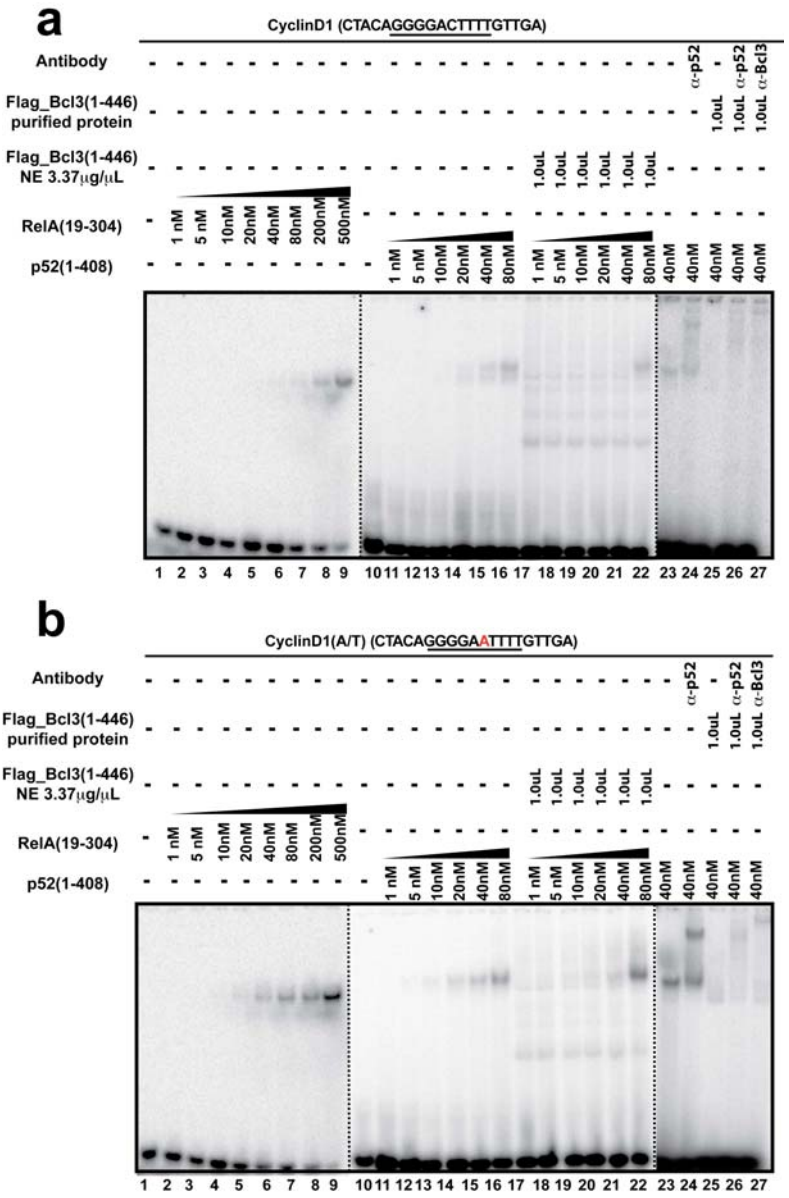

Figure 2.18 EMSA of p52, Bcl3, and RelA on Cyclin D1 κB DNAs. Recombinant p52, RelA, Flag-tagged Bcl3 protein and Bcl3 NE binding to a) wt (G/C)-centric, b) mutant (A/T)-centric Cyclin D1 κB DNA.

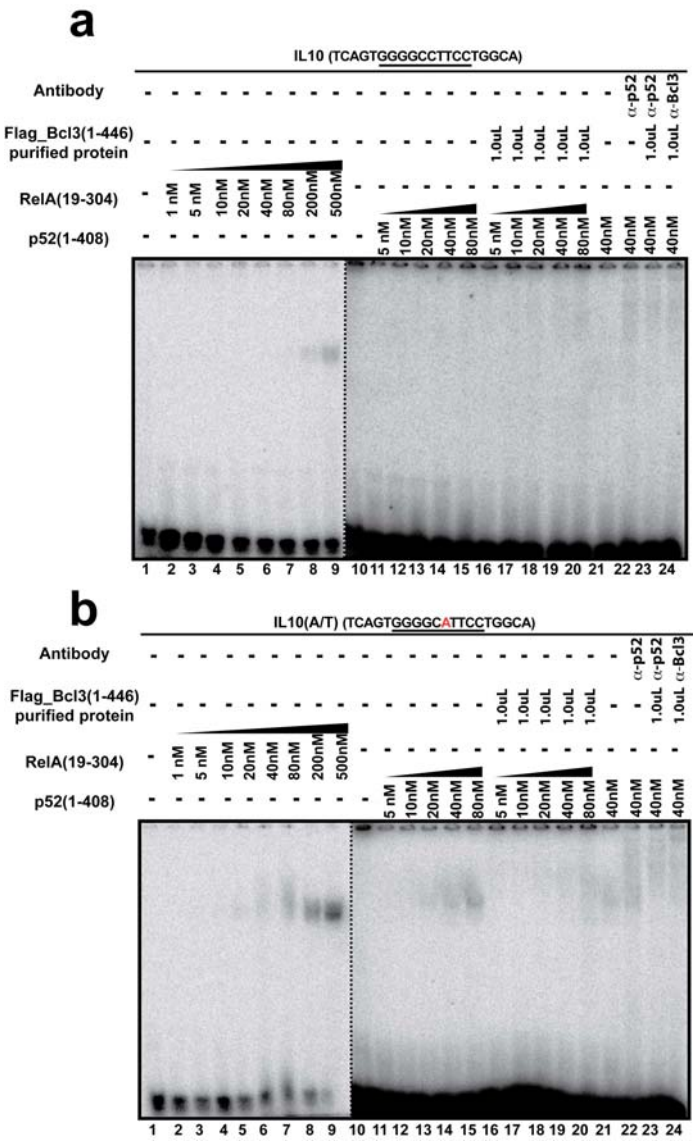

Figure 2.19 EMSA of p52, Bcl3, and RelA on IL-10 κB DNAs. Recombinant p52, RelA, Flag-tagged Bcl3 protein binding to a) wt (G/C)-centric, b) mutant (A/T)-centric IL-10 κB DNA.

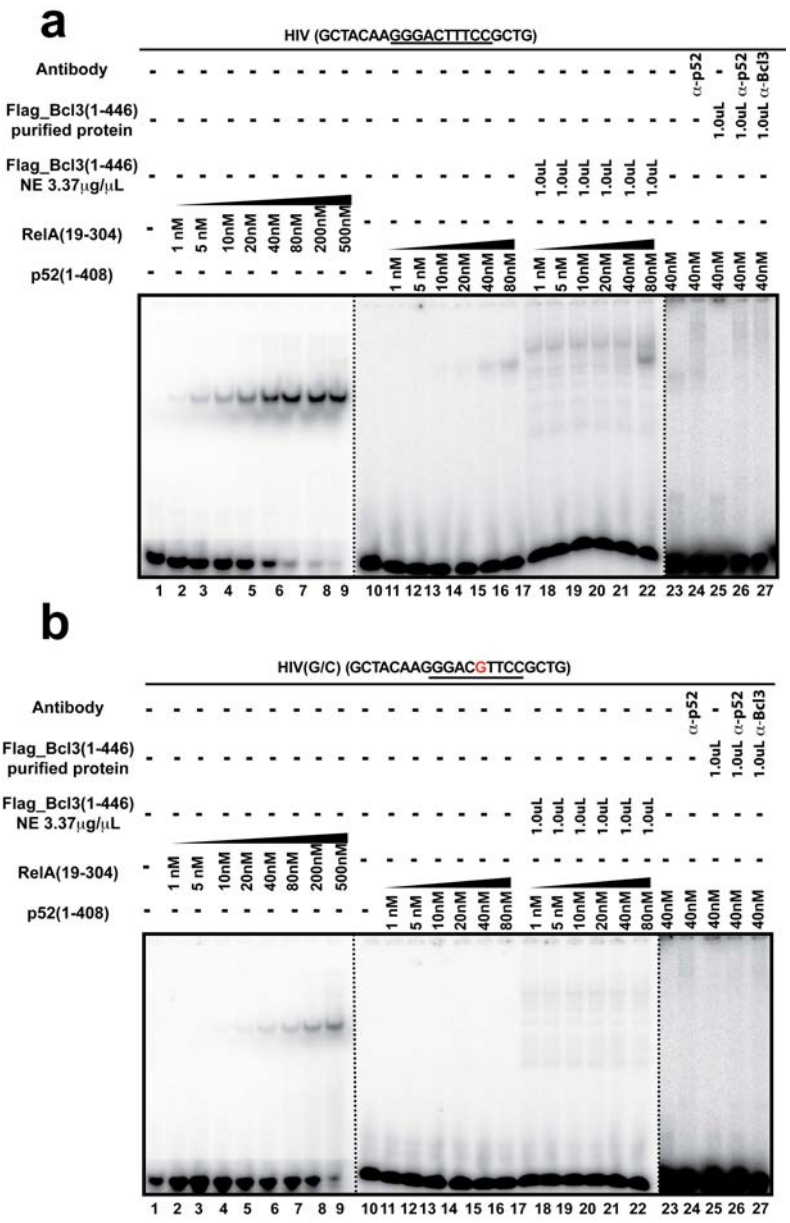

Figure 2.20 EMSA of p52, Bcl3, and RelA on HIV κB DNAs. Recombinant p52, RelA, Flag-tagged Bcl3 protein and Bcl3 NE binding to a) wt (A/T)-centric, b) mutant (G/C)-centric HIV κB DNA.

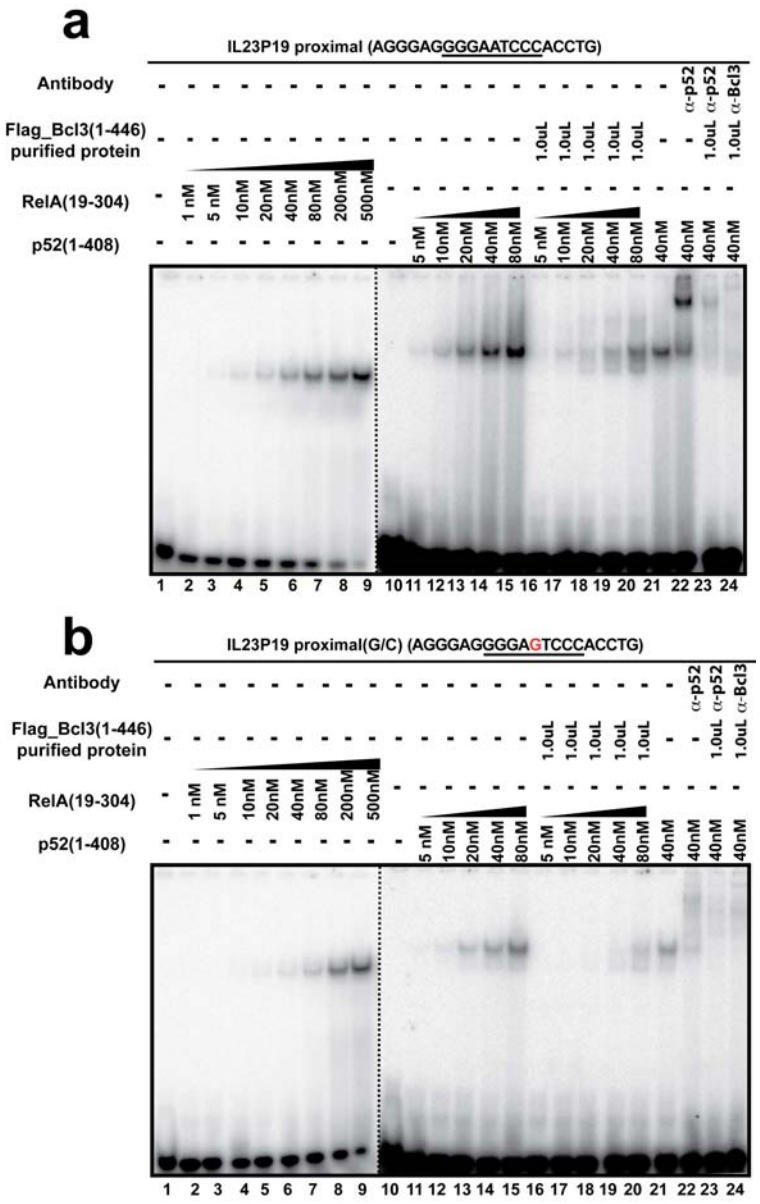

Figure 2.21 EMSA of p52, Bcl3, and RelA on IL23p19 proximal κB DNAs. Recombinant p52, RelA, Flag-tagged Bcl3 protein binding to a) wt (A/T)-centric, b) mutant (G/C)-centric IL23p19 proximal κB DNA.

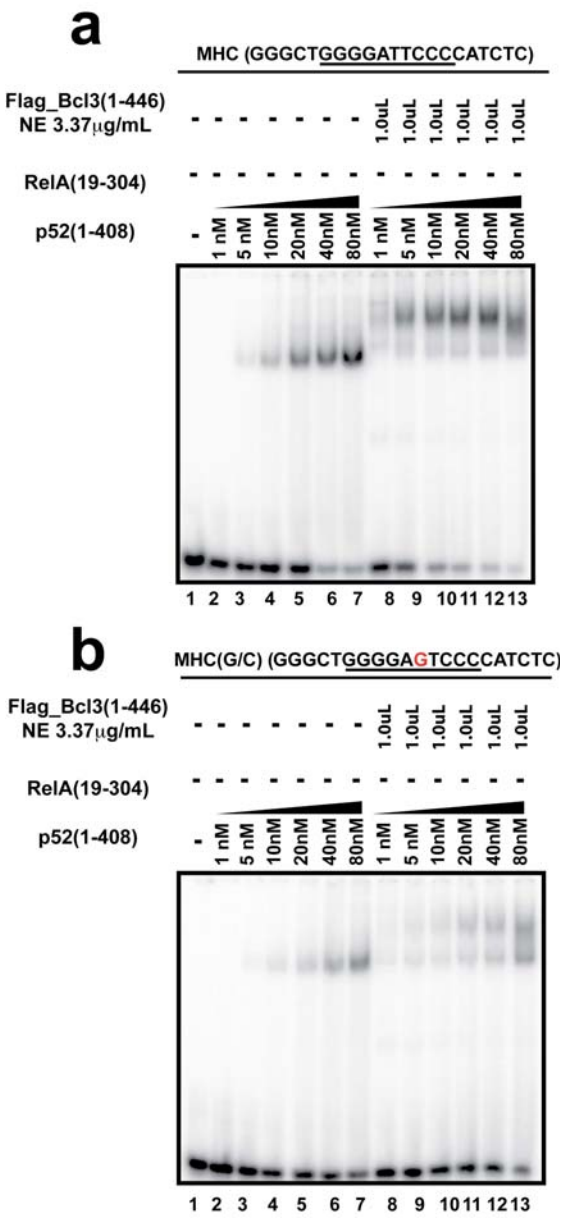

Figure 2.22 EMSA of p52, Bcl3, and RelA on MHC κB DNAs. Recombinant p52 and Flag-tagged Bcl3 NE binding to a) wt (A/T)-centric, b) mutant (G/C)-centric MHC κB DNA.

D. Discussion

This study show how the transcriptional activity of NF-κB dimers is linked to the target κB DNA sequences. We showed RelA (as either a homodimer or heterodimer with p50) binds strongly and activate κB sites with A/T bp but not with G/C bp in the central position. Therefore, genes with G/C-centric κB site(s) in their promoters, such as Skp2, Cyclin D1 cannot be activated by RelA. The p52:Bcl3 complex performs more complex functions; it is capable of binding to κB sites with both G/C and A/T bps at their central position. However, it only activates the G/C-centric κB sites. Our results give a hint of how the p52:Bcl3 complex coordinate biological programs such as the control of cell cycle and inflammation. Through highly selective regulation of the G/C-centric κB sites within the promoters of Skp2 and Cyclin D1, p52:Bcl3 complex regulates cell cycle progression (Massoumi et al., 2006). Results in this study explains how this p52:Bcl3 complex can control cell cycle by binding and activating genes with G/C-centric κB DNA sequences in the promoters. This complex also controls inflammation by activating a class of anti-inflammatory cytokines such as IL-10 through binding to their G/C-centric κB sites; and at the same time it represses pro-inflammatory cytokines such as IL-23, IL-6, IL-8 by binding to their A/T-centric κB sites. The p52:Bcl3 complex also tamper inflammation by restructuring effector genes that would undergo uncontrolled expression. Our result can explain severity lack of immunological tolerance in nfκb2$^{-/-}$/bcl3$^{-/-}$ double knockout mice where an entire program is

affected due to impair regulation of a large set of genes. Our study also suggests that small variations of nucleotide sequences within a κB DNA severely compromise binding of certain NF-κB dimers and allow other dimers with a distinct conformation. This ‘new look’ complex now could recruit a different set of transcriptional complex. In sum, our study thus links a single bp switch in the κB DNA response element to the proper functioning of the two oncogenic proteins, p52 and Bcl3.

E. Chapter II Acknowledgements

I would like to thank member of my committee, Dr. Christopher Glass, for providing me with RAW 264.7 cells and the primary macrophages. And also his lab members, Dr. Wendy Huang, Dr. Nathan Spann, and Jesse Fox, for helping me with the RNAi, ChIP and mRNA-RTqPCR experiments.

Chapter II is currently being prepared for submission for publication. Wang, Vivien Y.; and Ghosh, Gourisankar. “The central base pair of κB DNA sequences is a key regulator of the NF-κB dimer transcriptional specificity”. The dissertation author was the primary investigator and author of this paper.

Chapter III: Maturity of the p100:NF-κB Complex Determines p100 Processing vs. Complete Degradation in Response to Non-Canonical Signaling

A. Introduction

The dimeric NF-κB transcription factors are critical mediators of a diverse array of physiological processes through transcriptional regulation of hundreds of target genes. Inhibitor IκB proteins ensure appropriate NF-κB activation in stimulus- and cell-specific manners. Two proteins, p105 (NF-κB1) and p100 (NF-κB2) reside at the interface of both NF-κB and IκB activities by virtue of having both NF-κB and IκB domains (Ghosh and Hayden, 2008; Sun and Ley, 2008). p100 and p105 are processed into NF-κB p52 and p50, respectively. Processing is carried out by the proteasome, which completely degrades the C-terminal IκB region. Unlike constitutive processing of p105, p100 undergoes inducible processing (Ghosh and Karin, 2002). NF-κB inhibitory activity of unprocessed p100, which is referred to as IκBδ, has been demonstrated to be critical in different cellular settings (Basak et al., 2007; Ishikawa et al., 1997; Ishikawa et al., 1998; Novack et al., 2003). Lack of IκBδ activity in osteoclast progenitor cells blocks osteoclast differentiation whereas p100 deficiency sensitizes differentiation. Similarly, cells devoid of p100 is defective in terminating pathogen-triggered NF-κB responses generated through sustained TLR (Shih et al., 2009). TCR stimulated expression of p100 through canonical pathway dampens NF-κB responses and IL-2 production in T cells (Legarda-Addison and Ting, 2007). All together these observations suggest that like IκBα, IκBδ functions both pre- and post-stimulations.

The processing of p100 into p52 is induced by a distinct class of stimuli such as LTβ, BAFF and CD40; and this NF-κB activation pathway is known as the non-canonical signaling pathway (Xiao et al., 2001; Senftleben et al., 2001). The predominant NF-κB dimer that is activated from these stimuli is the p52/RelB heterodimer (Bonizzi et al., 2004; Claudio et al., 2002; Coope et al., 2002; Dejardin et al., 2002; Senftleben et al., 2001). The non-canonical NF-κB signaling pathway induces p100 processing through the activation of NF-κB inducing kinase (NIK) and IKKα/IKK1 (Xiao et al., 2001a; Xiao et al., 2004). Several studies have demonstrated that in resting cells NIK has a short half-life where it undergoes constitutive degradation through the actions of E3 ubiquitin ligases, TRAF2, TRAF3 (TNF receptor associated factor 3) and cIAPs (inhibitor of apoptotic proteins) (He et al., 2007; Liao et al., 2004; Vallabhapurapu et al., 2008; Varfolomeev et al., 2007; Zarnegar et al., 2008). When inducers of non-canonical pathways, such as LTβ, bind to their specific receptors, it alters the conformation of the cytoplasmic tail of the receptors which induces receptor association with the TRAF3:TRAF2 complex by competitively removing NIK from the NIK:TRAFs complex (Sanjo et al. 2010). Stabilized NIK promotes p100 processing by associating with IKK1 and inducing phosphorylation of p100 at residues S866, S870 and S872 (Sanjo et al.; Zarnegar et al., 2008). Receptor bound TRAF3:TRAF2 complex undergo degradation and effectively block the induction of canonical pathways (Vallabhapurapu et al., 2008). Unregulated p100 processing has been

reported to link to cancers (Courtois and Gilmore, 2006). Recent reports have shown that hyper-activation of p100 processing in multiple myeloma patients is due to aberrant stabilization of NIK caused by mutations of different components in the NIK degradation pathway underscoring the importance of non-canonical NF-κB activation pathway. Several of these mutations have been mapped in TRAF3 (Annunziata et al., 2007; Keats et al., 2007).

Previous experiments revealed that p100 processing is blocked in the presence of protein synthesis inhibitor cycloheximide (CHX) (Mordmuller et al., 2003). Although it was thought that new p100 synthesis is required for processing, in light of recent reports on NIK, it is unclear if continuous synthesis of NIK or p100 or both are essential for processing. Previous reports suggested that in addition to signal induced processing of p100 to p52, p100 might undergo complete degradation releasing other NF-κB subunits. However, there has been no clear experimental evidence to support the complete degradation or the consequence of complete p100 degradation.

It has been previously showed in our lab that the p100: RelB complex was highly stable where all domains of both p100 and RelB were engaged (Fusco et al., 2008). These observations were consistent with prior reports that in unstimulated cells RelB is primarily associated with p100 (Solan et al., 2002). This high specificity of RelB for p100 and its processed product p52 led us to hypothesize that RelB might play an important role in the life cycle of p100 both in steady state and during non-canonical signaling. In this chapter,

we investigated if and how RelB influences p100's fate during non-canonical NF-κB signaling. We found that LTβ-mediated non-canonical signaling is a NIK-dependent biphasic event; in the first phase, p100 undergoes complete degradation in a translation independent manner leading to RelA activation. In the second phase, processing of newly synthesized p100 occurs in a translation-dependent manner. We further show that the processing is a dynamic event and that a pool of p100 is protected from processing and degradation during signaling. The protection of p100 requires RelB which enables p100 to re-associate with RelA upon signal termination, thereby promoting NF-κB inhibitory activity of NF-κB2/p100. Non-canonical signaling thus induces both activation and suppression of NF-κB activity.

B. Materials and methods

1. Antibodies

The RelB (sc-226), RelA (sc-372), IκBα (sc-371), αTubulin (sc-5286), βActin (sc-1615), GST (sc-138), and all the secondary HRP-conjugated antibodies were purchased from Santa Cruz Biotecnology. Flag (M2), GFP (A6-455) and penta-His antibodies were from Sigma, Invitrogen and Qiagen, respectively. NIK (#4994) and Phospho-p100 (Ser866/870) (#4810) antibody were from Cell Signaling. p52 and αLTβR antibody were gifts from Dr. Nancy Rice (NIH, Bethesda, MD) and Dr. Carl F. Ware (La Jolla Institute for Allergy & Immunology), respectively.

2. Mammalian Cell Culture and Transient Protein Expression

Wild type and knock out 3T3 cells (MEF cells) were grown in Dulbecco's modified Eagle's medium (CellGro) supplemented with 10% calf serum, 2 mM glutamine and antibiotics.

HEK 293T cells were maintained in DMEM supplemented with 10% fetal bovine serum and 2 mM glutamine and antibiotics. HEK 293T cells were transfected using Lipofectamine 2000 reagent (Invitrogen). Cell lysates were prepared 24-48 hours after transfection or as indicated.

3. Transgenic Cell Lines

All constructs were cloned into the pBABE vector and transgenic cell lines were prepared as described previously (Basak et al., 2007).

4. Cytoplasmic/Nuclear Fractionation

Cytoplasmic/nuclear fractionation was performed as described (Savinova et al., 2009). In brief, cells were lysed in two cell pellet volumns of cytoplasmic extract (CE) buffer containing 60 mM KCl, 10 mM HEPES-KOH pH 7.9, 1 mM EDTA, 0.5% NP-40, and 1 mM DTT supplemented with Protease Inhibitor Cocktail. Cytoplasmic extracts were collected by centrifuging at 500 × g. After collecting the cytoplasmic fractions, the nuclei were washed with additional five volumes of CE buffer and then lysed in three pellet volumes of nuclear extract buffer containing 60 mM KCl, 250 mM Tris-HCl pH 7.5, 1 mM EDTA, and 1 mM DTT supplemented with Proteasome Inhibitor Cocktail. The nuclear extracts were collected by freeze-thaw three times on dry ice and 37°C water bath and then centrifuging.

5. Gel Filtration Chromatography

Gel filtration chromatography was performed as described (Savinova et al., 2009). In brief, cytoplasmic extracts from two 15 cm plates were prepared and filtered using Ultrafree-MC Centrifugal filter units (Millipore, Durapore PVDF 0.22 μm). Each sample was injected onto Superose 6 10/300GL column and resolved in 15 mM Tris-HCl pH 7.5, 140 mM NaCl, and 1 mM DTT

at 0.5 mL/min flow rate. 500 μL fractions were collected, and 20 μL sample from each fraction was analysed by western blotting.

6. Immunoblotting and Co-immunoprecipitation

Cell extracts were prepared by harvesting cells followed by lysis with buffer containing 20 mM Tris-HCl pH 8.0, 0.2 M NaCl, 1% Triton-X-100, 2 mM Na_2VO_4, 2 mM dithiothreitol (DTT), 1 mM phenyl-methylsulfonyl fluoride (PMSF), 5 mM 4-nitrophenyl phosphate di(Tris) Salt, and protease inhibitor mixture (Sigma). 15-30 μg protein from the total cell extracts or nuclear and cytoplasmic extracts were separated by SDS-PAGE followed by transfer to nitrocellulose membrane. Immunodetection was done using specific antibodies. Co-immunoprecipitation was done with 600 μg of identical cell extracts with specific antibody by incubating overnight in the presence of 25 μl protein G sepharose (Upstate Biotechnology). Bound complex was washed three times and separated by SDS-PAGE followed by IB.

7. RNA Isolation and Real-time qPCR

Total RNA (isolated by RNeasy kit, Qiagen) was prepared from *wt* and *relb-/-*MEF cells treated with α-LTβR (0.5μg/mL) as indicated. 0.1μg of total RNA was used for cDNA synthesis (using Invitrogen SuperScriptIII First-Strand Synthesis System) and 1μL of cDNA was used for real-time qPCR analysis. Values are normalized with GAPDH content (Livak and Schmittgen,

2001). Data are represented as mean ± standard deviations (SD) of three independent experiments in duplicates. Primer sequences are listed in Table 2.2.

C. Results

1. RelB protects p100 during induction

It has been previously reported that RelB is a protease sensitive unstable protein and that p100 protects RelB from degradation through multi-site protein-protein interactions (Fusco et al., 2008). We reasoned that such intimate interaction between p100 and RelB must have an impact on p100 stability and function. Dr. Amanda Fusco, a previous graduate student in our lab had tested this hypothesis by examining p100 levels in *wt* and *relb*$^{-/-}$ MEF cells. In the absence of RelB a dramatic decrease of steady state p100 level was observed (Figure 3.1a). Stimulus-responsive p100 processing remained intact in these cells as p52 levels increased over time during stimulation with agonistic anti-LTβ receptor antibody (α-LTβR). However, in contrast to the p100 levels in stimulated *relb*$^{-/-}$ cells, p100 levels in *wt* cells reduced only marginally. These observations suggested that RelB might play a role in stabilization of p100 during α-LTβR signaling. To further test p100 stabilization by RelB, we reconstituted wt *relb* in *relb*$^{-/-}$ cells and induced these cells with α-LTβR. p100 was significantly stabilized in reconstituted cells and the degree of stabilization appeared to be correlated with RelB levels (Figure 3.1a). And in all cases, a fraction of p52 was localized to the nucleus whereas most remained in the cytoplasm (Figure 3.1b). In order to further confirm that RelB's effect on p100 stabilization was not due to its transcriptional activity. Nfkb2/p100 mRNA levels were measured using RT-qPCR in both *wt* and *relb*$^{-/-}$

cells. In Figure 3.1c, it showed that α-LTβR was able to induce p100 transcription in both *wt* and *relb*$^{-/-}$ cells suggesting that RelB mostly affects p100 stability at the protein level.

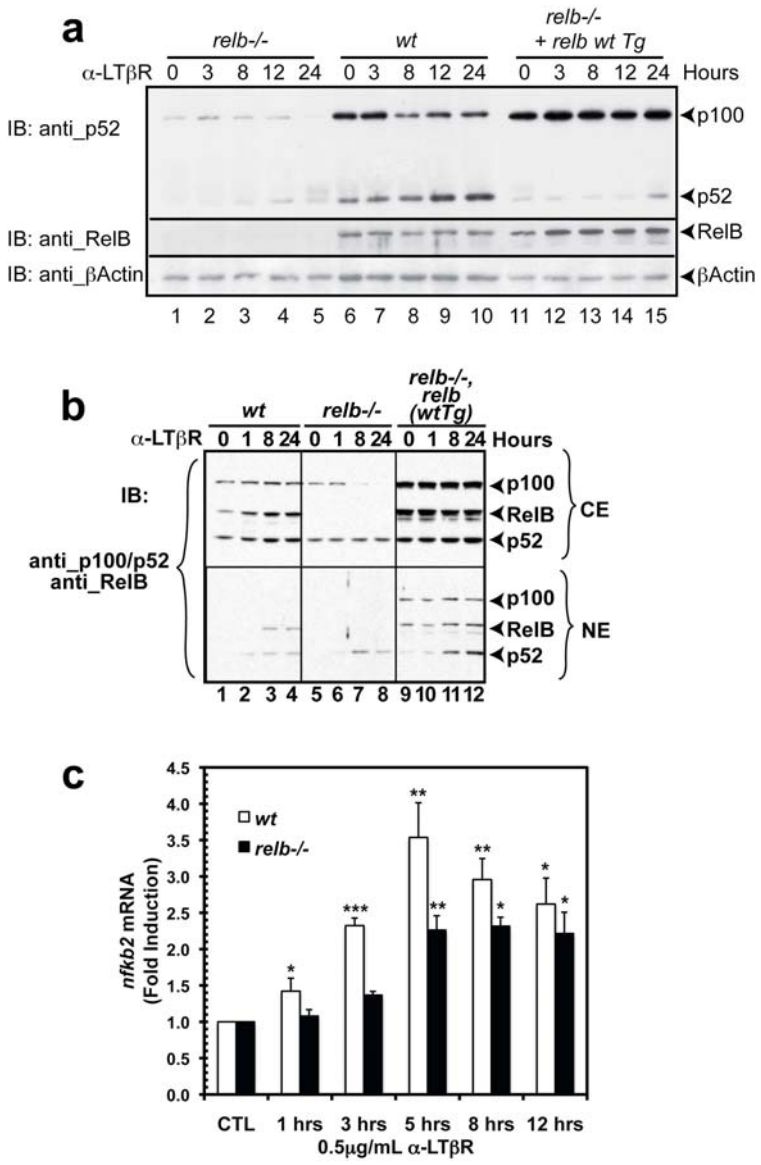

Figure 3.1 RelB inhibits stimulus dependent p100 degradation. a) Wild type (*wt)*, *relb*$^{-/-}$, and *relb*$^{-/-}$ MEF cells with transgenic *wt relb (relb wt Tg)* were stimulated with α-LTβR for up to 24 hours. p100 processing, the levels of RelB and βActin (loading control) were analyzed by western blot. b) p52 processing and nuclear localization in *wt, relb*$^{-/-}$*, relb wt Tg* reconstituted *relb*$^{-/-}$ cells. c) nfkb2/p100 gene expression upon α-LTβR stimulation for indicated time in both *wt* and *relb*$^{-/-}$ MEF cells. *p < 0.05, **p < 0.01, ***p < 0.001 versus nontreated controls. Error bars represent SD.

(Figure 3.1a courtesy of Dr. Amanda Fusco; Figure 3.1b courtesy of Dr. Olga Savinova.)

2. p100 protection is a unique function of RelB not shared by other NF-κB subunits

Although above experiments showed RelB is essential for p100 protection, it was not clear if RelB alone is responsible, i. e., if RelB is necessary and sufficient for p100 protection during stimulation or if other NF-κB members are also required for this function. To investigate this, Dr. Soumen Basak from the Hoffmann lab extended the studies into two different types of MEF cells, one devoid of both RelA and RelB subunits (*rela/relb*$^{-/-}$/$^{-/-}$ double knock out MEFs) and the other devoid of all three transcription activation competent NF-κB subunits; RelA, RelB and c-Rel (*rela/relb/crel*$^{-/-}$/$^{-/-}$/$^{-/-}$ triple knock out MEFs). α-LTβR treatment induced processing however; stabilization of p100 was not observed in *rela/relb*$^{-/-}$/$^{-/-}$ cells (Figure 3.2a). This is consistent with the notion that wt RelB must be present to stabilize p100. As expected, p100 protein level in *rela/relb/crel*$^{-/-}$/$^{-/-}$/$^{-/-}$ cells was extremely low, as the p100 transcription is regulated by NF-κB (Basak et al., 2007). The small amount of p100 present was completely degraded in response to α-LTβR (Figure 3.2b, high exposure). To enhance the level of p100, p100 was reconstituted in *rela/relb/crel*$^{-/-}$/$^{-/-}$/$^{-/-}$ MEF cells and its expression was driven by a constitutive heterologous promoter. In these cells, α-LTβR induced processing without significant stabilization of p100 (Figure 3.2b; third panel). To further test if RelB is sufficient for the stabilization of p100, both *nfκb2* and *wt relb* were reconstituted in *rela/relb/crel*$^{-/-}$/$^{-/-}$/$^{-/-}$ cells (Figure 3.2b, fourth

panel). In both of the reconstituted cells, p100 was stabilized upon treatment with α-LTβR. Therefore, RelB was essential and sufficient to protect p100 during induction. All together, these observations demonstrated a new role of RelB which is to retain at least a pool of p100 remain intact during non-canonical signaling. This is intriguing as processing of p100 into p52 is thought to be the major outcome of non-canonical signaling and p52:RelB is the resultant active dimer.

RelB's protective function of p100 without completely inhibiting p100 processing as seen in Figure 3.1 and 3.2 suggests that under physiological concentrations of these proteins both activities are balanced and that excess RelB could in principle inhibit processing. To test this, we used transient transfection experiments in HEK 293T cells. It has been shown that exogenous p100 could undergo processing in the presence of constitutively active NIK bypassing the requirement of upstream signals (Xiao et al., 2001a). Under the condition of constant amount of NIK, we tested the processing of p100 in the presence of increasing amounts of RelB. Indeed, we found that p100 protection is related to processing and with increasing dose of RelB the processing of p100 is inhibited (Figure 3.2d). These results thus suggest that excess RelB is able to inhibit p100 processing. Although p100 stabilization is opposite to its function as precursor of p52, nevertheless our result indicates that there must be a dynamic balance of p100 processing and stabilization mediated by RelB. This suggests that under physiological concentration of

RelB and the strength of non-canonical signaling (NIK and IKK activities) a pool of p100 is protected and another pool undergoes processing to generate p52.

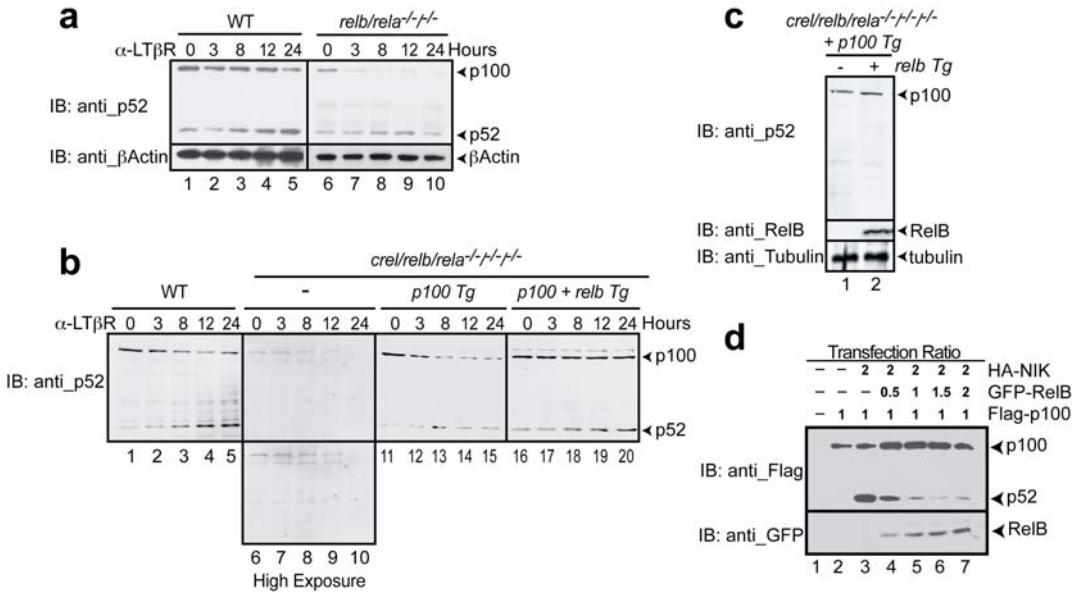

Figure 3.2 RelA and c-Rel cannot substitute RelB function in stabilizing p100 during stimulation. a) Wild type and *rela/relb*$^{-/-}$ MEF were stimulated with α-LTβR for up to 24 hours. Processing of p100 was observed by western blot. b) *rela/relb/crel*$^{-/-/-/-}$ MEF cells and *rela/relb/crel*$^{-/-/-/-}$ MEF cells with *Tg p100* and both *Tg p100 and relb* are stimulated with α-LTβR for up to 24 hours and p100 processing is observed by western blot. A higher exposure of *rela/relb/crel*$^{-/-/-/-}$ MEF cells upon stimulation is shown (bottom panel) due to the low endogenous p100 expression in the knockout cells. c) Tubulin (loading control) and transgenic RelB and p100 expression levels were observed by western blot. d) RelB blocks p100 processing in HEK 293T cells transient transfected with Flag-p100, GFP-RelB and HA-NIK.

(Figure 3.2a-c courtesy of Dr. Soumen Basak.)

3. RelB displays a dominant effect on p100 life cycle

To further investigate how RelB protects p100 during signaling, Dr. Amanda Fusco had tested the effect of a RelB dimerization mutant, Y300A (Figure 3.3a). Y300 is located at the NF-κB dimer interface and is expected to destabilize RelB heterodimer formation with p52. The corresponding residue in p50 (Y267) significantly reduced p50 homodimer formation (Sengchanthalangsy et al., 1999). RelB Y300A did not bind p52 RHR; however, it was still able to bind p100, perhaps as the other contacts between RelB and p100 remained unaltered (Figure 3.3b-d). Surprisingly, little or no induced processing of p100 was observed in *relb Y300A* reconstituted cells, and instead, p100 level diminished progressively with increasing time of stimulation (Figure 3.3a). This is the first clear indication that in response to stimulus p100 can undergo complete degradation, not just processing and generate p52. To further test the effect of RelB Y300A mutant, Flag-p100, HA-NIK and GFP-wt RelB or GFP-RelB Y300A mutant were overexpressed in HEK 293T cells, and p100 was found to undergo processing in the presence of either HA-NIK alone or HA-NIK co-expressed with GFP-RelB. However, in the presence of GFP-RelB Y300A, processing was negligible, and further, p100 level appeared to be significantly reduced suggesting that p100 underwent complete degradation (Figure 3.3d). These observations suggested that dimer formation might be a key regulatory event for the stabilization of the processed product; and also suggested that perhaps there are two modes of

binding interaction between p100 and wt RelB, and the different binding mode would dictate whether processing or stabilization would occur. In the case of RelB Y300A, a processing competent complex between p100 and RelB could not be formed; and it resulted in the complete degradation of p100.

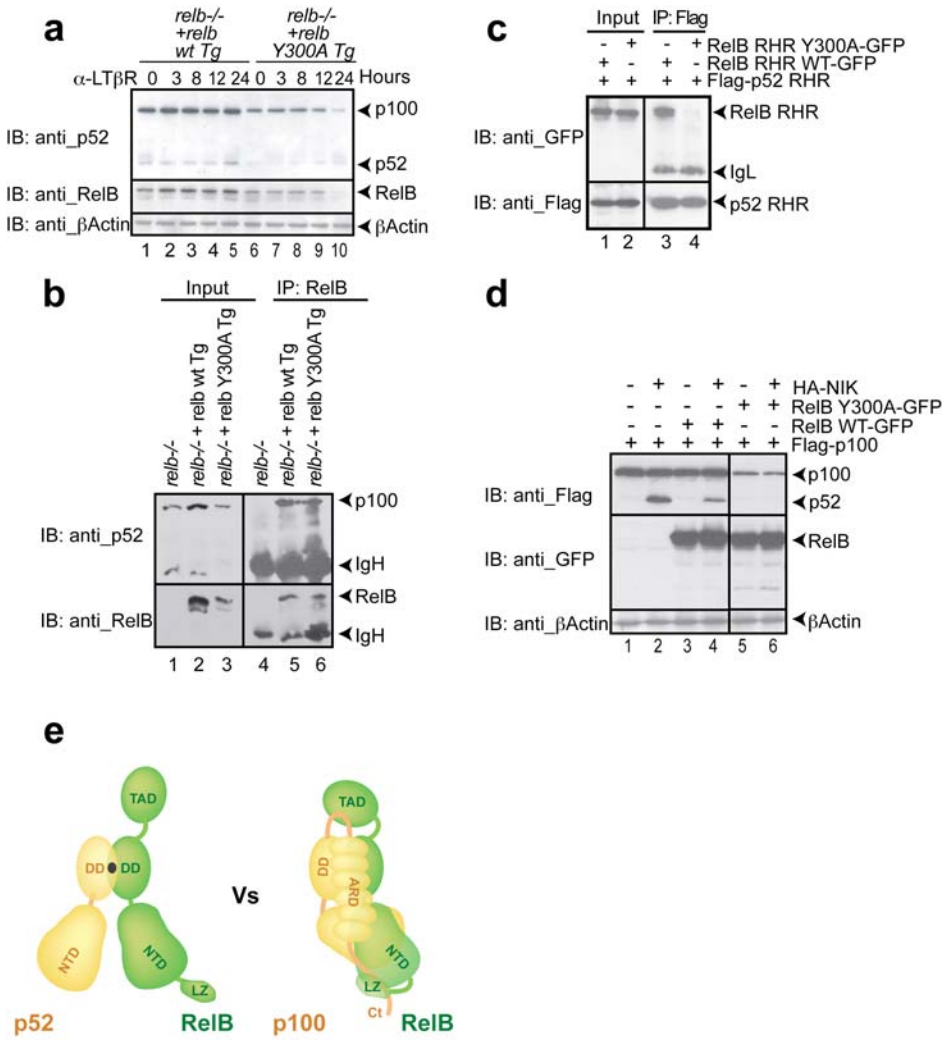

Figure 3.3 RelB dimerization defective mutant affect p100 processing. a) p100 processing was monitored in *relb*$^{-/-}$ MEF cells expressing either *Tg wt relb* or *relb Y300A* mutant. These cells were stimulated with α-LTβR for up to 24 hours and p100 processing was observed by western blot. The levels of RelB and βActin (loading control) were analyzed by western blot. b) Co-IP showing the interactions of endogenous p100 with wt RelB and RelB Y300A mutant. c) Co-IP showing the interaction of p52 RHR with wt RelB and RelB Y300A mutant in transcient transfected HEK 293T cells. d) RelB Y300A blocks p100 processing with transient transfected Flag-p100, HA-NIK, GFP-RelB, and GFP-RelB Y300A in HEK 293T cells. e) Models showing the interactions of p52:RelB vs. p100:RelB complexes. Different domains of both RelB and p100 are labeled. Domains of these proteins have been identified by structural, sequence homology or biochemical analysis. The (●) circle in the dimerization domain denotes the location of the critical tyrosine residue at the dimer interface. The p52:RelB heterodimer formation relies exclusively on the contacts through the dimerization domain whereas p100:RelB complex formation relies on contacts through multiple sites.

(Figure 3.3a-d courtesy of Dr. Amanda Fusco.)

4. Both complete degradation and processing of p100 are regulated by the same signaling pathway

We wanted to investigate if the same signal transduction pathway induces both processing (partial degradation and generation of p52) and complete degradation of p100. Because it is known that p100 processing requires new protein synthesis, we investigated the state of p100 in the presence of both the inducer of signal transduction and the inhibitor of protein synthesis. Wild type and *relb*$^{-/-}$ MEF cells were treated with an inhibitor of protein synthesis, cycloheximide (CHX), or the combination of both CHX and α-LTβR (Figure 3.4a and b). As reported previously, we also observed that processing was completely inhibited in the presence of CHX with no or little degradation of p100. However, in the presence of both CHX and α-LTβR, p100 underwent complete degradation without any processing. This suggests that the signaling pathway induced by α-LTβR remained intact even in the presence of CHX. One way to test pathway sharing is to test if degradation of p100 by the α-LTβR pathway requires NIK. We looked for NIK stabilization in cells treated with α-LTβR or α-LTβR plus CHX (Figure 3.4c). As expected, NIK was stabilized in α-LTβR treated cells (Figure 3.4c, upper panel, compare lanes 1and 2). However, NIK was also observed, albeit in lesser amounts, in cell treated with combined α-LTβR and CHX (upper panel; compare lanes 1 and 3). Marked NIK stabilization was seen when cells were treated with the

proteasome inhibitor MG-132. These results confirm that under conditions when translation is inhibited p100 cannot undergo processing; however, p100 undergoes complete degradation by the action of stabilized NIK. In all, our results suggest that the non-canonical NF-κB signaling pathway activates both processing and complete degradation of p100 through stabilization of NIK. An important question, however, is, being a labile protein itself, how could NIK be stabilized when translation is blocked. Kinetics of α-LTβR and CHX activity might be responsible for this event. It is likely that sufficient NIK was accumulated by the action of α-LTβR before CHX action initiated, and accumulated NIK was stable as long as α-LTβR was present to block the NIK degrading activity. To further recapitulate the difference between processing and complete degradation of p100, we carried out similar experiments in transiently transfected HEK 293T cells. We found that in the presence of CHX, p100 underwent complete degradation when NIK was over expressed (Figure 3.4d). In these cells, cellular E3 ligases are unable to down regulate NIK and artificially higher NIK level induced complete degradation of p100. However, degradation of p100 is blocked under these conditions when excess RelB is present. Over-expression of a catalytically inactive NIK [NIK(KK429-430AA)] (Xiao et al., 2001b) also failed to induce p100 degradation which further confirmed the key role of NIK in complete degradation of p100.

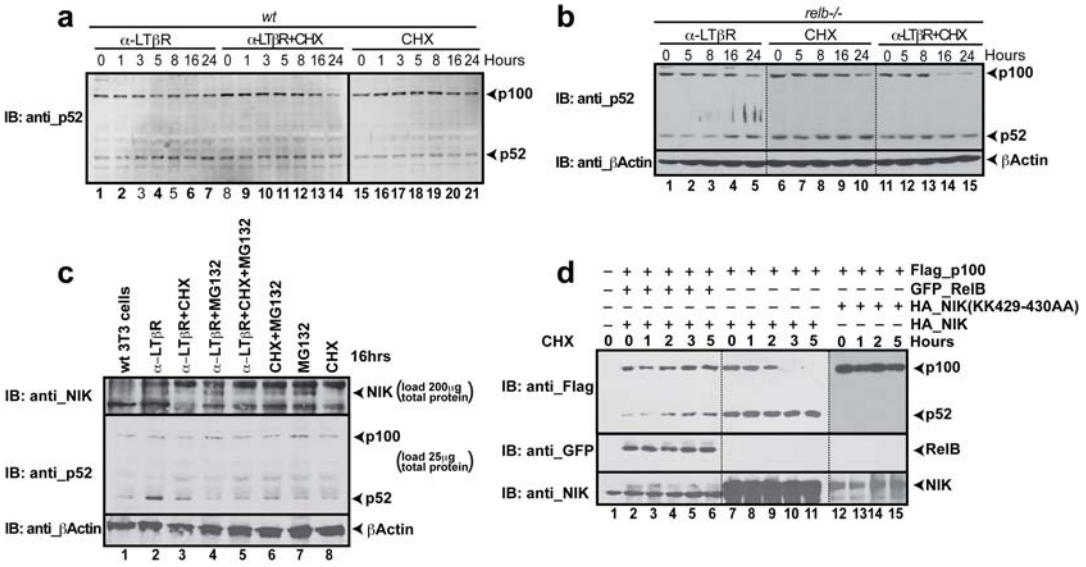

Figure 3.4 α-LTβR induces complete degradation of p100 in the presence of cycloheximide. p100 processing was monitored in a) *wt* and b) *relb*$^{-/-}$ MEF cells. These cells were stimulated with α-LTβR alone, CHX alone, or both α-LTβR and CHX for up to 24 hours c) NIK stabilization in *wt* MEF cells with α-LTβR, CHX, and MG132 treatments at 16 hours. d) p100 degradation in the presence of CHX with transient transfected Flag-p100, GFP-RelB, HA-NIK or catalytic inactive HA-NIK(KK429-430AA) in HEK 293T cells.

(Figure 3.4a courtesy of Dr. Soumen Basak.)

5. Non-canonical signaling is a composite of translation-independent and -dependent processes

It was previously reported that LTβ-induces p50:RelA heterodimer activation (Basak et al., 2007). Our model suggests induction of RelA activity is the result of complete degradation of p100. Indeed, we observed that LTβ induced NF-κB RelA localization to the nucleus between 1 to 3 hours of inducer treatment (Figure 3.5a). This result suggests that RelA localization precedes p100 processing which can be identified earliest around 3 to 5 hours. Under these conditions IκBα level was also enhanced with increasing time of induction, which further suggested that classical IκB degradation pathway was not responsible for the RelA activation, and instead activated RelA induced new IκBα synthesis. To test if RelA might be activated from the p100:RelA complex, we co-transfected p100 and RelA or RelB along with NIK in HEK 293T cells. And CHX was used to treat the cell in order to monitor only complete degradation, but not processing. We found that while RelB-bound p100 is protected from complete degradation, RelA bound p100 undergoes degradation (Figure 3.5b). Moreover, RelA-bound p100 undergoes processing as seen in cell extracts prepared before CHX treatment. These results suggest that RelA movement to the nucleus seen in *wt* MEF resulted primarily, if not exclusively, from the complete degradation of p100 that was bound to RelA. Our results further suggested that RelA activation not only induced new p100 and RelB synthesis, but also new IκBα synthesis (Figure 3.5a). Our

experiments clearly dissects two events in non-canonical signaling; first, activation of RelA through complete degradation of p100 which is translation independent; and second, processing of p100 into p52 which is translation dependent. These results further support the notion that one of the important functions of RelB is to protect p100 from being completely exhausted through processing and degradation.

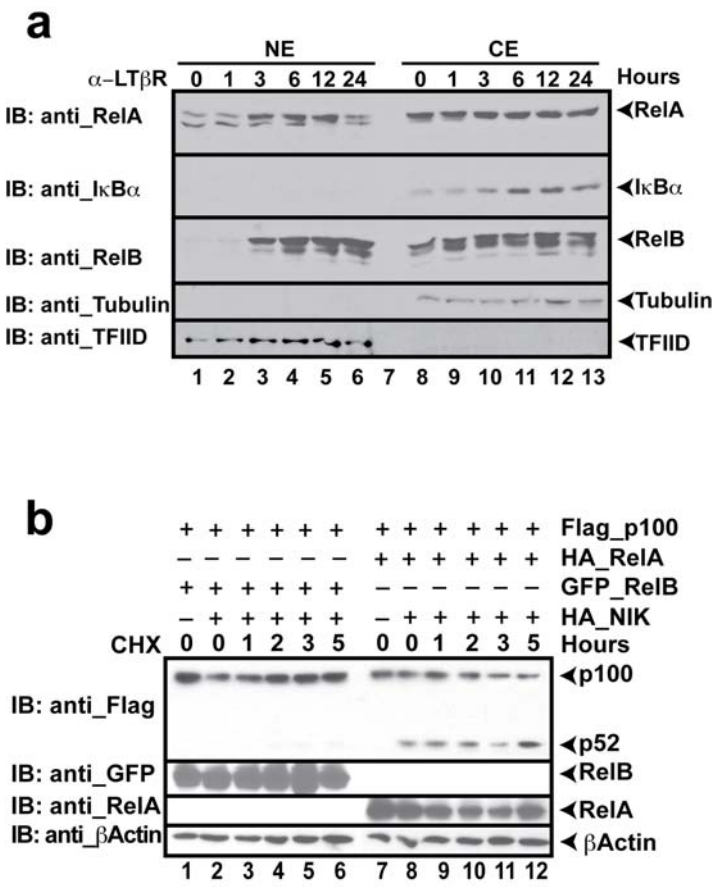

Figure 3.5 RelA activation by α-LTβR requires complete degradation of p100. a) RelA nuclear localization upon α-LTβR treatment in *wt* MEF cells. b) RelB-bound p100 is stable whereas RelA-bound p100 undergo degradation in transiently transfected HEK 293T cells.

6. p100 undergoes dynamic assembly modes during induced processing

Using size fractionation of endogenous proteins, it has been previously showed that endogenous p105 exists mostly as the high MW complex (Savinova et al., 2009). And p105 transforms from a low MW processing competent state to a high MW processing incompetent state. These two states could only be clearly observed in the transient transfection system where p105 was continuously synthesizing. We have carried out fractionation of the cytoplasmic extracts prepared from *wt* MEF cells before and after 12 hours induction with α-LTβR. As shown previously in different other cell types such as HEK 293T and macrophage cells (Savinova et al., 2009), we found that p100 in MEFs primarily exists as a high MW complex in uninduced cells (Figure 3.6a). As expected, RelB appeared in the same high MW fractions as p100. Fractionation of 12 hours post stimulated *wt* MEF cells cytoplasmic extracts clearly showed p100 was distributed in two distinct peaks; one as a high MW species and the other as a low MW species (Figure 3.6a). The high MW species closely resembles the high MW species in the uninduced sample. The newly formed low MW p100 is similar to the low MW species observed for p105 in the transient transfection experiment. We suggest that upon induction newly synthesized p100 partitioned into two distinct complexes; the high MW complex which we propose is stable and processing incompetent and the low MW complex which we propose is a transient state and processing competent complex, similar to what was observed for p105. If our hypothesis is true then

the processing competent low MW state must undergo induced phosphorylation at specific serines (S866, S870 and S872) (Liang et al., 2006). To test phosphorylation of p100 in each fraction, we used a phospho-specific antibody raised against a p100 peptide with S866 and S870 phosphorylated. Because of low sensitivity of phospho-specific antibody to fractionated p100, we carried out immunoprecipitation of the peak fractions in high and low MW complexes (Figure 3.6a, fraction #22 and #26). As expected, p100 in the low MW complex, but not in the high MW complex, underwent phosphorylation (Figure 3.6b). No phosphorylation was observed at the corresponding fractions of uninduced samples. This indicates that the high MW complex does not undergo processing and can be referred to as the processing incompetent stable complex. The low MW complex is capable of undergoing processing and can be referred to as the processing competent transient complex. The lesser level of RelB in the low MW p100 transient complex might be due to quick mobilization to and accumulation of RelB in the nucleus as the p52:RelB heterodimer. If our suggestion that high MW complex formation relies on the presence of RelB during stimulation is true, then p100 should not fractionate into two distinct peaks upon stimulation when RelB is absent. It has been shown previously by Dr. Olga Savinova in our lab that in *relb*$^{-/-}$ MEFs, upon α-LTβR stimulation p100 primarily fractionated in the low MW factions comparing with un-induced cells. Based on these observations we suggest that newly synthesized p100 interacts with newly

synthesized RelB in an initial transient interaction mode, which then can transform into a stable interaction mode. In the stable mode, p100 cannot be phosphorylated by NIK/IKK1/α. However, these kinases can phosphorylate p100 when its phosphorylation sites are still free, i. e., the complex is still in the transient low MW state (Figure 3.6c).

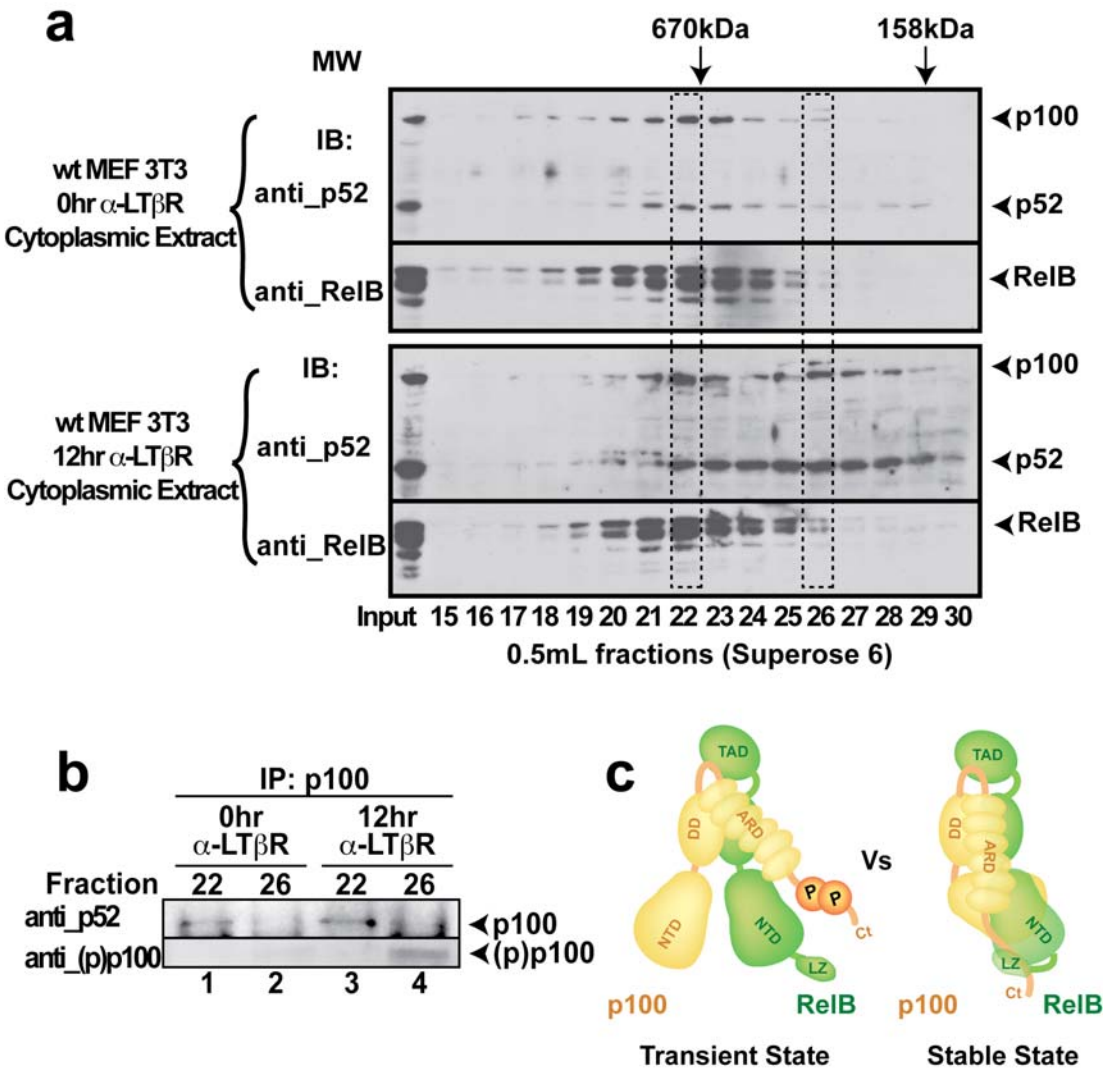

Figure 3.6 p100 processing is a dynamic event. a) Fractionation of the cytoplasmic extracts of *wt* MEF 3T3 cells with or without α-LTβR treatment. b) Immunoprecipitation of fractions #22 and #26 from both induced and uninduced fractionated samples followed by WB against anti-p52 and anti-phospho-p100 antibodies. c) Models of p100:RelB complex in transient state vs. stable state. This model shows that the C-terminal IκB-like domain of p100 can exist in two states. In transient state, C-terminal tail of p100 is accessible and can be phopshorylated; in stable state, the tail is masked by RelB, so processing becomes inhibited.

7. RelB permits p100 to function as an inhibitor of NF-κB

Finally, we investigated the significance of RelB's protective role in p100 processing/degradation during non-canonical signaling. Our hypothesis is that by protecting at least a pool of p100 during stimulation RelB allows p100 to function as an inhibitor of NF-κB in steady state. We suggest that p100 bound RelA depletes during signaling whereas RelB bound p100 persists, and when stimulus is withdrawn p100 rebinds RelA. To test this model, both *wt* MEF cells were treated with α-LTβR for 12 hours or grown for another 12 hours after withdrawal of stimulus. We observed, as expected, that in *wt* cells RelA was bound to p100 in resting cells and levels of bound RelA diminished significantly after 12 hours of α-LTβR stimulation. However, RelA was found to re-associate with p100 after the stimulus was withdrawn for additional 12 hours (Figure 3.7a). During this time course RelB remained bound to p100. This suggests a dynamic assembly mode of p100, where it associates, dissociates and re-associates with RelA as depicted in Figure 3.7b. Similar experiments were carried out in *relb*$^{-/-}$ MEF cells, negligible re-association of p100 with RelA was observed post induction (Data not shown). Therefore, dynamic assembly mode relies on the presence of RelB, which preventing p100 from being completely degraded/processed through the non-canonical signaling and permitting p100 to function as an NF-κB inhibitor, which referred as IκBδ activity of NF-κB2/p100.

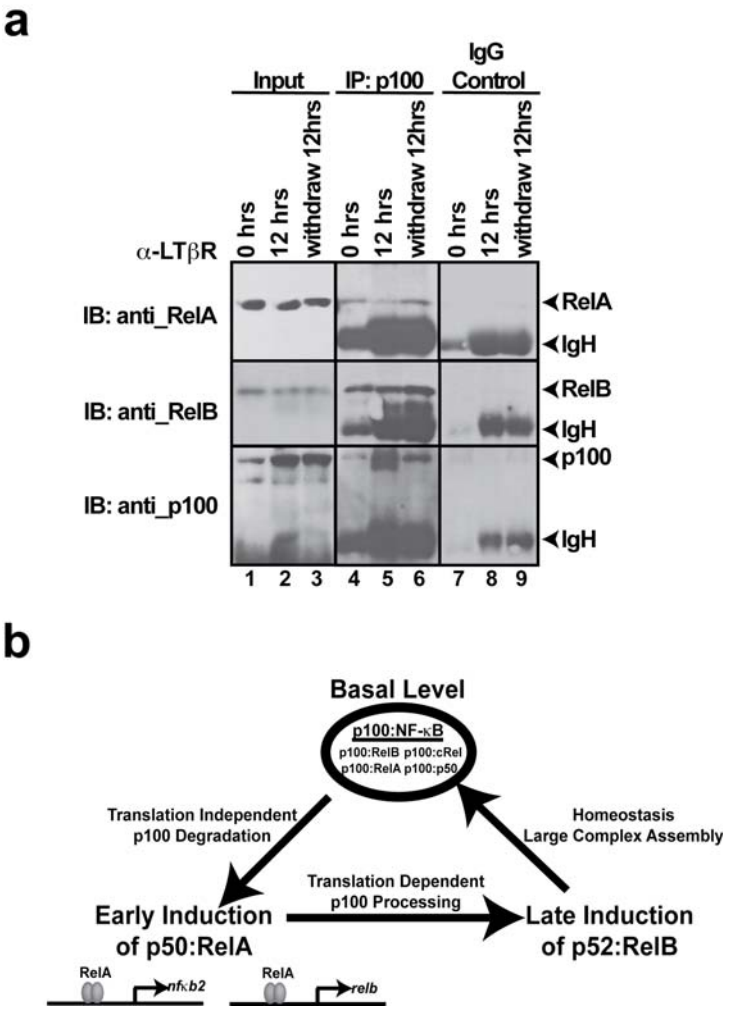

Figure 3.7 Association and dissociation of p100:RelA complex. a) Co-immunoprecipitation demonstrates the binding of RelA to p100 before (0 hrs); during (12 hrs) and after (withdraw 12 hrs) α-LTβR stimulation in *wt* MEF cells. b) Model of p100 translation independent degradation, translation dependent processing, and large complex assembly which functions as an inhibitor of NF-κB.

D. Discussion

Having both NF-κB activation and IκB inhibition functions, NF-κB2/p100 poses a complex problem of maintaining both the processed (p52) and unprocessed (p100) molecules in appropriate levels for their cellular activities. Excessive processing or lack of it results in devastating physiological consequences including cancer (Annunziata et al., 2007; Keats et al., 2007). Dissection of highly intertwined activities generated by the same molecule is a challenging task. We describe here the molecular mechanisms of three important events in non-canonical NF-κB signaling pathway: First, we show that the non-canonical signaling pathway induces both processing and complete degradation of p100 and that the complete degradation is translation independent whereas the processing is translation dependent. Second, we show that the processing of p100 requires a distinct structural state induced by signaling. Finally, we show that RelB plays a protective role that allows p100 to function as an effective inhibitor of NF-κB. RelB also plays a critical mediatory role in balancing between complete degradation and processing of p100.

1. Complete degradation of p100 releases RelA in the first phase of non-canonical NF-κB signaling

The RelA activation by non-canonical NF-κB signaling was shown before (Basak et al. Cell, 2007). However, the precise mechanism of how

RelA is activated was not clear. Work presented here demonstrates that p100 undergoes complete degradation which releases free RelA to localize to the nucleus. To demonstrate complete degradation in the backdrop of p100 processing is challenging. There are several reasons for this: processing of p100 results in a new product, p52, which can be visualized, and in this background complete degradation of p100 can be missed. In order to demonstrate the complete p100 degradation requires NIK but occurs in a translation independent manner, the use of translation inhibitor CHX is required. However, CHX is expected to block both p100 synthesis and NIK synthesis. We show that in cells treated with both CHX and α-LTβR, p100 undergoes complete degradation, which becomes more evident in cells devoid of RelB (Figure 3.4b and d). Our results show that indeed, in the presence of CHX, low level of NIK is stabilized in α-LTβR-treated cells, which might be sufficient to act on its downstream effectors. One can suspect that under native condition where NIK level is expected to get higher, complete degradation of p100 would occur at a faster rate.

2. Processing is the result of dynamic p100 assembly event in the second phase of non-canonical NF-κB signaling

The RelA activation in the first phase of the non-canonical signaling, within the first three hours, apparently induces expression of both *nfκb2* and *relb* genes. New p100 can undergo processing or remained protected. In this

study we establish the underpinnings of the highly complex event of p100 processing/degradation. Our study reveals that p100 alters its assembly during signaling where processing occurs in a distinct structural state, which we refer to as transient low MW state (Figure 3.8). RelB is not essential for this structural state, however, if RelB is present in cells then it also interact with p100 at this transient structural state. Processing competency is supported by phosphorylation of the C-terminal serines of p100. In resting cells, the transient state is not observed and p100 only remains as the high MW complexes which bound to other NF-κB subunits. Of these steady state heterogeneous p100 complexes, RelB-bound p100 is insensitive to induced phosphorylation. Newly synthesized p100 during signaling forms a similar stable complex with newly synthesized RelB and this stable p100:RelB complex is unable to undergo phosphorylation. It is unclear at this stage the precise structural states of the p100:RelB complexes that accurately describe high and low MW compositions. Structural studies are essential to understand the conformational states of p100 steady and induced conditions. Because phosphorylation of p100 requires it to be in transient low MW state, it is tempting to speculate that NIK/IKK1 may play a role in the transition of p100 from low to high MW state. As the level of NIK/ IKK1 increases, they might interact with more p100 in low MW state resulting in greater degree of processing. Our results thus show how the strength of a stimulus can be the deciding factor of the relative amounts of p100 and p52.

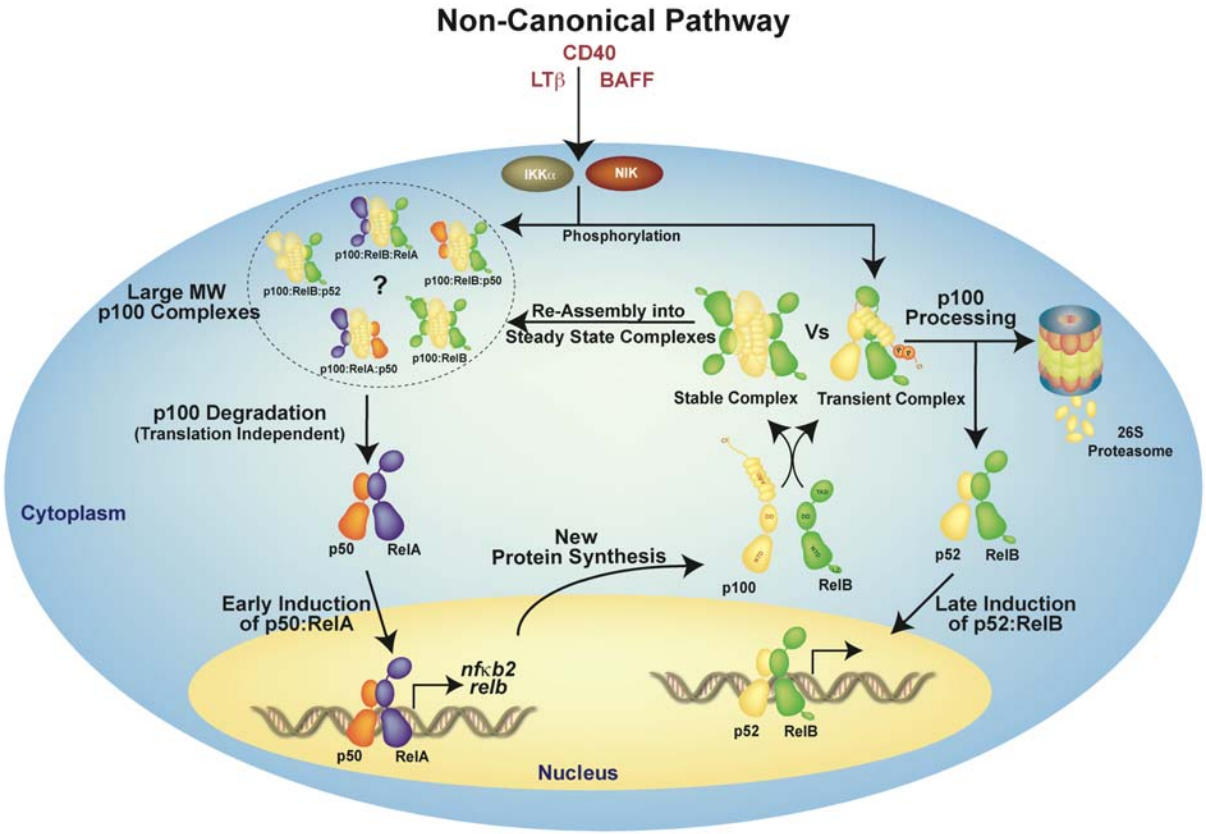

Figure 3.8 Biphasic NF-κB activation model by non-canonical signaling. α-LTβR activates RelA (possibly as the p50:RelA heterodimer) through complete degradation of p100, which in turn activates the expression of p100 and RelB. Newly synthesized p100 and RelB proteins assemble into two modes, a transient mode that is capable of p100 phosphorylation and processing; and a stable mode that is incapable of p100 phosphorylation and processing. It is also possible that all interactions occurs transiently which experience two competing events; phopshorylation by NIK/IKK1 and rapidly transformation into stable mode. The stable p100:RelB complex further incorporates RelA and other NF-κB subunits post stimulation to return to the steady state.

3. RelB is the enforcer of NF-κB inhibitory activity of NF-κB2/p100

Finally, our study identifies a novel mechanism of post stimulation re-establishment of NF-κB inhibition by p100. Protection of p100 during stimulation by RelB has an important purpose. This protected pool of p100 can rebind RelA or c-Rel and prime the complex for the next wave of activation. The mechanism of RelA rebinding to p100 is still unclear. It may competitively remove RelB from p100 forming the p100:RelA complex or associate with the p100:RelB complex forming a higher order assembly. We suggest that p100:RelB complex is probably an inconsequential signaling complex because degradation of p100 from this complex leaves free RelB which is a highly unstable protein. This would result in loss of both proteins. On the other hand, RelA is activated from the p100:RelA complex and participates in transcription. Therefore, transfer of p100 to RelA or accommodation of RelA in the p100:RelB complex is a specialized activity of RelB which cannot be compensated by other NF-κB subunits. Another potential indirect function of RelB could be that it limits RelA binding to p100. In *relb*$^{-/-}$ cells p100 is present as complexed to RelA (as p50:RelA) and perhaps with c-Rel. In the absence of RelB, more RelA (and/or c-Rel) can associate with p100 at homeostatic level which could be potently activated by non-canonical signaling through complete degradation of p100. Higher levels of RelA/c-Rel activation could result in high-level expression of inflammatory genes.

In conclusion, our results demonstrate that the non-canonical NF-κB signaling pathway simultaneously induces complete degradation and processing of p100 and that both events are necessary for the NF-κB activation cycle. The non-canonical signaling pathway induces both RelA and RelB activation and p52 generation. Therefore, in addition to the well recognized activation of p52:RelB heterodimer, this pathway has the component of canonical signaling embedded in it. NF-κB2/p100 displays distinct inhibitory activities toward RelA and RelB: it inactivates RelA in steady state and in post-stimulation steady state, but not during stimulation; on the other hand, RelB controls p100 at three cellular states. RelB protected p100 during stimulation allows RelA to re-bind to p100 post-stimulation. Therefore, RelB functions directly as a transcription activator and indirectly as a transcription repressor.

E. Chapter III Acknowledgements

Chapter III is currently being prepared for submission for publication. Fusco, Amanda J.; Wang, Vivien Y.; Basak, Soumen; Tao, Zhihua; Savinova, Olga V.; Hoffmann, Alexander; and Ghosh, Gourisankar. “RelB plays a critical role in regulating both processing and stabilization of NF-κB2/p100”. The dissertation author was the co-primary investigator and author of this paper.

Chapter IV: Identification of Bcl3 Phosphorylation Sites and its Functions

A. Introduction

The gene expression repertoire of cells is constantly modulated by a variety of extracellular stimuli. Excluding those small lipophilic molecules which can cross the plasma membrane and affect the ligand binding transcription factors allosterically; most signals such as bacterial or viral infection and stresses transmit from cell surfaces to the nucleus rapidly and accurately through different signaling pathways. And these signaling pathways rely on protein phosphorylation and lead to the activation of specific transcription factors that can induce the expression of appropriate target genes. The Rel/NF-κB family proteins regulate hundreds of target genes that are essential for inflammation, immunity, cell proliferation, and apoptosis. In unstimulated cells, NF-κB proteins are maintained in a latent state in the cytoplasm through stable protein-protein association with a class of inhibitor proteins known as IκBs. NF-κB signaling pathways are triggered by a variety of extracellular signals which lead to the phosphorylation and subsequent proteasome mediated degradation of the IκBs.

Bcl3 is a putative oncoprotein identified in a t(14;19) translocation in a subgroup of B cell lymphocytic leukemias. In B cells containing the t(14;19) translocation, Bcl3 is expressed at a 3-4 fold higher level (Ohno et al., 1990). Bcl3 is a distinctive member of the IκB family; it has a strong preference towards NF-κB p50 or p52 homodimers. IκB proteins regulates NF-κB activities in two ways: IκBs can retain NF-κB in the cytoplasm of resting cells by blocking the nuclear localization signal (NLS) sequences; IκB can also

inhibit NF-κB transcription activity by actively removing NF-κB from κB DNAs. The role of Bcl3 in modulating NF-κB mediated gene regulation is complex. Some earlier reports showed Bcl3 could, like the classical IκBs, dissociate its preferred NF-κB p50 or p52 homodimer from κB DNAs, thereby functions as a repressor of transcription (Nolan et al., 1993). Other reports showed that, under some circumstances, Bcl3 could associate with p50 or p52 homodimer forming an activation complex on the promoter (IκB:NF-κB:κB DNA) (Bours et al., 1993; Dechend et al., 1999; Fujita et al., 1993; Massoumi et al., 2006; Rocha et al., 2003). Therefore, Bcl3 can function to co-activate NF-κB transcription.

It has been shown that in B and T cells as well as in transiently transfected cells, Bcl3 is present predominantly in the nucleus and the NLS located at its N-terminal portion is required for its efficient nuclear localization (Zhang et al., 1994). In several other cell types, such as erythroblasts, hepatocytes, and keratinocytes, Bcl3 resides in the cytoplasm and requires activation prior to nuclear translocation (Brasier et al., 2001; Massoumi et al., 2006; Zhang et al., 1998). However, the signals which activate Bcl3 and recruit Bcl3 to the NF-κB p50 and p52 homodimers in the nucleus are not known.

Bcl3 mRNA and protein expression are induced by NF-κB activating agents. Promoter analysis of Bcl3 gene identified two high affinity NF-κB binding sites; κB1 site located at -872 to -861 bp and κB2 site located at -106

to -96 bp upstream of transcription start site. RelA binds to both κB1 and κB2; however, only κB2 is required for NF-κB dependent induction of the Bcl3 promoter (Brasier et al., 2001). Bcl3 deficient mice have been generated to study the physiological functions of Bcl3. It has been shown that Bcl3 is required for T cell dependent immunity. Bcl3 deficient mice are defective in antigen specific antibody production and germinal center formation (Franzoso et al., 1997; Schwarz et al., 1997).

An interesting feature of Bcl3 is the high density of proline and serine residues present at its C-terminus. Previous studies have shown that upon stimulation, Bcl3 C-terminal domain is highly phosphorylated, and the phosphorylation may affect its regulation of NF-κB-dependent transcription *in vivo* (Bundy and McKeithan, 1997; Massoumi et al., 2006; Nolan et al., 1993; Viatour et al., 2004b, 2005). For example, in anaplastic large cell lymphoma (ALCL), Bcl3 is further upregulated upon stimulation. In the resting cells, Bcl3 is present as an intermediate phosphorylation state; in response to CD30 stimulation, Bcl3 protein becomes hyperphosphorylated. The CD30 stimulation also promotes the *de novo* synthesis of NF-κB2/p100 as well as the p100 processing to p52. Processed p52 associates with hyperphosphorylated Bcl3 in CD30 stimulated ALCL (Nishikori et al., 2005). However, there are only two Bcl3 phosphorylation sites, Ser394 and Ser398, have been identified so far. These two serine residues are phosphorylated by GSK3β and lead to the subsequent Bcl3 degradation through the proteasomal pathway (Viatour et al., 2004a). This GSK3-mediated Bcl3 phosphorylation is

inhibited by Akt activation and modulates Bcl3's association with HDAC1, -3, and -6 which in turn prevents its cellular accumulation and attenuates its oncogenic potential.

Since little is known about the regulation of Bcl3 phosphorylation at molecular level and its integration into gene regulatory pathway, we set out to identify additional Bcl3 phosphorylation sites and study its functions in this chapter. We successfully expressed and purified full length human Bcl3 protein from HEK 293T cells and identified two new Bcl3 phosphorylation sites, Ser33 and Ser446, using mass spectrometry. Bcl3 Ser33 phosphorylation modulates its protein expression and probably nuclear localization; Ser446 modulates its interaction with NF-κB p52 homodimer. Taken together, phosphorylation of Bcl3 at these two newly identified serines would enhance its transactivation potential on NF-κB p52 homodimer specific gene transcription. And inhibitor studies suggested that these two phosphorylation sites might be regulated by the Akt pathway.

B. Materials and methods

1. Antibodies and Reagents

Anti-Flag (M2) (F3165) antibody, LPS (L6529), Cycloheximide (C1988), and Wortmannin (W1628) were from Sigma. MG-132 (#474791) and Akt Inhibitor VIII (124018) (Bain et al., 2007) was from Calbiochem. Anti-Akt1/2/3 (sc-8312) antibody was from Santa Cruz Biotechnology. and Anti-phospho-Akt (Ser473) (#9271) antibody were from Cell Signaling. Anti-p100/p52 (#1495) and Anti-Bcl3 (#1348) rabbit antisera were a kindly gift from Dr. Nancy (NIH, Bethesda, MD).

2. Mammalian Cell Culture and Transient Protein Expression

HEK 293T cells and HeLa cells were grown in Dulbecco's modified Eagle's medium (CellGro) supplemented with 10% fetal bovine serum, 2 mM glutamine and antibiotics. Cells were transfected using Lipofectamine 2000 reagent (Invitrogen). Cell lysates were prepared 48 hours after transfection or as indicated.

3. Protein Expression and Purification

Mouse HA-tagged Akt wt is a general gift from Dr. Alexandra Newton.

Recombinant non-tagged human p52(1-408) in pET11a vector was expressed and purified from *E.coli* BL21(DE3) cells as described in Chapter II.

Human Flag-Bcl3(1-446) in pEYFP-C1-YFP+NT-Flag+CT-His8 vector was transfected into HEK 293T cells and purified using Anti-Flag affinity resin as described in Chapter II.

4. Graded Dephosphorylation of Bcl3

Typically, 23 μg (70 μL in volumn) of affinity purified Flag-tagged Bcl3(1-446) protein was incubated with 50 units of intestinal calf phosphatase (CIP) (NEB) in NEB buffer 3 at room temperature. 10 μL aliquots of the reaction mixtures were removed from at each time point from 0 to 3 hours from the starting point of the reaction. The last aliquot was left at room temperature for overnight to see the complete de-phosphorylation of the Bcl3 protein. At each time point, the reaction was stopped by boiling the samples with SDS buffer at 95°C for 5 minutes. The samples were then analyzed by 12.5% SDS-PAGE.

5. Generation of p50-RelA(TAD) and p52-RelA(TAD) Fusion Protein Constructs

p50-RelA(TAD): Mammalian expression plasmids of Flag-tagged p50-RelA(TAD) in pEYFP-C1-YFP+NT-Flag+CT-His8 (described in Chapter II) vector was generated by two-step PCR reaction. During the first round of PCR reaction, Flag-tagged mouse p50(1-435) and human RelA(325-551) were generated separately. For Flag-tagged p50(1-435) fragment, pEYFPC1-YFP+NT-Flag-p50(1-435) was used as PCR template, the N-terminal primer

containing EcoR I restriction site: p105_EcoRI_1F: 5’-CG AAT TCT ATG GCA GAC GAT GAT CCC-3’; C-terminal primer linked mouse p50 residue 435 with human RelA residue 325: mp105-435_hp65-325_R: 5’-GCG TCG AGG TGG AGG CCG GGT GTT TAT GGT GCC ATG-3’.

For RelA(325-551) fragment, HA-tagged human RelA(1-551) was used as PCR template, the N-terminal primer was complimentary to primer mp105-435_hp65-325_R, which linked mouse p50 residue 435 with human RelA residue 325: mp105-435_hp65-325_F: 5’-CAT GGC ACC ATA AAC ACC CGG CCT CCA CCT CGA CGC-3’; C-terminal primer containing EcoR V restriction site: hmp65_sEcoRV_550/551R: 5’-TC GAT ATC TTA GGA GCT GAT CTG ACT C-3’.

The resulting PCR products of the two DNA fragments were then used as templates in the second round PCR reaction, and the two primers p105_EcoRI_1F and hmp65_sEcoRV_550/551R were used. The resulting p50(1-435)RelA(325-551) fragment was then gel purified and double digested with EcoR I and EcoR V restriction enzymes (NEB), and gel purified again. The DNA fragment was then ligated in pEYFP-C1-YFP+NT-Flag+CT-His8 vector at EcoR I and EcoR V cut sites.

p52-RelA(TAD): Mammalian expression plasmids of Flag-tagged p52-RelA(TAD) in pEYFP-C1-YFP+NT-Flag+CT-His8 vector was generated by two-step PCR reaction similar as p50-RelA(TAD) fusion construct. During the first round of PCR reaction, Flag-tagged human p52(1-415) and human

RelA(325-551) were generated separately. For Flag-tagged p52(1-415) fragment, pEYFPC1-YFP+NT-Flag-p52(1-415) was used as PCR template, the N-terminal primer containing EcoR I restriction site: p100_EcoRI_1F: 5'-CG AAT TCT ATG GAG AGT TGC TAC AAC C-3'; C-terminal primer linked human p52 residue 415 with human RelA residue 325: hp100-415_hp65-325_R: 5'-GCG TCG AGG TGG AGG CCG GTC CCT GCT GGG CAC CG-3'. For RelA(325-551) fragment, HA-tagged human RelA(1-551) was used as PCR template, the N-terminal primer was complimentary to primer hp100-415_hp65-325_R, which linked human p52 residue 415 with human RelA residue 325: hp100-415_hp65-325_F: 5'-CG GTG CCC AGC AGG GAC CGG CCT CCA CCT CGA CGC-3'; C-terminal primer containing EcoR V restriction site: hmp65_sEcoRV_550/551R: 5'-TC GAT ATC TTA GGA GCT GAT CTG ACT C-3'.

The resulting PCR products of the two DNA fragments were then used as templates in the second round PCR reaction, and the two primers p100_EcoRI_1F and hmp65_sEcoRV_550/551R were used. The resulting p52(1-415)RelA(325-551) fragment was then gel purified and double digested with EcoR I and EcoR V restriction enzymes (NEB), and gel purified again. The DNA fragment was then ligated in pEYFP-C1-YFP+NT-Flag+CT-His8 vector at EcoR I and EcoR V cut sites.

6. Phosphopeptide enrichment and LC-MS/MS analysis

Proteolysis of the sample: 25 µL 5% RapiGest (Waters Corporation, 5 Pack of 1 mg Vials, 186001860) in 10 X TNE was mixed with 225 µL protein mixture in water. Sample was boiled for 5 minutes after which 375 µL of water was added. TCEP (tris(2-carboxyethyl)phosphine) was added to the final concentration of 1 mM and incubated at 37°C for 30 minutes. Idoacetamide was then added to the final concentration of 2 mM and incubated at 37°C for 30 minutes. Before the addition of trypsin another aliquot of TCEP was added to the final concentration of 2 mM. Trypsin was then added to the final concentration of 1:50 trypsin:protein and incubated overnight at 37°C. To remove RapiGest, HCl was added to a final concentration of 250 mM and incubated at 37°C for 1 hour. The sample was then centrifuged at 14K at 4°C for 30 minutes. The supernatant was removed from the pellet into a fresh tube. The peptides were then extracted using Aspire RP30 desalting columns (Thermo Scientific) before injection into the mass spectrometer.

Phosphopeptide enrichment

For phosphopeptide enrichment of the samples the waters "MassPREP^{TM} phosphopeptide enrichment kit" (Waters Corporation) was used. The peptides were lyophilized and subsequently hydrated in 80% acetonitrile, 0.1% TFA, 0.5mM EDTA, and 100 mg/mL Enhancer^{TM} (Waters Corporation) and passed through the TiO_2 solid phase extraction wells. The wells are then washed with water and later with 80% acetonitrile and 0.1%

TFA. The peptides are finally eluted with 100 mM ammonium phosphate dibasic solution.

LC-MS/MS analysis

Trypsin-digested peptides or the phosphopeptide enriched peptide samples were analyzed by liquid chromatography (LC)-MS/MS with nanospray ionization. All nanospray ionization experiments were performed using a QSTAR-Elite hybrid mass spectrometer (ABSCIEX™) interfaced to a nanoscale reversed-phase high-pressure liquid chromatography (Tempo) using a 10 cm-180 ID glass capillary packed with 5-μm C18 Zorbax™ beads (Agilent). The buffer compositions were as follows. Buffer A was composed of 98% H_2O, 2% ACN, 0.2% formic acid, and 0.005% TFA; buffer B was composed of 100% ACN, 0.2% formic acid, and 0.005% TFA. Peptides were eluted from the C-18 column into the mass spectrometer using a linear gradient of 10–80% Buffer B over 60 minutes at 400 μL/min (10-40% buffer B for 50 minutes followed by 5 minutes at 80% B, followed by 5 minutes 10% B). LC-MS/MS data were acquired in a data-dependent fashion by selecting the 6 most intense peaks with charge state of 2 to 4 that exceeds 20 counts, with exclusion of former target ions set to "120 seconds" and the mass tolerance for exclusion set to 100 ppm. Time-of-flight MS were acquired at *m/z* 400 to 2000 Da for 0.5 seconds with 12 time bins to sum. MS/MS data were acquired from *m/z* 50 to 2,000 Da by using "enhance all" function and 24 time bins to sum, dynamic background subtract, automatic collision energy, and automatic

MS/MS accumulation with the fragment intensity multiplier set to 6 and maximum accumulation set to 2 second before returning to the survey scan (in iTRAQ acquisition mode).

7. Mutagenesis of human Bcl3

Bcl3 Serine 33 single mutations: Phospho-mimic Flag_Bcl3(1-447)S33E, and Flag Bcl3(1-447)S33A mutations were generated by PCR reaction using human Flag_Bcl3(1-447) wt as a template, N-terminal primer containing EcoRI restriction site, and C-terminal primer containing BamHI restriction site. The PCR reaction product was first gel purified, then double digested with EcoRI and BamHI restriction enzymes (NEB), and gel purified again. The DNA fragment was then ligated in pEYFP-C1-YFP+NT-Flag+CT-His8 vector at the corresponding cut sites. Plasmids isolated from transformations were sequenced to verified the presence of mutations. The mutagenic DNA oligonucleotide primers listed bellowed were used to amplify the mutated gene construct:

Bcl3_EcoRI_1_S33E_101F(pEYFPC1): 5’-CG AAT TCT ATG GAC GAG GGG CCC GTG GAC CTG CGC ACC CGG CCC AAG GCC GCC GGA CTC CCG GGC GCC GCG CTG CCG CTC CGC AAG CGC CCG CTG CGC GCG CCC GAA CCG GAG CC-3’

Bcl3_EcoRI_1_S33A_107F(pEYFPC1): 5’-CG AAT TCT ATG GAC GAG GGG CCC GTG GAC CTG CGC ACC CGG CCC AAG GCC GCC GGA CTC

CCG GGC GCC GCG CTG CCG CTC CGC AAG CGC CCG CTG CGC GCG CCC GCA CCG GAG CC-3’

Bcl3_sBamHI_447R(pEYFPC1): 5’-CG GGA TCC TCA GCT GCC TCC TGG AGC TGG-3’

Bcl3 Serine 446 single mutations: Phospho-mimic Flag_Bcl3(1-447)S446E, and Flag Bcl3(1-447)S446A mutations were generated by PCR reaction using human Flag_Bcl3(1-447) wt as a template, N-terminal primer containing EcoRI restriction site, and C-terminal primer containing BamHI restriction site. The PCR reaction product was first gel purified, then double digested with EcoRI and BamHI restriction enzymes (NEB), and gel purified again. The DNA fragment was then ligated in pEYFP-C1-YFP+NT-Flag+CT-His8 vector at the corresponding cut sites. Plasmids isolated from transformations were sequenced to verify the presence of mutations. The mutagenic DNA oligonucleotide primers listed bellowed were used to amplify the mutated gene construct:

Bcl3_EcoRI_1F(pEYFPC1): 5’-CG AAT TCT ATG GAC GAG GGG CCC G-3’

Bcl3_sBamHI_446R_S446E(pEYFPC1): 5’-CG GGA TCC TCA TTC GCC TCC TGG AGC TGG-3’

Bcl3_sBamHI_446R_S446A(pEYFPC1): 5’-CG GGA TCC TCA TGC GCC TCC TGG AGC TGG-3’

Bcl3 Serine 33 and 446 double mutations: Flag_Bcl3(1-447)S33,446E, Flag Bcl3(1-447)S33,446A, Flag_Bcl3(1-447)S33E,S446A, and Flag_Bcl3(1-447)S33A,S446A double mutations were generated by PCR reaction using human Flag_Bcl3(1-447)S33E and Flag_Bcl3(1-447)S33A as a template respectively, N-terminal primer containing EcoRI restriction site, and C-terminal primer containing BamHI restriction site. The PCR reaction product was first gel purified, then double digested with EcoRI and BamHI restriction enzymes (NEB), and gel purified again. The DNA fragment was then ligated in pEYFP-C1-YFP+NT-Flag+CT-His8 vector at the corresponding cut sites. Plasmids isolated from transformations were sequenced to verified the presence of mutations. The mutagenic DNA oligonucleotide primers listed bellowed were used to amplify the mutated gene construct:

Bcl3_EcoRI_1_S33E_101F(pEYFPC1): 5’-CG AAT TCT ATG GAC GAG GGG CCC GTG GAC CTG CGC ACC CGG CCC AAG GCC GCC GGA CTC CCG GGC GCC GCG CTG CCG CTC CGC AAG CGC CCG CTG CGC GCG CCC GAA CCG GAG CC-3’

Bcl3_EcoRI_1F(pEYFPC1): 5’-CG AAT TCT ATG GAC GAG GGG CCC G-3’

Bcl3_sBamHI_446R_S446E(pEYFPC1): 5’-CG GGA TCC TCA TTC GCC TCC TGG AGC TGG-3’

Bcl3_sBamHI_446R_S446A(pEYFPC1): 5’-CG GGA TCC TCA TGC GCC TCC TGG AGC TGG-3’

8. Cytoplasmic/Nuclear Fractionation

Cytoplasmic/nuclear fractionation was performed as described (Savinova et al., 2009). In brief, cells were lysed in two cell pellet volumns of cytoplasmic extract (CE) buffer containing 60 mM KCl, 10 mM HEPES-KOH pH 7.9, 1 mM EDTA, 0.5% NP-40, and 1 mM DTT supplemented with Protease Inhibitor Cocktail. Cytoplasmic extracts were collected by centrifuging at 500 × g. After collecting the cytoplasmic fractions, the nuclei were washed with additional five volumes of CE buffer and then lysed in three pellet volumes of nuclear extract buffer containing 60 mM KCl, 250 mM Tris-HCl pH 7.5, 1 mM EDTA, and 1 mM DTT supplemented with Proteasome Inhibitor Cocktail. The nuclear extracts were collected by freeze-thaw three times on dry ice and 37°C water bath and then centrifuging.

9. Flag-Immunoprecipitation

25 μg of Flag-tagged Bcl3(1-446) wt and different mutants' nuclear extracts were incubated with recombinant non-tagged p52(1-408) protein in binding buffer (20 mM Tris pH 7.5, 150 mM NaCl, 0.5% NP-40, and 1 mM DTT) overnight at 4°C. Complexes of p52 with Flag-tagged Bcl3 were then immunoprecipited using 50 μL Anti-Flag affinity resin (Sigman A2220) at 4°C for 2 hours. Bound complexes were washed three times with 1xTBS buffer supplemented with 0.1% NP-40, and dissolved in 4xSDS-dye by boiling at 95°C for 10 minutes followed by SDS-PAGE analysis.

C. Results

1. Full-Length Bcl3 is Required for its Transactivation Potential with p52 Homodimer

The IκB family member Bcl3 functions as transcriptional co-activator specific to NF-κB p52 homodimers. NF-κB p50 and p52 subunits do not contain the C-terminal transcription activation domains (TAD) and broadly function as the repressors of transcription. However, in the presence of Bcl3, p52 homodimer can activate target gene transcription. In essence, Bcl3 provides the TAD in trans. It is interesting to know whether the lack of C-terminal TAD is the only reason which terminate p52 homodimer to activate its target gene transcription, or Bcl3 plays some essential roles specific for p52 homodimer transactivation potential. Therefore, we generated fusion protein in which the RelA TAD was linked to the C-terminus of p52 named as p52-RelA(TAD). p50-RelA(TAD) fusion protein was also generated for comparison (Figure 4.1a). Both fusion proteins expressed to a similar level when transiently transfected to HEK 293T cells. Similar to the constitutive processing of NF-κB1/p105 to p50, the p50-RelA(TAD) was continuously processed to p50 when expressed; however, little or no p52 was generated from p52-RelA(TAD) (Figure 4.1b). Luciferase assays were performed to test the transactivation potential of the two fusion proteins on P-Selectin κB reporter and compared to p52 and p50 complexed with Bcl3. To our surprise, none of the fusion proteins could activate P-Selectin transcription (Figure 4.1c). It is possible that fusion of the RelA TAD to the C-terminus of p52 and

p50 hinders their ability to recognize DNA. In order to confirm that the fusion proteins could bind κB DNA, they were also tested on classical MHC κB reporter, RelA and p52:Bcl3 were used as controls. As expected, RelA and p50-RelA(TAD) activated MHC κB reporter since MHC κB DNA is a well known NF-κB binding site specific for the classical RelA/RelA, p50/p50, and p50/RelA dimers. However, neither p52:Bcl3 nor p52-RelA(TAD) could activate the MHC κB reporter (Figure 4.1d). Since P-Selectin κB DNA is a specific target site for p52 homodimer, but not the other NF-κB dimers, the p50-RelA(TAD) fusion protein dimer cannot bind to it and activate its transcription (Figure 4.1c). It is not clear, however, the reason for the inability of the p52-RelA(TAD) fusion protein to activate P-Selectin κB reporter. Different Bcl3 constructs with either N- or C-terminus deletion were also generated and tested in the P-Selectin κB reporter assay. Only the full-length Bcl3 could confer transactivation potential to p52 and activate P-Selectin reporter (Figure 4.2). Full-length Bcl3 probably help targeting p52 homodimer to its specific κB DNA in the promoter. Another possible explanation might be the NF-κB dimer affinity. Different IκB family proteins might have differential preferences towards different NF-κB dimers, such as IκBα preferentially binds to p50/RelA heterodimer, IκBβ and IκBε prefers RelA and c-Rel homodimer and RelA/c-Rel heterodimer, and IκBζ only binds to p50 homodimer (Vallabhapurapu and Karin, 2009). The diversity in the activity of IκB family members suggests that different IκBs might have distinct and synchronous

roles in the regulation of specific NF-κB activity. And this NF-κB:IκB interaction specificity is required not only for the specificity in NF-κB dimer inhibition, but also for the transcription activation by some IκB members such as the p52:Bcl3 complex. p52:Bcl3 complex exhibited relatively higher transcriptional activity towards G/C-centric κB sites. These experiments showed that the highly potent TAD of RelA could not activate transcription when fused to p52; however, when fused to p50, the fusion construct showed higher transcription potency than wt RelA in reporter assays.

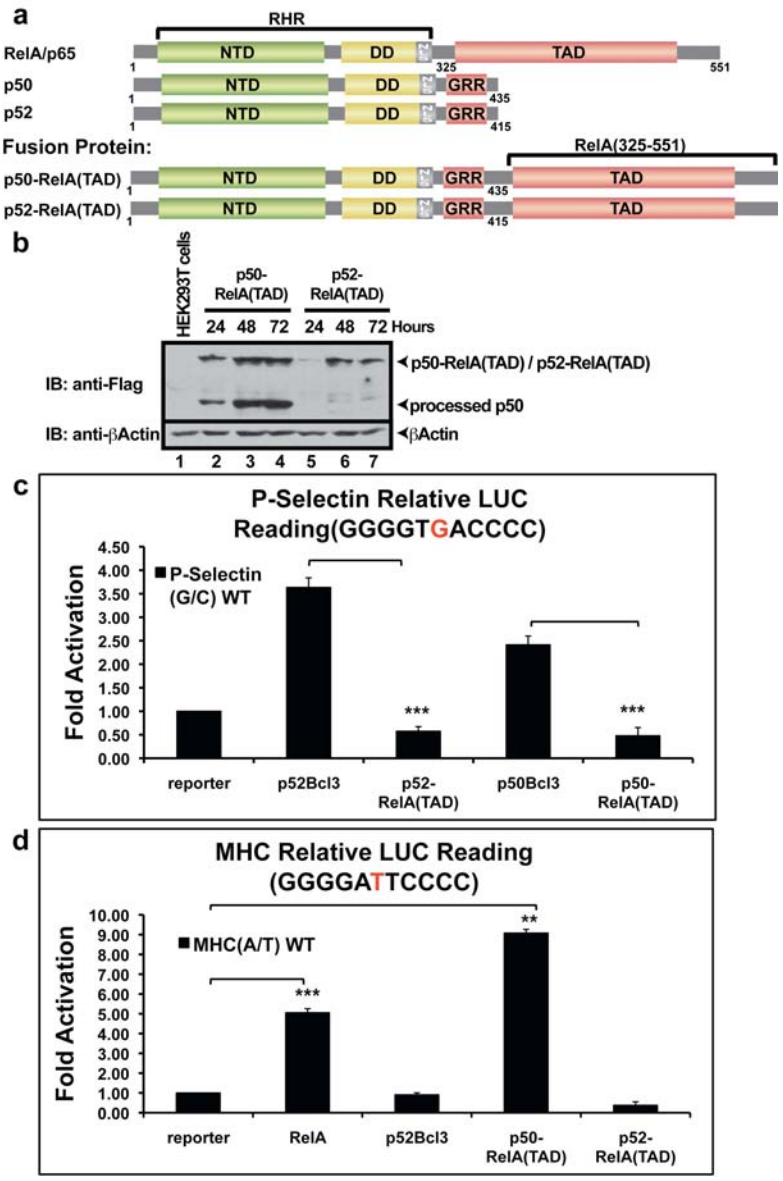

Figure 4.1 Bcl3 is required for p52 transcription activity. a) Schematic representation of NF-κB RelA, p50, p52 and their fusion constructs. b) Expression of p50-RelA(TAD) and p52-RelA(TAD) fusion proteins in HEK 293T cells. Constitutively processed p50 was generated from the p50-RelA(TAD) fusion protein. Transcriptional activities on c) P-Selectin, d) MHC κB luciferease reporters. Neither p50-RelA(TAD) nor p52-RelA(TAD) can activate P-Selectin reporter; p52:Bcl3 was done as a control. However, p50-RelA(TAD) can activate MHC κB reporter. The data was analyzed from three independent experiments performed in triplicate. **p<0.01, ***p<0.005. Error bars represent standard deviation (SD).

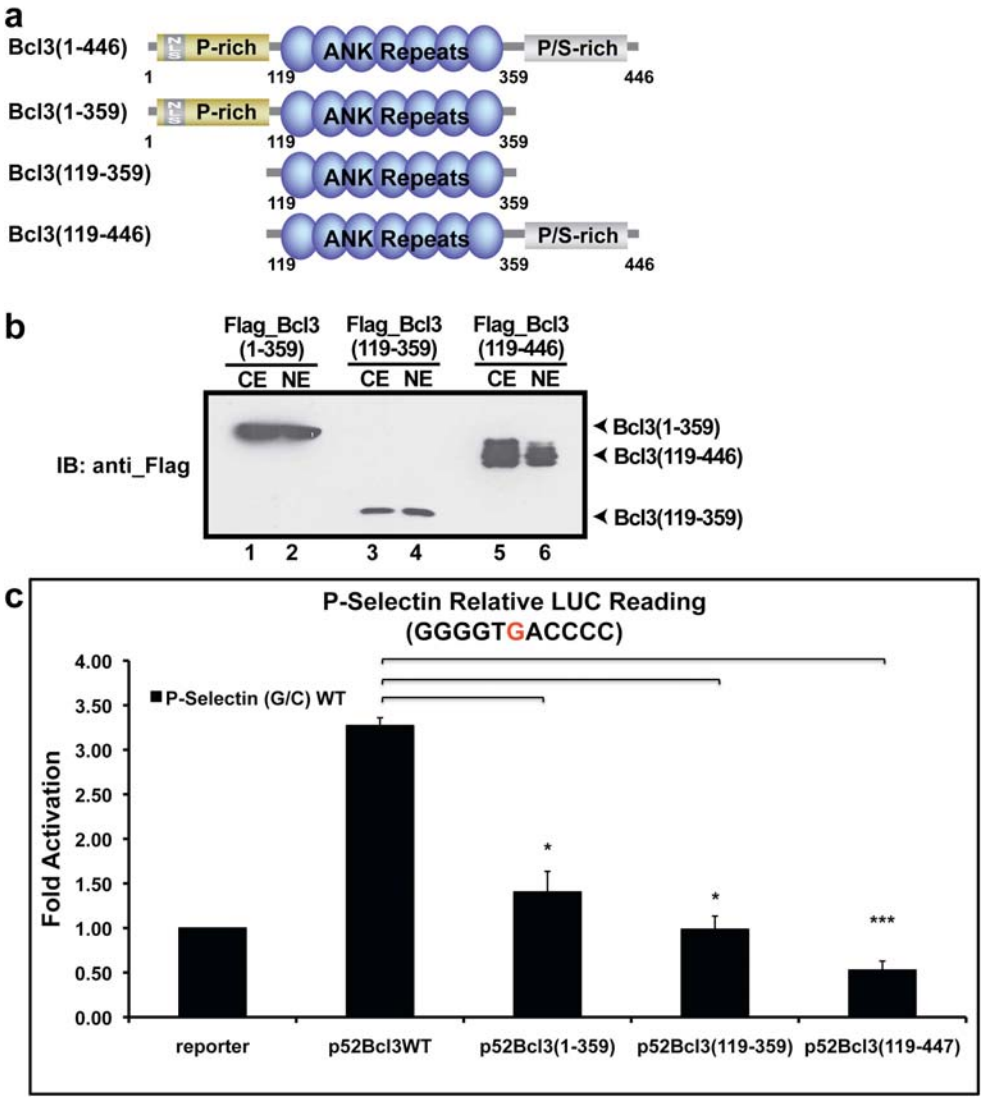

Figure 4.2 Full-length Bcl3 is required for its transcription potential with p52. a) Schematic representation of full length Bcl3 and its truncated constructs. b) Nuclear and cytoplasmic expression of different Bcl3 constructs. Flag-tagged Bcl3 plasmids were transfected into HEK 293T cells; expressions were analyzed by anti-Flag Western Blot. c) Transcriptional activities of different Bcl3 constructs complex with p52 on P-Selection luciferase reporter. Only full-length Bcl3 showed transcriptional activity with p52 on P-Selectin reporter. The data was analyzed from three independent experiments performed in triplicate. *$p<0.05$, ***$p<0.005$. Error bars represent SD.

2. Bcl3 is Phosphorylated at Ser33 and Ser446

We have previously noticed that Bcl3 expression induced in response to LPS stimulation in macrophages, and it accumulated in the nucleus. Since nuclear localization of many proteins is regulated at the level of protein phosphorylation, we would like to investigate if Bcl3's localization is also regulated at the level of phosphorylation. It has been previously reported that the C-terminus of Bcl3 is extensively phosphorylated and different phosphorylation form of Bcl3 modulates the NF-κB p52 homodimer binding to DNA (Bundy and McKeithan, 1997); and only two phosphorylation sites have been identified at its C-terminal to date (Viatour et al., 2004a). Therefore, we set out to identify new Bcl3 phosphorylation sites in order to further study the effects of Bcl3 phosphorylation in terms of modulating its nuclear localization and transcriptional activation.

Since recombinant full-length Bcl3 from *E.coli* is insoluble and continuously degrading during purification, we expressed and purified Flag-tagged full-length Bcl3 from HEK 293T cells. With a predicted molecular weight of 48 kDa, purified full-length Flag-tagged Bcl3 migrates as multiple bands of approximately 60 kDa in SDS-PAGE analysis (Figure 4.3a). To determine whether the Flag affinity purified full-length Bcl3 is phosphorylated or not, the protein was subjected to graded phosphatase treatment. Figure 4.3b shows Bcl3 was de-phosphorylated within 30 minutes treatment of phosphatase. These data, as well as previous reports, suggested transiently expressed full-length Bcl3 is extensively and constitutively phosphorylated.

To identify new phosphorylation sites, purified full-length Bcl3 protein was digested with trypsin and then subjected to LC-MS/MS analysis. Phosphopeptides consistent with phosphorylations at Ser33 and Ser446 were identified (Figure 4.4 and 4.5). These two serine residues are evolutionarily conserved in mouse and human Bcl3.

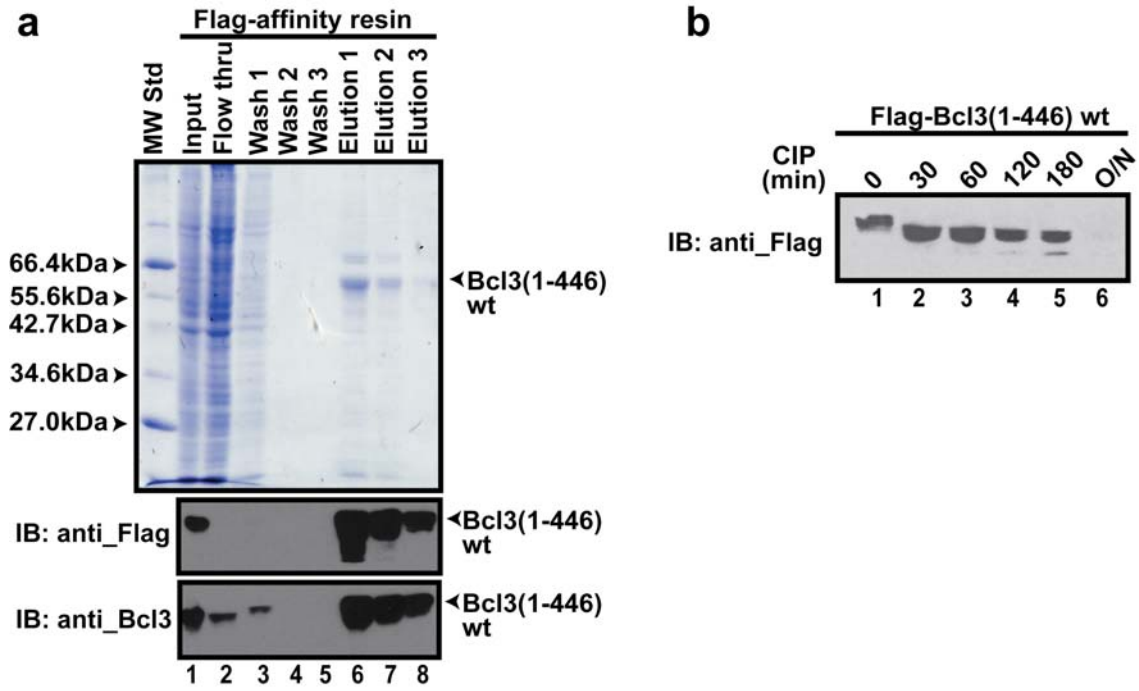

Figure 4.3 Purification of Flag-tagged human Bcl3(1-446). a) Full length Flag-tagged Bcl3 was expressed and purified from HEK 293T cells using Flag affinity chromatography. 12.5% SDS-PAGE analysis of the elutions from Flag affinity resin. Western blots using both Flag and Bcl3 antibody were used to confirm the purity of the protein. b) Calf intestinal phosphatase (CIP) dephosphorylates Flag-Bcl3(1-446). 3 μg of purified Flag-tagged Bcl3 was treated with CIP at room temperature for various time points as indicated and subsequently subjected to anti-Flag Western analysis.

a

b

Bcl3 N-Terminus Alignment

```
Mouse-Bcl3  1     MDEGPVDLRT RPK--GTPGA ALPLRKRPLR PASPEPATTR SPAG---PLD
Human-Bcl3  1     MDEGPVDLRT RPKAAGLPGA ALPLRKRPLR APSPEPAAPR GAAGLVVPLD
Consensus         MDEGPVDLRT RPKaaG-PGA ALPLRKRPLR --SPEPA--R --AGlvvPLD
                                                   Phospho Ser
Mouse-Bcl3  46    ALRSGCDVPV VPGPPHCVAR PEALYYQGPL MPIYSTPTMA PHFPLLNLPT
Human-Bcl3  51    PLRGGCDLPA VPGPPHGLAR PEALYYPGAL LPLYPTRAMG SPFPLVNLPT
Consensus         -LR-GCDvP- VPGPPH-vAR PEALYY-G-L mPiY-T--Ma --FPLlNLPT

Mouse-Bcl3  96    HPYSMICPME HPLSADIA
Human-Bcl3  101   PLYPMMCPME HPLSADIA
Consensus         --Y-MiCPME HPLSADIA
```

c

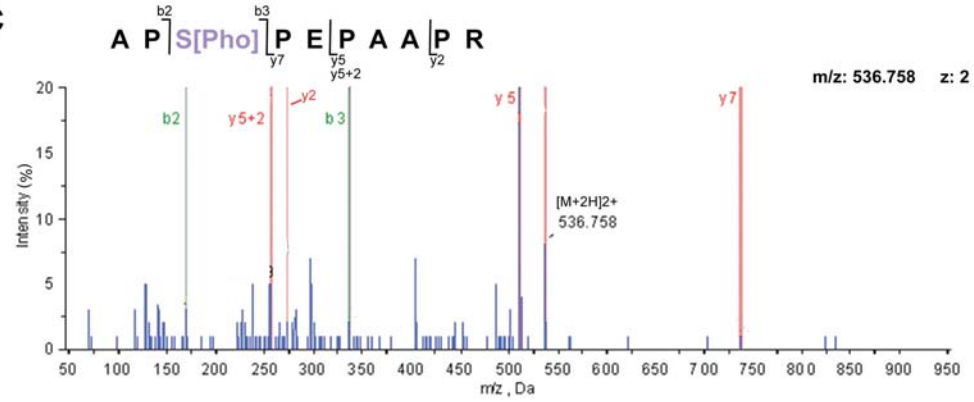

d

Fragment Ion Table (monoisotopic masses)

Residue	b	y
A	72.0444	1072.4823
P	169.0972	1001.4452
S[Pho]	336.0955	904.3924
P	433.1483	737.3941
E	562.1909	640.3413
P	659.2436	511.2987
A	730.2807	414.2459
A	801.3179	343.2088
P	898.3706	272.1717
R	1054.4717	175.1190

Figure 4.4 Identification of Bcl3 phosphorylation at Ser33. a) Schematic representation of full length Bcl3. b) Sequence alignment of N-terminus of human and mouse Bcl3. c) MS/MS spectrum showing the phosphorylation of Ser33 of Bcl3. d) Fragment ion mass table of the phosphopeptide.

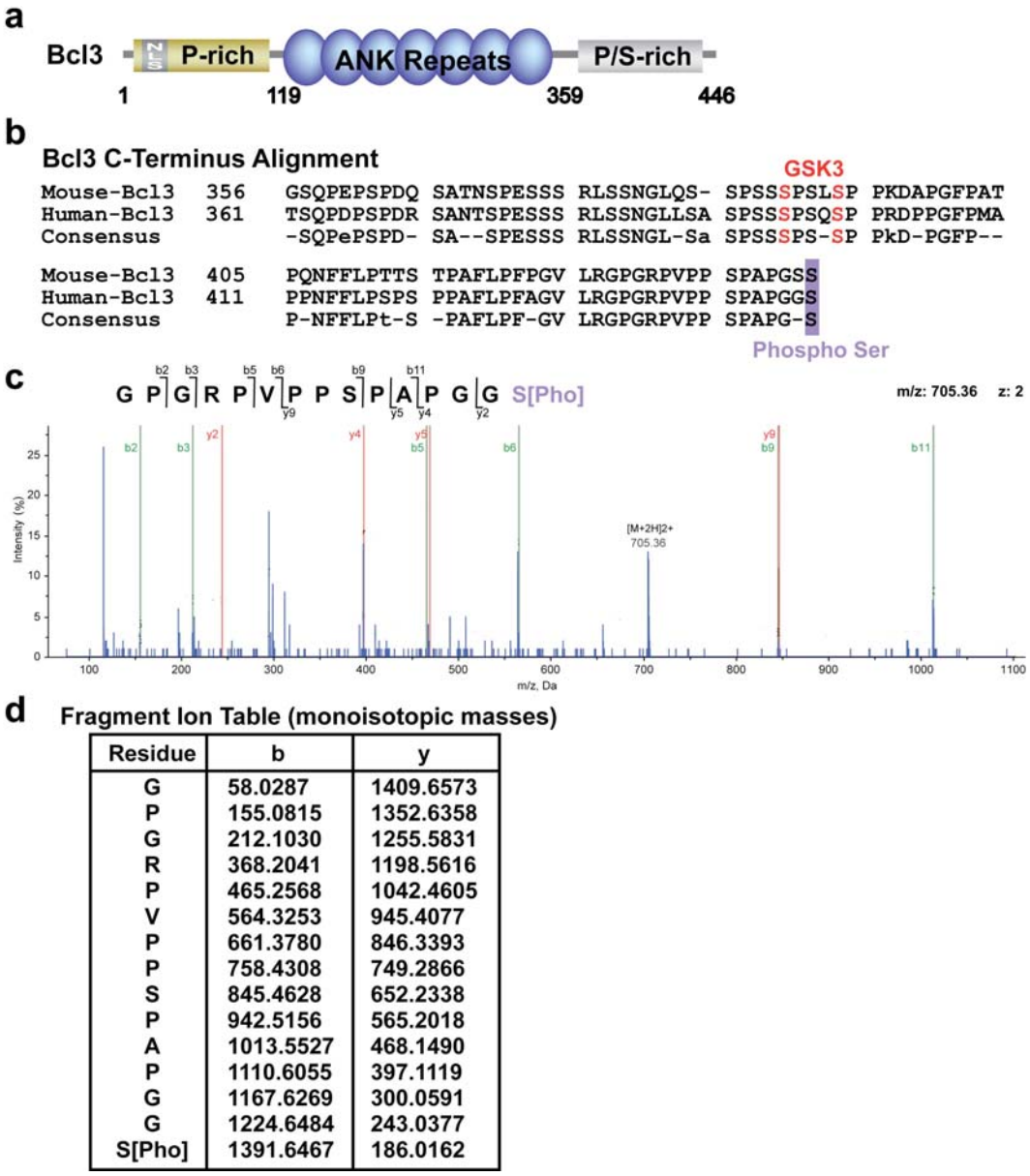

d **Fragment Ion Table (monoisotopic masses)**

Residue	b	y
G	58.0287	1409.6573
P	155.0815	1352.6358
G	212.1030	1255.5831
R	368.2041	1198.5616
P	465.2568	1042.4605
V	564.3253	945.4077
P	661.3780	846.3393
P	758.4308	749.2866
S	845.4628	652.2338
P	942.5156	565.2018
A	1013.5527	468.1490
P	1110.6055	397.1119
G	1167.6269	300.0591
G	1224.6484	243.0377
S[Pho]	1391.6467	186.0162

Figure 4.5 Identification of Bcl3 phosphorylation at Ser446. a) Schematic representation of full length Bcl3. b) Sequence alignment of N-terminus of human and mouse Bcl3. Two GSK3-mediated phosphorylation sites were indicated. c) MS/MS spectrum showing the phosphorylation of Ser446 of Bcl3. d) Fragment ion mass table of the phosphopeptide.

3. Phosphorylation of Bcl3 Enhances its Transactivation Potential with p52 Homodimer

Protein phosphorylation plays critical roles in cellular signaling to transmit signals from cell surface to the nucleus which ultimately lead to the activation of specific transcription factors that induce the expression of appropriate target genes. Since Bcl3 is a known co-activator for NF-κB p52 homodimer, we hypothesized that phosphorylation of Bcl3 might play a role in the regulation of p52 mediated transcriptional activity. To investigate the function of Bcl3 phosphorylation at Ser33 and Ser446, phospho-mimic and phospho-inactive mutants at Ser33, Ser446, and both residues were made. To our surprise, the phospho-inactive mutation of Ser33, S33A, showed very low total protein level (Figure 4.6a) and was mostly located in the cytoplasmic fraction (Figure 4.6e) in transiently transfection studies; and the corresponding phospho-mimic mutant, S33E, showed enhanced protein level and appeared in both cytoplasm and nucleus. Mutations at Ser446, both S446E and S446A, showed similar expression levels as wt Bcl3 and partitioned both in cytoplasm and nucleus (Figure 4.6b and f). Due to the high serine content at it C-terminus, Bcl3 with different phosphorylation states usually migrates abnormally as multiple bands in transient transfection studies as shown in Figure 4.2b lane 5,6 and Figure 4.3a, as well as previous reports (Bundy and McKeithan, 1997; Viatour et al., 2004a). One interesting observation is that the S446E mutant mostly migrated as the higher molecular weight band (Figure 4.6b lane 4); and the S446A mutant mostly migrated as the lower

molecular weight band (Figure 4.6b lane 6) compared to the wt protein, which normally migrates as the broad smear band. Double mutations of residue Ser33 and Ser446 were also made in different combination; S33A/S446A (AA), S33E/S446E (EE), S33E/S446A (EA). Similar to the S33A mutant, the total protein level of the AA mutant was low and mostly localized in the cytoplasm. The EE and EA double mutants showed enhanced protein level and appeared in both cytoplasm and nucleus (Figure 4.6c, d, g, h). These observations suggest that phosphorylation at Ser33 plays an important role for Bcl3 protein level. And phosphorylation of Ser33 may also play a role in Bcl3 nuclear translocation.

The transactivation potential of Bcl3 and all its mutants was investigated by performing the luciferase assays using P-Seletin κB reporter. As shown in Chapter II, when expressed alone, Bcl3 did not induce the luciferase activity; however, when coexpressed with p52, Bcl3 strongly enhanced the luciferase activity on P-Selectin reporter than the reporter alone control (Figure 2.3). Therefore, all the expressing Bcl3 mutants, S33E, S446E, S446A, EE, and EA, were expressed to a similar level in the nucleus (Figure 4.7b) and tested in luciferase assays in complex with p52 homodimer to activate P-Selectin κB reporter. Compare to wt Bcl3, S446E showed enhancement of the transcriptional activity and S446A significantly reduced the activity; double mutant EE further enhanced the transcriptional activity slightly compare to that of the S446E single mutant (Figure 4.7a). Taken together, these results demonstrate that Bcl3 phosphorylation at Ser446

enhances its activity as co-activator with p52 homodimer. As discussed above, phosphorylation at Ser33 was important for the protein expression/stability; therefore, the strongest transcriptional activity displayed by the EE double mutant was due to the higher protein level in the nucleus.

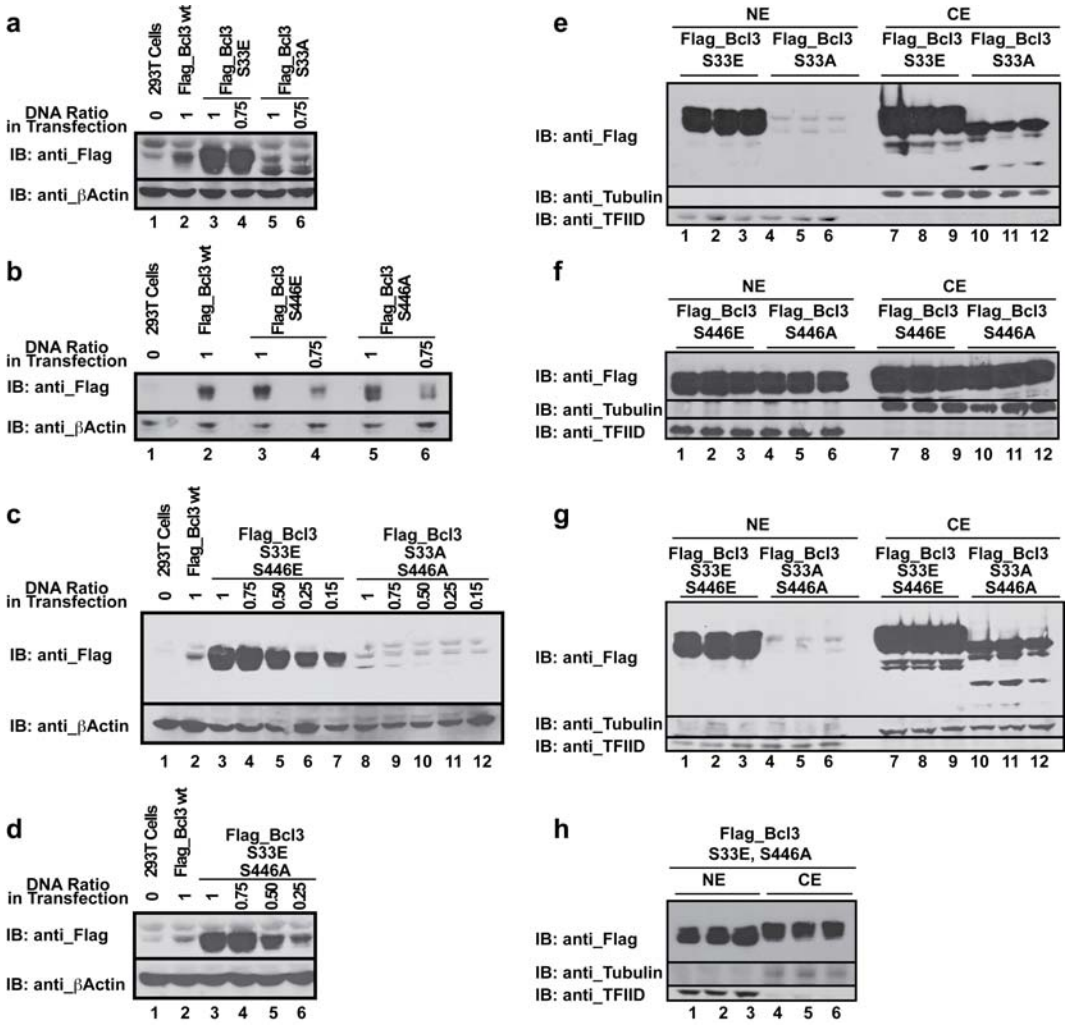

Figure 4.6 Phosphorylation of Bcl3 Ser33 regulates its protein expression. Total protein expressions of a) Bcl3 S33E and S33A; b) Bcl3 S446E and S446A; c) Bcl3 S33E/S446E and S33A/S446A; d) Bcl3 S33E/S446A mutants. Different amounts of DNA were used for the transfection in HEK 293T cells in order to monitor the expression levels. Nuclear and cytoplasmic expressions of e) Bcl3 S33E and S33A; f) Bcl3 S446E and S446A; g) Bcl3 S33E/S446E and S33A/S446A; h) Bcl3 S33E/S446A mutants.

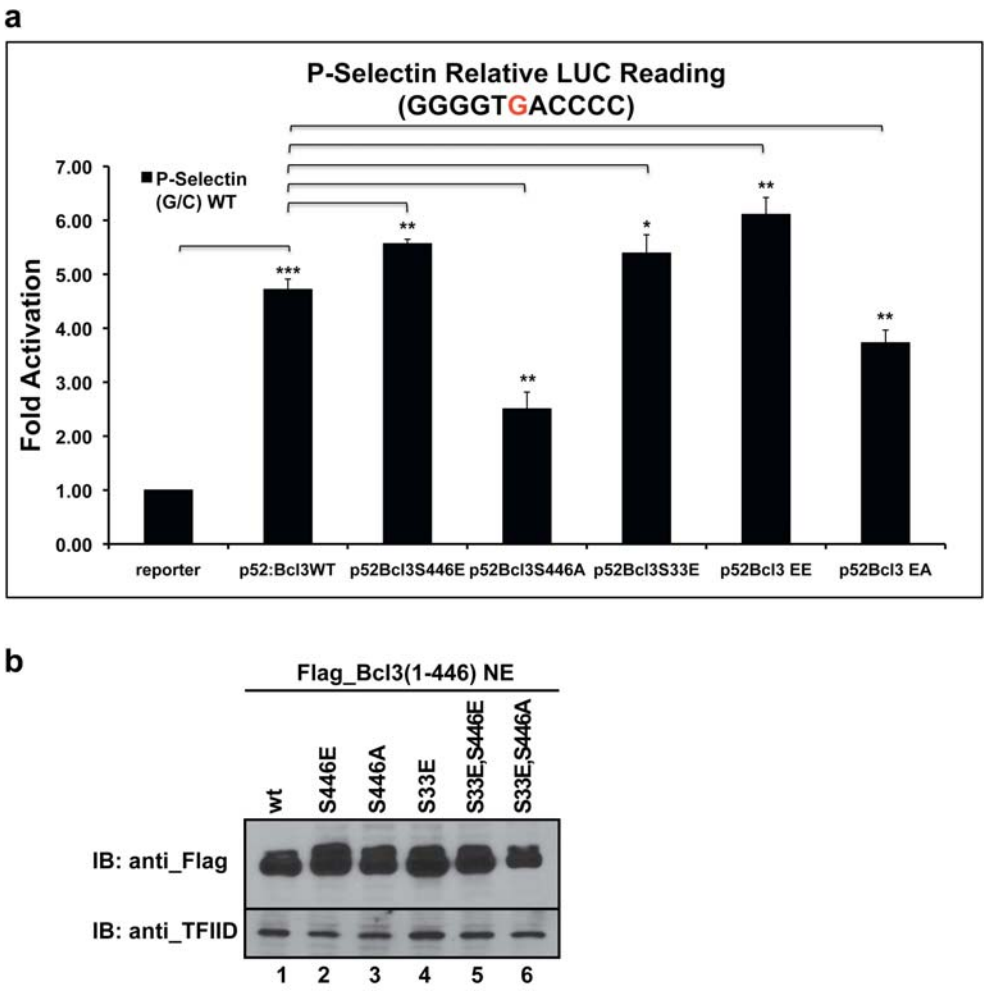

Figure 4.7 Phosphorylation of Bcl3 Ser446 enhance p52:Bcl3 transcriptional activity. a) Transcriptional activities of wt and different mutants of Bcl3 complex with p52 on P-Selection luciferase reporter. The data was analyzed from three independent experiments performed in triplicate. *p<0.05, **p<0.01, ***p<0.005. Error bars represent SD. b) Nuclear expression of wt and different Bcl3 mutants analyzed by anti-Flag Western Blot.

4. Phosphorylation of Bcl3 Modulates its Interaction with p52 Homodimer

It is know that the GSK3-mediated Bcl3 phosphorylation at Ser394 and Ser398 targets its proteasomal degradation (Viatour et al., 2004a). To determine whether the phosphorylations at Ser33 and Ser446 of Bcl3 also regulate its degradation, Flag-tagged Bcl3 wt and all the phosphomimic and phospho-inactive mutants were expressed in HEK 293T cells and treated with an inhibitor of protein synthesis, cycloheximide (CHX), up to 24 hours in order to monitor the protein half-life. We observed no significant differences between wt Bcl3 and all the mutants (Figure 4.8). This suggested that the impaired activity of Bcl3 S446A mutant on p52 homodimer transcription did not result from the short protein half-life.

As phospho-mimic mutations at Bcl3 Ser33 and Ser446 enhance its transactivation potential on p52 target reporter. And Bcl3 controls p52 homodimer transcription through the formation of hetercomplexes with p52 homodimer (Bours et al., 1993; Franzoso et al., 1993; Fujita et al., 1993). We investigated whether Ser33 and Ser446 phosphorylation regulates Bcl3's ability to bind with p52 protein. Since full-length Bcl3 could not be purified from *E.coli*, constant amount of nuclear extracts from HEK 293T cells transfected with Flag-tagged Bcl3 wt and mutants plasmids were Flag immunoprecipitated with recombinant non-tagged p52(1-408) at various concentration. Anti-p52 and anti-Bcl3 Western Blots were performed on the immunoprecipitates (Figure 4.9). In these conditions, recombinant p52 homodimer interacted with

Bcl3 S446E mutant with high affinity than wt Bcl3; and S446A mutant significantly impaired its interaction with p52 (Figure 4.9a and b). And the interaction was further enhanced by the double phospho-mimic EE mutant (Figure 4.9c and d). Taken together, these results demonstrated that Bcl3's ability to interact with p52 was modulated by the phosphorylations at Ser33 and Ser446. Phosphorylated Bcl3 interacts with p52 with higher affinity; and therefore enhancing the transactivation potential on p52 regulated gene transcription.

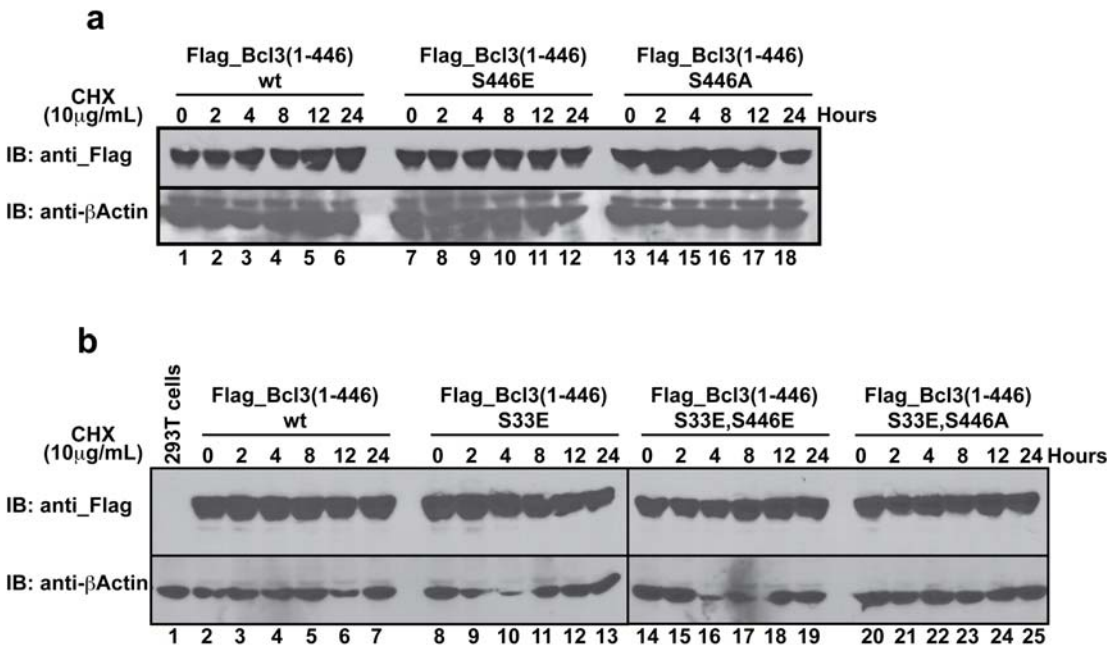

Figure 4.8 Phosphorylation of Bcl3 Ser33 and Ser446 does not affect its protein stability. a) Flag-tagged Bcl3 S446E and S446A b) Flag-tagged Bcl3 S33E, S33E/S446E, and S33E/S446A together with wt Flag-tagged Bcl3 were transfected into HEK 293T cells and followed by CHX treatment for different time as indicated. All Bcl3 mutants showed similar half-life comparable to wt protein.

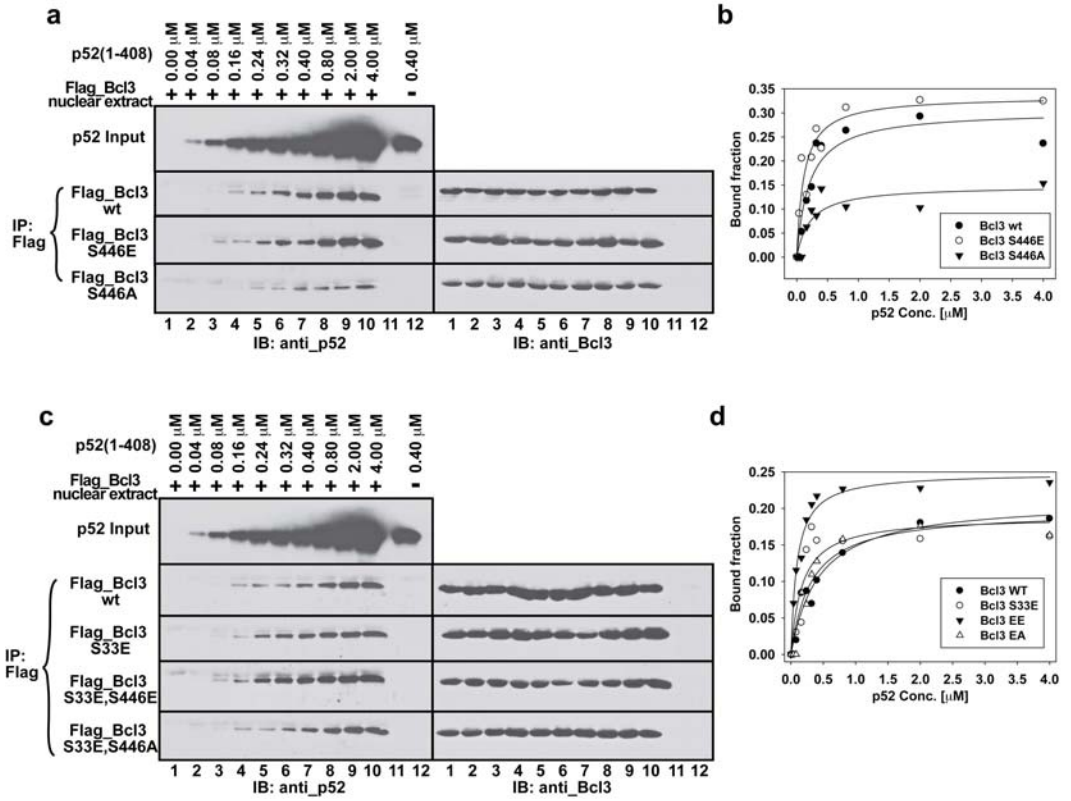

Figure 4.9 Phosphorylation of Bcl3 Ser33 and Ser446 enhance its interaction with p52. Flag immunoprecipitation demonstrates the binding of recombinant p52(1-408) to different Flag-tagged Bcl3 mutants a) Western analysis showing Flag-tagged Bcl3 wt, S446E, and S446A binding to p52 at various concentrations. b) Bound p52 was plotted against the total p52 input at various concentrations, demonstrating that Bcl3 S446E has greater binding affinity towards p52 homodimer than wt Bcl3; and Bcl3 S446A inhibits the binding. c) Western analysis showing Flag-tagged Bcl3 wt, S33E, S33E/S446E, and S33E/S446A binding to p52 at various concentrations. d) Bound p52 was plotted against the total p52 input at various concentrations. Bcl3 S33E/S446E showed the greatest affinity towards p52 homodimer.

5. Phosphorylation of Bcl3 might be Mediated by Akt

In the process of further studying the regulation of Bcl3 phosphorylation, group-based prediction system (GPS 2.1) (Xue et al., 2008) was used to search for Bcl3 kinases targeting residue Ser 33 and Ser446. Serveral potential kinase candidates were identified including Akt and NIK. Previous studies have shown that Akt, a downstream effector of the PI3K, regulates both canonical and non-canonical NF-κB signaling pathways. In particular, it regulates both basal and induced NF-κB2/p100 processing to p52 through IKK1 (Gustin et al., 2006). The GSK3β-mediated Bcl3 phosphorylation and proteasomal degradation is also prevented by the Akt activation (Viatour et al., 2004a). In addition, recent study from the Perkins' group has shown that the Akt/GSK3β pathway regulates Skp2 promoter activity through p52 NF-κB subunit and tumor suppressor p53 (Barre and Perkins). Therefore, we hypothesized that phosphorylation of Bcl3 at residue Ser33 and Ser446 might also be regulated by the Akt pathway. To determine whether Bcl3 is phosphrylated by Akt, a potent inhibitor of PI3Ks, wortmannin, and also a specific Akt inhibitor, Akt inhibitor VIII which is a highly selective non-competitive inhibitor of Akt1 and 2 (Bain et al., 2007), were used in the P-Selectin κB reporter assay when p52 and Bcl3 were co-expressed in HeLa cell. Addition of both wortmannin and Akt inhibitor VIII decreased the p52:Bcl3 complex transcriptional activity in the reporter assay (Figure 4.10a). Treatment of wortmannin and Akt inhibitor in HeLa cells only decreased the amount the active Akt without affecting the total protein amount (Figure 4.10b). This

suggested that the kinase activity of Akt might play a role in the phosphorylation of Bcl3 at Ser33 and Ser446 which in turn regulating its transactivation potential with p52.

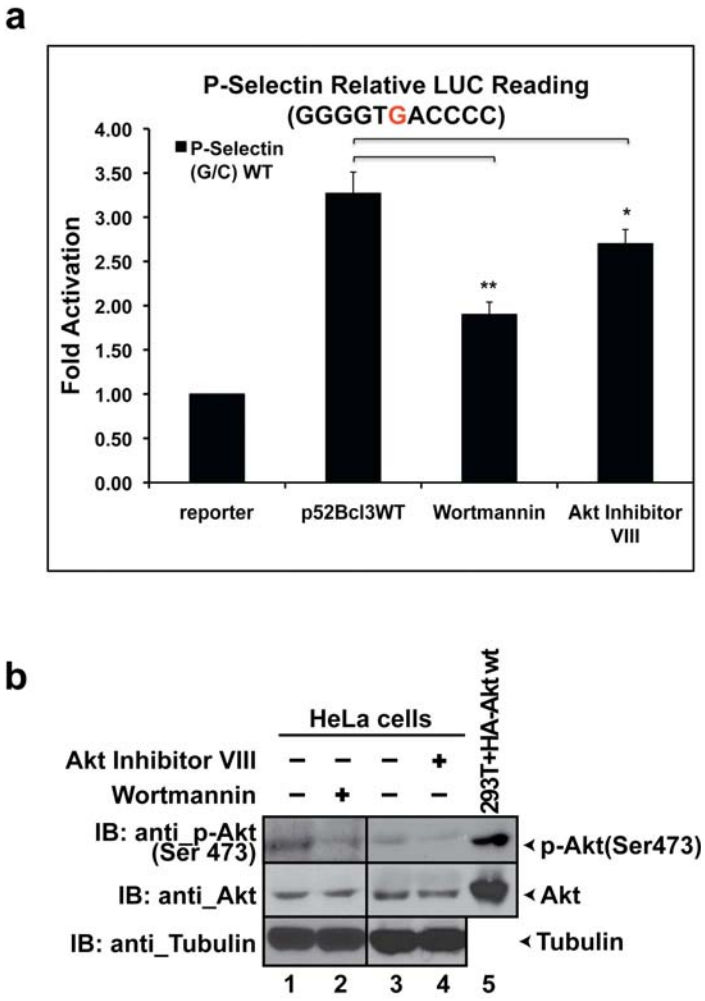

Figure 4.10 Bcl3 phosphorylation is regulated by Akt pathway. a) Wortmannin and specific Akt Inhibitor VIII inhibits Bcl3 transcriptional activity with p52 on P-Selectin luciferase reporter. The data was analyzed from three independent experiments performed in triplicate. *p<0.05, **p<0.01. Error bars represent SD. b) Both wortmannin and Akt Inhibitor VIII inhibits Akt kinase activity in HeLa cells. HeLa cells were left untreated (lane 1 and 3) or treated with 0.5 μM wortmannin (lane 2) or 5 μM Akt Inhibitor VIII (lane 4) for 48 hours. Cell extracts were subjected to anti-p-Akt(Ser473) and anti-Akt Western analysis. HA-tagged wt Akt was transiently transfected into HeLa cells used as a control for Akt expression (lane 5).

D. Discussion

1. Insight of Bcl3's Physiological Role

Bcl3 is a known specific transcriptional co-activator for NF-κB p52 homodimer; however, the mechanistic role of how Bcl3 activates p52 homodimer dependent transcription is not well understood. The Bcl3 activity *in vivo* may potentially be controlled at several levels: the NF-κB dimer identity, κB DNA sequence, protein phosphorylation, and interaction with other transcription factors and co-activators. Thus, the physiological role of Bcl3 might be dependent on the local influences in cells. Previous studies demonstrated that there are multiple phosphorylation states of Bcl3. However, only phosphorylation at residues Ser 394 and Ser 398 has been shown to link to the proteasome mediated degradation of Bcl3. In this study, we have identified two more phosphorylation sites, Ser33 and Ser446. Phosphorylation at Ser446 is required for the transcriptional activity of p52 homodimer. And this specificity is irreplaceable with RelA transcription activation domain as shown in Figure 4.1. This observation suggested that Bcl3 help targeting p52 homodimer at its specific κB DNA in the promoter.

In addition, based on our lab's unpublished data, we know that although the dimer interface of different NF-κB dimers looks very similar in the X-ray structures, and a set of similar residues are involved in the dimer formation; however, the dimerization affinities vary significantly among different NF-κB homo- or hetero-dimers. The strength of p52 homodimer is about 1000-fold weaker than p50 homodimer from the analytical

ultracentrifugation (AUC) analysis of recombinant p52 and p50 DD dimers. This raises another possibility which is p52 homodimer formation *in vivo* might require special “induced” condition; and Bcl3 could function as the inducer which enforces p52 homodimer formation. This explains the reason that the p52-RelA(TAD) fusion protein could not activating gene transcription since it could not form a stable dimer on it own in cells. As mentioned before, IκB induced NF-κB dimerization might be specific; IκBα preferentially stabilize p50/RelA heterodimer, IκBε was reported to bind specifically to RelA and c-Rel homodimers, IκBβ might be specific to the RelA/c-Rel heterodimer at least in association with DNA, IκBζ exhibited specificity towards the p50 homodimer. Therefore, only in the presence of Bcl3, it would stimulate p52 homodimer formation as well as help p52 targeting its κB DNA to form a ternary p52:Bcl3:DNA ternary complex and activate gene transcription. The weak p52 homodimer affinity might also influence the processing of NF-κB2/p100 to generate p52. Both NF-κB p50 and p52 subunits are generated from their precursor protein NF-κB1/p105 and NF-κB2/p100 respectively. p105 constitutively processes to p50 *in vivo*; however, p100’s processing to p52 is stimulus dependent. Despite of the high molecular similarity between these two proteins, the detail mechanistic differences in constitutive versus stimulus dependent processing of p105 and p100, respectively, are yet to be elucidated. To answer these questions, our lab is currently making efforts to generate mutations in p52 dimerization domain which will stabilize the p52 homodimer. Once the p52 stabilized DD mutants were generated, the

combination of structural, biochemical, and structure-based cell biological experiments will be carried out to further understand the connection between p100 processing, p52 dimer stability and its transcriptional activity. These will provide further understanding of the mechanism of p52:Bcl3 regulation both biochemically and physiologically.

2. Phosphorylation of Bcl3 at Ser33 and Ser446

In this chapter, we also identified two new Bcl3 phosphorylation sites, Ser33 and Ser446. These two are residues constitutively phosphorylated in cells. Phosphorylation at Ser446 enhances Bcl3's interaction with p52 homodimer, and hence increases its transactivation potential of the p52:Bcl3 complex. Luciferase assay with specific kinase inhibitors suggested the two new phosphorylation sites of Bcl3 might be regulated by the Akt pathway (Figure 4.7, 4.9, and 4.10). Phosphorylation at Ser33 plays an important role in the protein expression/stability of Bcl3 and perhaps its nuclear localization. When Ser33 was mutated to Ala, the total protein level of Bcl3 is decreased and only a small fraction translocated into nucleus. It is known that wt Bcl3 migrates abnormally as multiple bands in SDS-PAGE analysis due to the extensive phosphorylation at its C-terminus. In transfection studies, Bcl3 S33A as well as the AA double mutant migrated much faster (lower molecular weight) than wt Bcl3, S33E, EE, and EA mutants; and the phosphorylation states of the S33A and AA mutants seemed to be different than wt as the multiple bands pattern disappeared (Figure 4.6). However, the N-terminal

truncated construct of Bcl3(119-446) did not show either protein expression or nuclear localization problems, it migrated as multiple bands similar to the wt Bcl3 protein (Figure 4.2). All these observations suggested that the expression level, nuclear localization, and phosphorylation of Bcl3 are regulated by a complicated mechanism in cells. Since Ser33 is very close to the NLS sequence of Bcl3, we speculate that when Ser33 is de-phosphorylated in cells, it might block the NLS sequence; and there might be conformational change upon Ser33 phosphorylation which will expose the NLS sequence enabling Bcl3 translocated to the nucleus. In addition, lack of Ser33 phosphorylation resulted in less phosphorylation states of the total protein. This suggested that some of Bcl3's C-terminal phosphorylation might happen in the nucleus; once certain serine residues got phosphorylated in the nucleus, Bcl3 could be shuttle between nucleus and cytoplasm since both nuclear and cytoplsmic wt Bcl3 migrates in a similar pattern as multiple bands. It is not clear to us at this point why the N-terminal truncated Bcl3 could localize in the nucleus; probably there are other mechanisms regulate Bcl3's nuclear localization other than the NLS sequence.

Currently, we are generating phospho-specific antibodies targeting Bcl3 phospho-Ser33 and phospho-Ser446 using phospho-peptides. Once we get the good quality phospho-specific antibodies, we could use these antibodies to study phosphorylation of endogenous Bcl3 in different cell lines. We will use siRNA to knockdown endogenous Akt to further confirm if both of these newly identified phosphorylation sites are regulated by Akt in cells. Previous studies

have showed that in certain cell types, such as erythroblasts, hepatocytes, and keratinocytes, Bcl3 resides in the cytoplasm and requires activation prior to nuclear translocation (Brasier et al., 2001; Massoumi et al., 2006; Zhang et al., 1998). However, the signals activate Bcl3 and recruit Bcl3 to the NF-κB p52 homodimers in the nucleus are not known. Phospho-specific antibodies could be useful in the further study of the mechanism of Bcl3 regulation in cells both biochemically and physiologically.

E. Chapter IV Acknowledgements

I thank Dr. Majid Ghassemian at the UCSD Biomolecular and Proteomics Mass Spectrometry Facility for performing the phosphopeptide enrichment and LC-MS/MS analysis; and for all his help with interpreting the data.

Chapter V: Identification of a Crystallizable Construct of the p52:Bcl3 Core Complex and its Crystallization

A. Introduction

The Rel/NF-κB subsunits constitute a family by virtue of their high sequence homology near the N-terminus and this homologous region, known as the rel homology region (RHR) is responsible for subunit dimerization, DNA binding, and nuclear localization of NF-κB dimers. NF-κB subunits can be divided into two classes. The p50 and p52 subunits belong to class I by virtue of not having a transcription activation domain (TAD), thus categorizing them as transcriptional repressors. But instead TAD, p50 and p52 have a short glycine rich region (GRR) which caps the C-terminus (Baldwin, 1996; Ghosh et al., 1998). The function of GRR in transcription, if any, is unknown. The p50 and p52 subunits are generated from the precursor proteins p105 and p100, respectively. The other three subunits, RelA, cRel and RelB, constitute class II which contains a TAD. Homo- and heterodimers with at least one class II subunit have transcription activation (Baldwin, 1996; Ghosh et al., 1998).

NF-κB family regulates expression of hundreds of genes by binding to specific κB DNA sequences. In unstimulated cells, NF-κB dimers with transcription activation potential are maintained inactive through stable protein-protein association with a class of inhibitor proteins known as IκB. A large variety of extracellular signals activate NF-κB by degradation of IκB through concerted actions of IκB kinase (IKK), ubiquitin ligases, and the 26S proteasome (Karin and Ben-Neriah, 2000). This pathway, known as canonical pathway, initiated by a large number of physiological and non-physiological

stimuli activates RelA and c-Rel containing homo- and heterodimers (Ghosh and Karin, 2002).

NF-κB p50 and p52 are generated from their precursors, p105 and p100, respectively, through an event where the C-terminal regions of these two precursors are degraded. In both cases, however, the processing is limited. Only a fraction of these precursors are processed. The unprocessed p105 and p100 precursors act as the inhibitors of NF-κB subunits (Ghosh et al., 1998). However, the modes of processing are different in these two cases. In case of p105 processing, p105 undergoes constitutive processing which results in constitutive p50 in the nucleus (Moorthy et al., 2006). On the other hand, the processing of p100 into p52 is tightly regulated, which requires specific stimuli to activate the p100 processing pathway (Senftleben et al., 2001; Xiao et al., 2004), which is known as non-canonical signaling pathway.

In the nucleus, p52 functions in association with its specific transcriptional co-factor Bcl3 (Sun and Xiao, 2003). Bcl3 is a putative oncoprotein first discovered during the studies of B-cell chronic lymphocytic leukemias (Ohno et al., 1990). Bcl3 is a distinctive member of the IκB family because it can function to co-activate transcription and is present predominantly in the nucleus. The IκB family shares a conserved domain of six or seven ankyrin (ANK) repeats (Ghosh et al., 1998), a 33-residue sequence motif present in a large number of eukaryotic and prokaryotic proteins (Bork, 1993; Michaely and Bennett, 1992). Crystal structures of several such proteins reveal that ANK repeats form an L-shaped structure

composed of a β-hairpin and two antiparallel α-helices packing together to yeild a left handed superhelix (Sedgwick and Smerdon, 1999). Three groups of IκB ankyrin specificities can be distinguished: the precursor protein p100 and p105 bind to all known mammalian NF-κB factors; IκBα, IκBβ and IκBε strongly prefer dimers containing RelA or c-Rel; in contrast, Bcl3 has a strong preference towards p50 or p52 homodimers. Bcl3, in particular, has seven ANK in the middle region, called ANK domain (ARD); it also has proline rich N-terminal and proline/serine rich C-terminal domains (Figure 5.1) (Ghosh et al., 1998). Bcl3 has properties of a transcriptional co-activator, bridging transcription factors with the basal transcription machinery. Previous studies have shown that upon stimulation, Bcl3 C-terminal domain is highly phosphorylated, and this phosphorylation may affect its regulation of NF-κB-dependent transcription *in vivo* (Massoumi et al., 2006; Viatour P, 2004; Viatour P, 2005).

To investigate the differences in the activation and the regulation of different NF-κB dimers exhibited by the different IκB proteins, studying the precise molecular structures of the different NF-κB:IκB complexes would lead us a better understanding of their cellular functions. X-ray crystallography is one of the most widely used techniques for structural determination of biological macromolecules at atomic level. X-ray crystallography is usually preferred to study high molecular weight macromolecules comparing with nuclear magnetic resonance (NMR) spectroscopy. One of the major obstacles in protein X-ray crystallography is obtaining well-diffracting crystals of the

target macromolecules. In order to do so, one has to purify the target protein to homogeneity and crystallize it from the aqueous solution. However, many regions within proteins could be flexible and disordered which may lead to the failure in crystallization of the target protein. To overcome this difficulty, flexible regions with no biological significance could be removed to facilitate crystallization.

X-ray crystal structure of human Bcl3 ARD has been determined (Michel et al., 2001), and the overall structure of the Bcl3 ANK repeats are highly similar to the IκBα crystal structure. Therefore, we reasoned that determining the X-ray crystal structure of the p52:Bcl3 complex would provide us better understanding of the differences between NF-κB:IκB inhibition vs. activation complex in the atomic level; and also giving us better understanding of the mechanism of the gene regulation by the p52 and Bcl3. In this chapter, based on the knowledge of IκBα:p50/RelA and IκBβ:RelA crystal structures which have been solved in our lab previously, we determined that Bcl3 ARD bound to p52 homodimer asymmetrically, only one GRR of the p52 dimer was involved in the interactions with Bcl3 ARD. We also identified a crystallizable recombinant human p52:Bcl3 core complex. This core complex was expressed and purified in *E.coli* successfully, and small crystals were obtained.

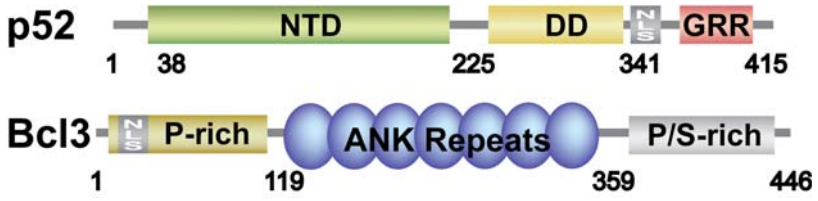

Figure 5.1 Schematic Representation of human p52 and Bcl3.

B. Materials and methods

1. Human p52 Expression Plasmids

p52(225-341): Non-tagged p52(225-341) in pET11a (Novagen) was provided by Don Vu.

p52(225-415): Non-tagged p52(225-415) in pET11a (Novagen) was generated by PCR reaction using human pHis8-p100(1-899) as a template, N-terminal primer containing NdeI restriction site: p100_NdeI_225F: 5'-G GAA TTC CAT ATG GCA TCA AAC CTG AAG ATT TC-3'

C-terminal primer containing BamHI restriction site: p100_BamHI_415R: 5'-CG GGA TCC GTC CCT GCT GGG CAC C-3'

The PCR reaction product was first gel purified, then double digested with NdeI and BamHI restriction enzymes (NEB), and gel purified again. The DNA fragment was then ligated in pET11a vector at the corresponding cut sites.

2. Mutagenesis of human p52

p52(225-415)D234N, Y247F: pET11a-p52(225-415) mutant contain two mutations at the dimmer interface was generated using QuickChange site-directed mutagenesis by introducing one mutations at a time. The QuickChange site-directed mutagenesis method was performed using *PfuTurbo* DNA polymerase (Stratagene). The mutagenic DNA oligonucleotide primers listed bellowed were used to amplify the mutated gene construct. The PCR product was first restriction digested by DpnI enzymes (NEB) to remove

template. The nicked products were then transformed into DH5α *E.coli* cells. Plasmids isolated from transformations were sequenced to verified the presence of mutations:

hp52D234N_F: 5'-C CTG AAG ATT TCT CGA ATG AAC AAG ACA GCA GGC-3'

hp52D234N_R: 5'-GCC TGC TGT CTT GTT CAT TCG AGA AAT CTT CAG G-3'

hp52Y247F_F: 5'-G GGT GGA GAT GAA GTT TTC CTG CTT TGT GAC AAG GTG C-3'

hp52Y247F_R: 5'-G CAC CTT GTC ACA AAG CAG GAA AAC TTC ATC TCC ACC C-3'

3. Human Bcl3 Expression Plasmid

Bcl3(119-359): Non-tagged Bcl3(119-359) in pET11a (Novagen) was generated by PCR reaction using human pEYFPC1-YFP+NTFlag+Bcl3(1-447) as a template, N-terminal primer containing NdeI restriction site: hBcl3_NdeI_119F: 5'- G GAA TTC CAT ATG ATG GCC ACC CGT GCA GAT G-3'

C-terminal primer containing BamHI restriction site: hBcl3_BamHI_359R: 5'-CG GGA TCC GGA AGC AGG CCG GGT GG-3'

The PCR reaction product was first gel purified, then double digested with NdeI and BamHI restriction enzymes (NEB), and gel purified again. The DNA fragment was then ligated in pET11a vector at the corresponding cut sites.

4. Human p52-Bcl3 Fusion Protein Expression Plasmid

p52(225-415)D234N, Y247F_5Gly_Bcl3(119-359): Expression plasmid of His-tagged p52(225-415)D234N, Y247F_5Gly_Bcl3(119-359) in pET29b (Novagen) vector was generated by two-step PCR reaction. During the first round of PCR reaction, p52(225-415)D234N, Y247F with five glycines linked at the C-terminus and Bcl3(119-359) were generated separately. For p52(225-415)D234N, Y247F_5Gly fragment, the pET11a-p52(225-415)D234N, Y247F was used as PCR template, the N-terminal primer containing NdeI restriction site: p100_NdeI_225F: 5'-G GAA TTC CAT ATG GCA TCA AAC CTG AAG ATT TC-3'; C-terminal primer containing BamHI restriction site and linked with five glycines sequence: p100_BamHI_415RGly: 5'-CG GGA TCC TCC TCC TCC TCC TCC GTC CCT GCT GGG CAC C-3'.

For Bcl3 fragment, the pET11a-Bcl3(119-359) was used as PCR template, the N-terminal primer containing NdeI restriction site: hBcl3_BamHI_119F: 5'-CG GGA TCC ATG GCC ACC CGT GCA GAT G-3'; C-terminal primer containing EcoRI restriction site: hBcl3_EcoRI_359R: 5'-CG GAA TTC GGA AGC AGG CCG GGT GG-3'.

The resulting PCR products of the two DNA fragments were then used as templates in the second round PCR reaction, and the two primers p100_NdeI_225F and hBcl3_EcoRI_359R were used. The resulting p52_5Gly_Bcl3 DNA fragment was then gel purified and double digested with

NdeI and EcoRI restriction enzymes (NEB), and gel purified again. The DNA fragment was then ligated in pET29b vector at NdeI and EcoRI cut sites.

5. Expression and Purification of Recombinant Protein Complexes

p52(225-415):Bcl3(119-359) Complex: *E.coli* BL21(DE3) cells transformed with pET11a-p52(225-415) and pET11a-Bcl3(119-359) respectively were grown in 2 L of LB/Ampicillin (100 μg/mL) broth to an $O.D._{600}$ of 0.6 at 37°C and induced with 0.5 mM IPTG for 3 hours at 37°C. Cells were harvested by centrifugation. Cell pellets of pET11a-p52(225-415) and pET11a-Bcl3(119-359) were resuspended together in 150 mL of lysis buffer containing 20 mM Tris pH 7.5, 100 mM NaCl, 5% glycerol, 2 mM EDTA, 0.5 mM PMSF, 10 mM βME, 100 μL of Sigma Protease Inhibitor Cocktail (Sigma/Alrich). The resuspended cells were lysed at 4°C by sonication five times at 1 minute burst intervals. The lysed cells were then centrifuged to remove insoluble fraction. The soluble fraction was loaded onto a fast flow S-sepharose column at 4°C. The column was washed and eluted with 100 mM to 1 M NaCl gradient. The peak fractions were analyzed by 12.5% SDS-PAGE. The pooled peak fractions were concentrated using Centriprep-10 (Amicon) at room temperature and loaded onto a Superdex-75 gel filtration column (GE Healthcare) which was pre-equalibrated with 350 mM NaCl, 20 mM Tris pH 7.5, 2 mM EDTA, 5% glycerol, 0.5 mM PMSF, 5 mM DTT. Pooled peak fractions were concentrated to ~50 mg/mL, aliquoted, flash frozen by liquid nitrogen and stored at -80°C.

p52(225-415) D234N, Y247F/p52(225-341):Bcl3(119-359) Complex: *E.coli* BL21(DE3) cells transformed with the corresponding p52 and Bcl3 were grown in LB/Ampicillin (100 μg/mL) broth to an $O.D._{600}$ of 0.6 at 37°C and induced with 0.5 mM IPTG for 3 hours at 37°C. Pelleted cells from 1 L culture of pET11a-p52(225-415) D234N, Y247F, 1 L culture of pET11a-p52(225-341), and 2 L culture of pET11a-Bcl3(119-359) were resuspended together in 150 mL of lysis buffer containing 20 mM Tris pH 7.5, 100 mM NaCl, 5% glycerol, 2 mM EDTA, 0.5 mM PMSF, 10 mM βME, 100 μL of Sigma Protease Inhibitor Cocktail (Sigma/Alrich). The resuspended cells were lysed at 4°C by sonication five times at 1 minute burst intervals. The lysed cells were then centrifuged to remove insoluble fraction. The soluble fraction was loaded onto a fast flow S-sepharose column at 4°C. The column was washed and eluted with 100 mM to 1 M NaCl gradient. The peak fractions were analyzed by 12.5% SDS-PAGE. The pooled peak fractions were concentrated using Centriprep-10 (Amicon) at room temperature, diluted 4-fold with 100 mM NaCl lysis buffer, and then loaded onto a 5 mL HiTrap-SP column (GE Healthcare) pre-equilibrated with 20 mM Tris pH 7.5, 100 mM NaCl, 5% glycerol, 2 mM EDTA, 0.5 mM PMSF, 5 mM DTT. The column was washed and eluted with 100 mM to 500 mM NaCl gradient. The peak fractions containing p52(225-415) D234N, Y247F/p52(225-341):Bcl3(119-359) complex were concentrated and loaded onto a Superdex-200 gel filtration column (GE Healthcare) which was pre-equalibrated with 350 mM NaCl, 20 mM Tris pH 7.5, 2 mM EDTA, 5%

glycerol, 0.5 mM PMSF, 5 mM DTT. Pooled peak fractions were concentrated to ~12 mg/mL, aliquoted, flash frozen by liquid nitrogen and stored at -80°C.

p52(225-415) D234N, Y247F_5Gly_Bcl3(119-359):p52(224-341) Complex: *E.coli* BL21(DE3) cells co-transformed with the corresponding plasmids were grown in 2 L of LB broth containing both Ampicillin (100 μg/mL) and Kanamycin (30 μg/mL) to an $O.D._{600}$ of 0.6 at 37°C and induced with 0.4 mM IPTG overnight at room temperature. Cell pellets were resuspended in 100 mL of lysis buffer containing 20 mM Tris pH 7.5, 100 mM NaCl, 2mM EDTA, 0.5 mM PMSF, 10 mM βME, 8 M Urea, and 100 μL of Sigma Protease Inhibitor Cocktail (Sigma/Alrich). The resuspended cells were lysed at 4°C by sonication four times at 30 second burst intervals. The lysed cells were then centrifuged to remove insoluble fraction. The soluble fraction was loaded onto a fast flow S-sepharose column at room temperature. The column was washed and eluted with 100 mM to 1 M NaCl gradient. The elutions were analyzed by 12.5% SDS-PAGE. The pooled peak fractions were dialysed overnight in three changes of 4 L buffer containing 20 mM Tris pH 7.5, 200 mM NaCl, 2 mM EDTA, 0.5 mM PMSF, 10% glycerol, and stepwise decrease of Urea from 5 M, 2 M, to 0 M Urea. The dialysed protein was centrifuged and filter using 0.22 μm filter to remove precipitates, and then diluted 2-fold with No-Salt buffer (20 mM Tris pH 7.5, 10% glycerol, 2 mM EDTA, 0.5 mM PMSF, and 2mM DTT) and then loaded onto a 5mL HiTrap-SP column (GE Healthcare) pre-equilibrated with 20 mM Tris pH 7.5, 100 mM NaCl, 5%

glycerol, 2 mM EDTA, 0.5 mM PMSF, 2 mM DTT. The column was washed and eluted with 100 mM to 500 mM NaCl gradient. The peak fractions containing p52(225-415) D234N, Y247F-5Gly_Bcl3(119-359):p52(225-341) complex were concentrated and loaded onto a Superdex-200 gel filtration column (GE Healthcare) which was pre-equalibrated with 350 mM NaCl, 20 mM Tris pH 7.5, 2 mM EDTA, 5% glycerol, 0.5 mM PMSF, 2 mM DTT. Pooled peak fractions were concentrated to ~15 mg/mL, aliquoted, flash frozen by liquid nitrogen and stored at -80°C.

6. Limited Proteolysis

Limited proteolysis reactions (1:2500 protein protease ratio) were performed using 88 μg (110 μL in volume) of p52(225-415):Bcl3(119-359) complex and 0.032 μg of either trypsin or chymotrypsin at room temperature. 10 μL aliquots of reaction mixtures were removed at each time point from 0 to 3 hours from the starting point of the reaction. The last aliquot was left at room temperature for overnight to see the completeness of the cleavage. At each time point, the reaction was stopped by boiling the samples with SDS buffer at 95°C for 5 minutes. The samples were then analyzed by 15% SDS-PAGE.

7. Crystallization of p52:Bcl3 complex

Initial crystallization trials of different p52:Bcl3 complexes were performed by the hanging drop vapor diffusion at room temperature using the Hampton Screen (Hampton Research). Each drop contained 1.5 μL of

p52:Bcl3 complex protein at ~12 mg/mL mixed with 1.5 μL of reservoir solution containing additional 2 mM DTT. The optimal condition for p52:Bcl3 protein complex crystallization was found to be 2 M ammonium sulfate, 100 mM sodium citrate pH 5.5 – 6.5, 5% PEG 8000, and 2 mM DTT in the reservoir.

C. Results

1. Identification of the core p52:Bcl3 complex

We have investigated if Bcl3 and p52 form a thermodynamically stable complex by examining the behavior of the complex under size exclusion chromatography. Although we invested significant amount of time to produce wt Bcl3 protein in *E. coli*, large amount of highly pure protein required for crystallization trials could not be isolated. Full length Bcl3 is proteolytically sensitive and degrades continuously as the protein is produced in the cell. Published reports clearly demonstrated that the ankyrin repeat domain (ARD) of Bcl3 is solely responsible for p52 binding (Bours et al., 1993), and thus I focused on the ARD of Bcl3. We found that the Bcl3 ARD binds to the p52 homodimer. We also found that the N-terminal domain of p52 is not essential for Bcl3 binding on size exclusion chromatography. Finally, we also found that the binding requires the GRR of p52. However, p52 homodimer containing the GRR are unstable and the GRR portion degrades during purification. To circumvent this problem, we have used a co-purification strategy where cell pellets containing over-expressed Bcl3 ARD and p52(225-415) are lysed together, sonicated and purified through multiple chromatographic steps. The complex is highly pure and does not undergo degradation (Figure 5.2). This complex has been tested for crystallization.

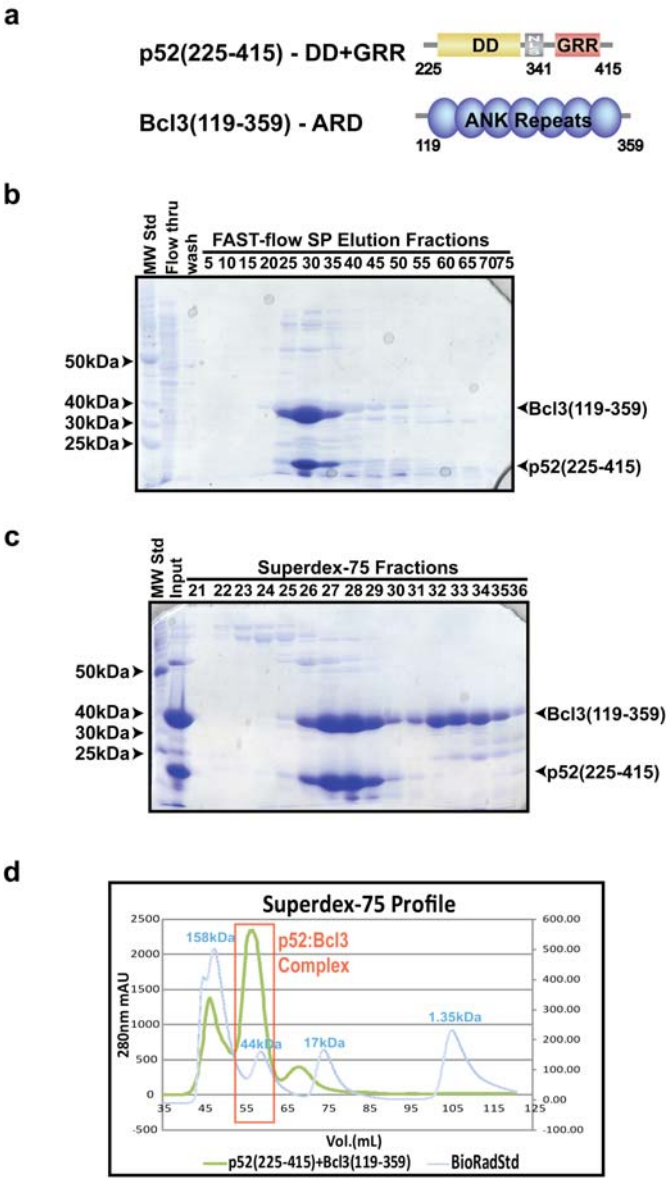

Figure 5.2 Purification of recombinant human p52(225-415):Bcl3(119-359) protein complex. a) Schematic representation of p52 and Bcl3 constructs used.Schematic representation of human p52 and Bcl3. b) 12.5% SDS-PAGE analysis of crude p52(225-415):Bcl3(119-359) lysate purified by cation exchange chromatography (fast flow S-sepharose). c) 12.5% SDS-PAGE analysis of fractions from Superdex-75 size exclusion chromatography. d) Superdex-75 size exclusion chromatography elution profile shows p52 and Bcl3 form a stable complex which eluted as a single peak. Overlaying with MW standards (BioRad) indicates the complex contains one molecule of p52 homodimer and one molecule of Bcl3.

2. The GRRs of p52 bind Bcl3 Asymmetrically

Based on the knowledge of the crystal structures of the IκBβ:RelA(p65) complex done previously in our laboratory, the ARD of IκBβ binds to RelA homodimer asymmetrically; only one of the RelA nuclear localization sequence (NLS) interacts with IκBβ (Malek et al., 2003). We reasoned that the symmetric p52 homodimer might bind Bcl3 protomer in an asymmetric manner; therefore, the binding of the two GRR molecules to the Bcl3 ARD must be different. To investigate whether both or only one GRR interacts with ARD of Bcl3, we used limited proteolytic digestions by using both trypsin and chymotrypsin. The results clearly show that one of the two p52 subunits remains fully intact even after several hours of protease treatments. However, the cleavage patterns of the second GRR are vastly different for the two proteases. Trypsin generates multiple shorter products (Figure 5.3a, smeared band indicated by double arrowhead). It appears that cleavage occurs within the NLS basic residues as there is no other arginine or lysines following the NLS of p52. Chymotrypsin generates a single moderately stable product (Figure 5.3b, double arrowhead). However, the length of this fragment is larger than the ones generated by trypsin. Based on the sequence it appears that the chymotrypsin cleavage site is located after residue Y376 or Y385. This limited protease digest experiment let us propose a model which is the asymmetrical binding of p52 GRR and Bcl3. In the model, one of the GRR binds to Bcl3, so it gets protected from the protease cleavage; another GRR remain flexible, so it can be cleaved by the protease (Figure 5.3d).

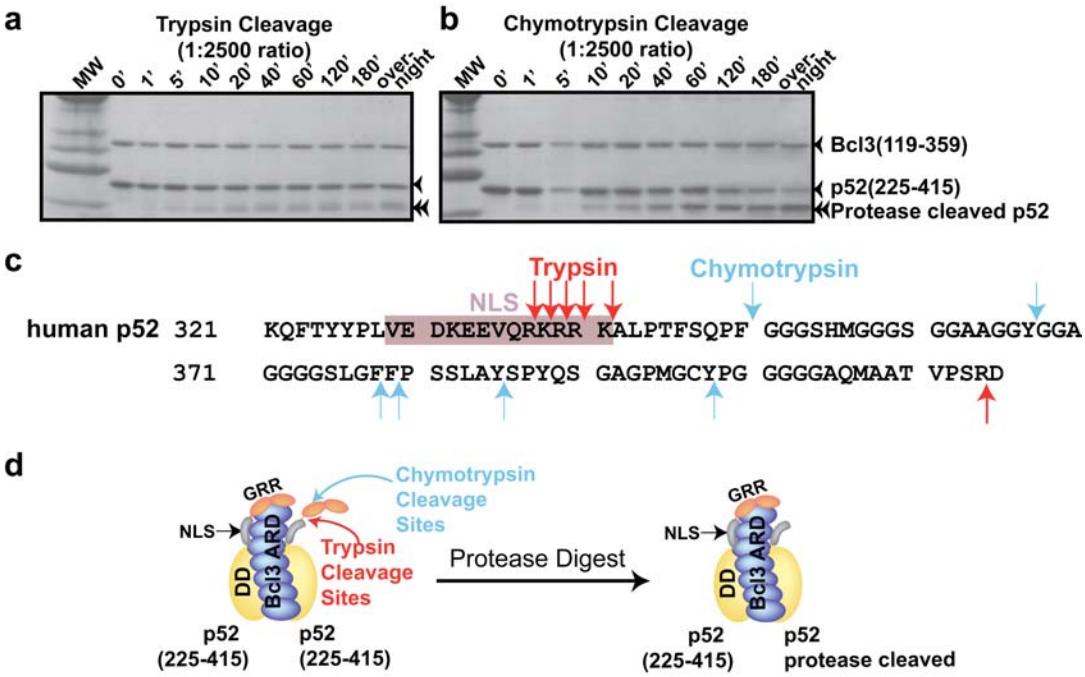

Figure 5.3 Asymmetrical binding of p52 GRR and Bcl3. 15% SDS-PAGE analysis of p52(225-415):Bcl3(119-359) complex and its partial digestion with a) trypsin and b) chymotrypsin. The single and double arrowheads denote uncleaved and cleaved p52. Please note that the cleaved product in chymotrypsin treated complex is longer than the trypsin treated complex. c) Human p52 sequence of NLS and GRR region. The potential trypsin (Red) and chymotrypsin (Blue) cleavage sites are indicated. d) Model of Bcl3 ARD bound to p52 DD-GRR. The putative cleavage sites are indicated.

3. Crystallization of the p52:Bcl3 core complex

Crystal screening of p52(225-415):Bcl3(119-359) core complex using commercially available sparse matrix screen was not fruitful. It is possible that the flexible GRR might be detrimental to crystallization. Therefore, 1:10000 ratio of either trypsin or chymotrypsin was used in the crystallization trials of the complex. The idea was small amount of protease, may cleave only the flexible portion allowing crystallization of the stable core complex. Small complex crystals were obtained in the conditions with trypsin (Figure 5.4). This condition contains 2M ammonium sulfate, 100mM sodium citrate pH 5.5, 5% PEG 8000 as the precipitant, and 2mM DTT in the reservoir. The SDS-PAGE analysis of the dissolved crystals shows one of the p52 remains intact with Bcl3, whereas the other p52 GRR gets cleaved by tryspin (Figure 5.4b). Indeed, this is exactly what we have observed during the limited proteolysis experiment (Figure 5.3). However, this method of crystallization is difficult to control. In order to overcome this problem, we decided to generate and purify proteolyzed complex that contains Bcl3 ARD and p52 dimer with only one GRR.

However, the proteolyzed complex, p52(225-415)/p52(225-341):Bcl3(119-359), could not been generated by the co-purification strategy as described above since all NF-κB subunits can form homo- or hetero-dimers in a combinatorial manner. If the co-purification method was used, there would be a mixture of complexes containing three different p52:Bcl3 complexes (Figure 5.5); one would contain both p52 GRRs; one would contain

no p52 GRR; and another would contain only one p52 GRR. In order to make the preferential one GRR p52:Bcl3 complex complex, two point mutations were introduced at the p52 dimerization interface. Based on crystal structure knowledge our lab has, we know that NF-κB subunits form a stronger heterodimer than homodimer. This is because the heterodimer interface has all four important residues Asp, Tyr, Asn, and Phe (Huang et al., 1997) (Figure 5.6). In the dimerization domain of p50:RelA heterodimer, the first amino acid contributes to the variation in dimmer affinity is the replacement of Asp254 in p50 DD with Asn200 in RelA DD. One of the carboxylate oxygens of Asp254 makes hydrogen bond with its own backbone nitrogen together with the backbone nitrogen of Tyr267; this hydrogen-bonding network constrains the other carboxylate oxygen of Asp254 in such an orientation that it will encounter the equivalent symmetrical functional group arising from the other subunit. Therefore, this like-charge interaction unflavored p50 homodimer; however the corresponding Asn in RelA DD appears not to play any role in dimerization. The second amino acid contributes to dimmer affinity is Tyr267 in p50 DD and the corresponding Phe213 in RelA DD which located at the center of the dimer interface. Tyr267 in p50 DD is involved in six hydrogen bonds, which is absent in RelA Phe213. Therefore, the absence of hydrogen bonds may account for the weaker RelA homodimer compared to p50/RelA heterodimer (Huang et al., 1997). Together, these are the reasons that RelA forms a stronger heterodimer with p50 than its own homodimer; and the reason that RelB forms a strong heterodimer with p52 or p50. Therefore, two

point mutations D234N, Y247F were introduced in p52(225-415) construct which allow this subunit to form a preferential dimer with wt p52(225-341) when both are present.

The one GRR core complex, p52(225-341)/p52(225-415)D234N, Y247F:Bcl3(119-359), was generated in high purity using multiple chromatographic steps (Figure 5.7). And small crystals of this complex were obtained in a similar condition as the previous condition. This condition contains 2M ammonium sulfate, 100mM sodium citrate pH 6.5, 5% PEG 8000 as the precipitant, and 2mM DTT in the reservoir. The SDS-PAGE analysis of the dissolved crystals confirm that the crystal were constituted of p52(225-341)/p52(225-415)D234N, Y247F:Bcl3(119-359) protein complex (Figure 5.8). However, extensive screening of crystallization conditions of this one GRR p52:Bcl3 complex did not produce suitable crystals for diffraction studies.

The one GRR p52:Bcl3 construct formed stable complex through both cation exchange and size-exclusion columns, however, this complex crystallized in a condition containing 2M ammonium sulfate, the p52 GRR portion of the complex might be flexible under such high salt concentration and hindered the growth of the crystals. Based on the knowledge of the crystal structures of the IκBβ:RelA(p65) complex, we know that the N-terminus of IκBβ is in close proximity to the RelA C-terminus NLS sequence (Malek et al., 2003) (Figure 5.9); therefore, a fusion construct was generated in which the N-terminus of Bcl3 ARD was linked to the C-terminus of p52 DD+GRR using five glycines. The idea of this fusion protein is that the p52

GRR portion would remain stable during crystallization even under high salt condition; and this might help the growth and the packing of the protein crystals. This fusion p52_5Gly_Bcl3 construct containing the two p52 dimerization mutations was co-expressed with wt p52 DD and purified through the de-nature and refolding method (Figure 5.9). And small crystals were obtained by microseeding using the previous one GRR p52:Bcl3 complex crystal as a seed in the similar conditions.

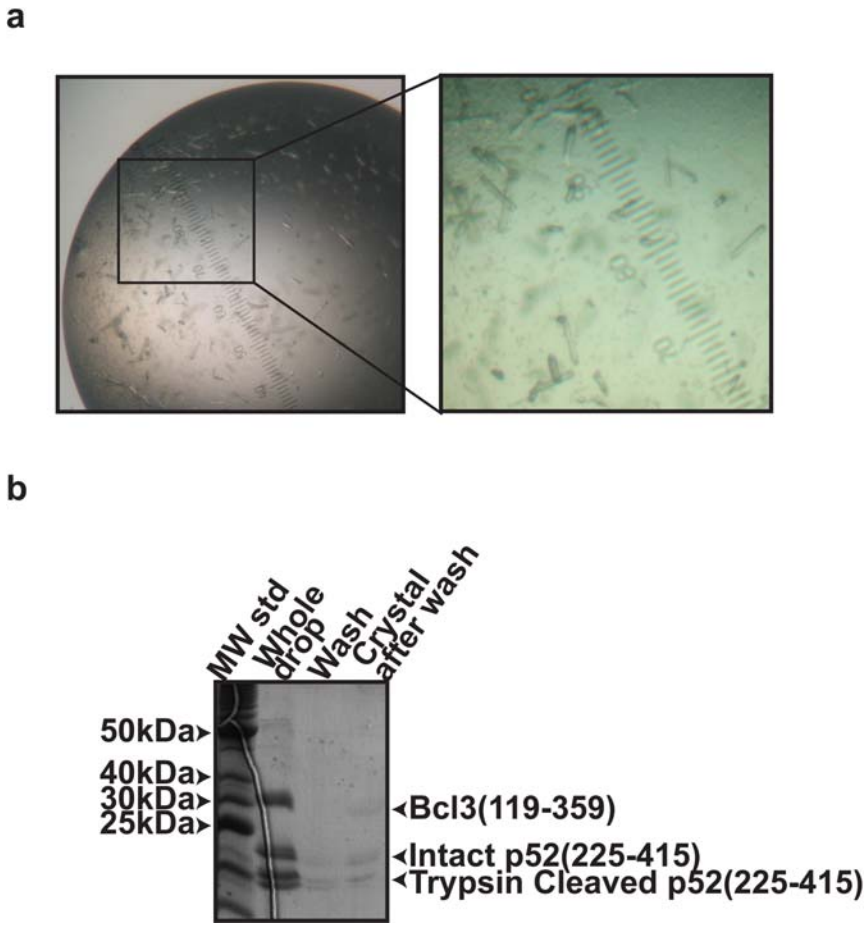

Figure 5.4 Crystallization of p52(225-415):Bcl3(119-359) complex. a) Microcrystals from a crystallization trial condition with 1:10000 ratio of trypsin which contained the recombinant p52(225-415):Bcl3(119-359) complex. b) SDS-PAGE analysis of the dissolved crystals in a).

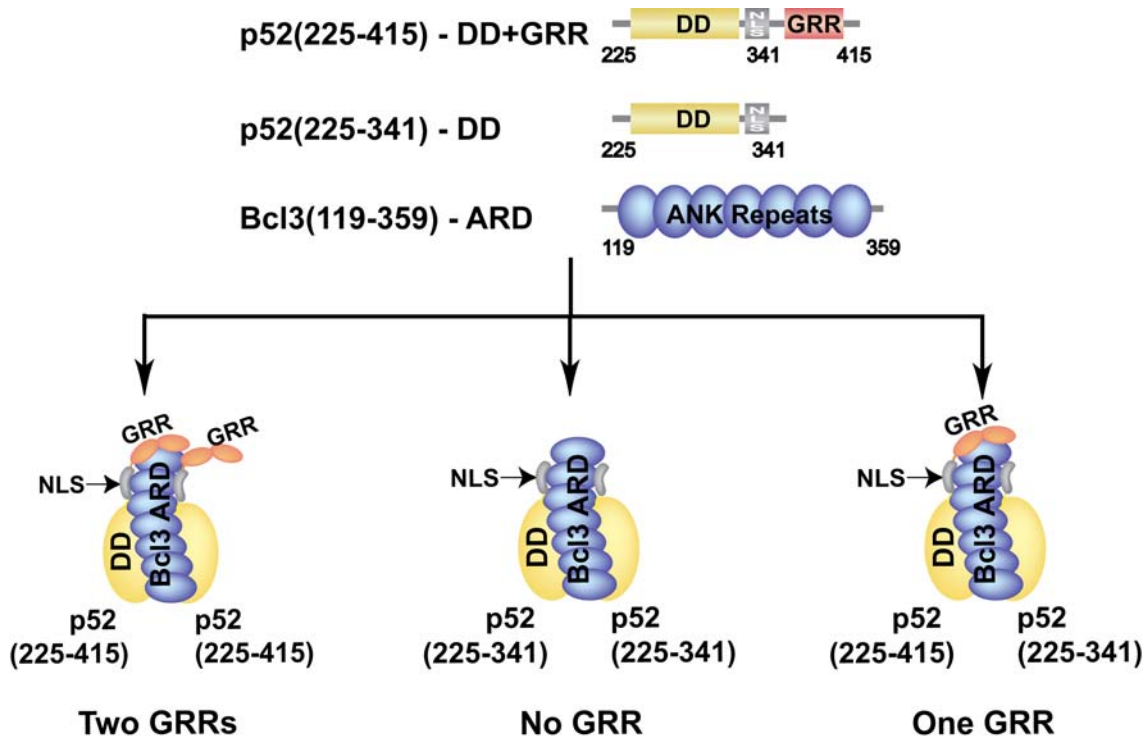

Figure 5.5 Model of co-purification of One GRR p52:Bcl3 complex.

a

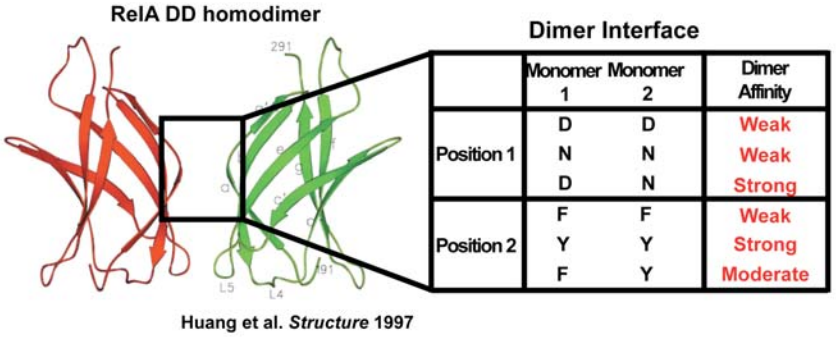

b

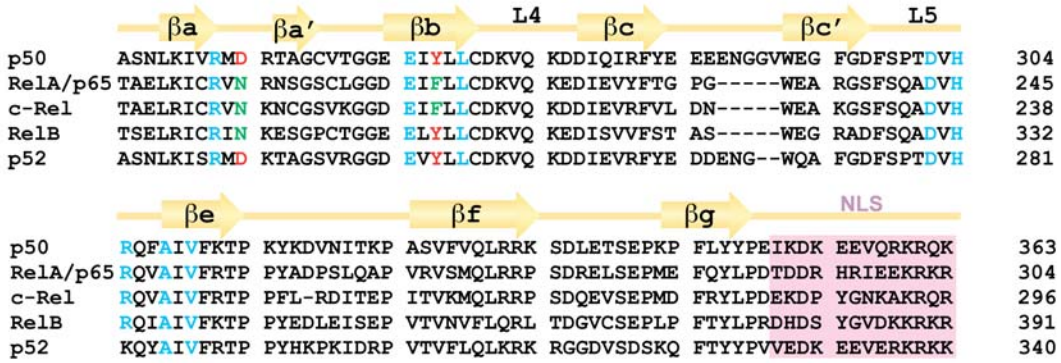

Figure 5.6 The NF-κB Dimer Interface. a) Ribbon diragram of the RelA dimerization domain homodimer indicating the secondary elements and the overall tertiary fold. Red and green are used to indicate the two monomeric RelA subunits in the homodimer. b) Sequence alignment of the dimerization domains of the NF-κB family proteins. Residues which contribute to the dimer interface are colored: blue indicates the conserved key residues in the dimerization interface; red and green indicates the non-conserved residues which significantly contribute to the determinacy of NF-κB dimer affinity. NLS sequences are boxed in light purple. Yellow arrows and lines indicate β-strands and loops respectively.

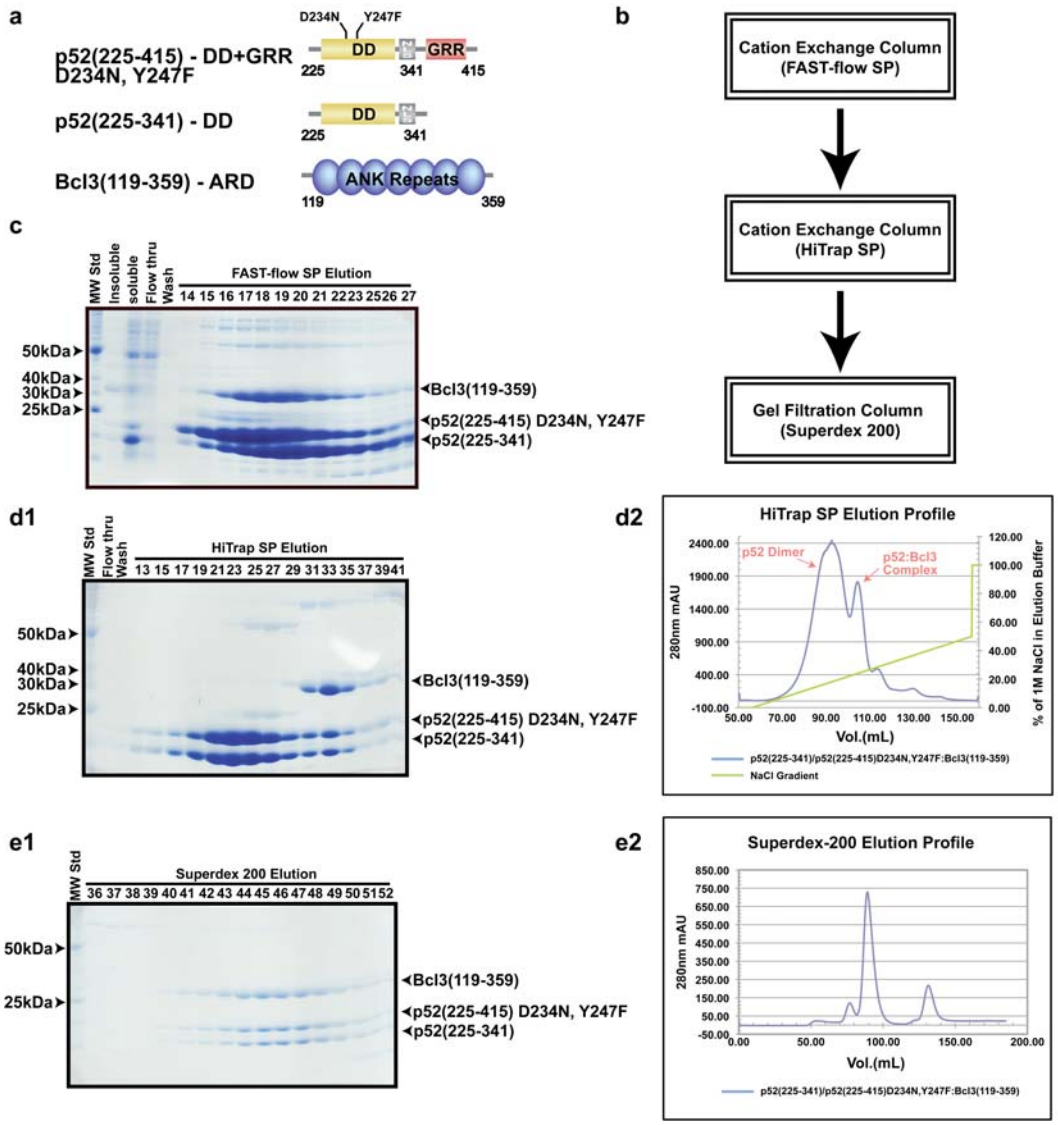

Figure 5.7 Purification of recombinant human p52(225-341) / p52(225-415) D234N,Y247F:Bcl3(119-359) protein complex. a) Schematic representation of p52 and Bcl3 constructs used. Two point mutation in p52 DD, D234N and Y247F, are indicated. b) Purification scheme. c) 12.5% SDS-PAGE analysis of crude complex lysate purified by cation exchange chromatography (fast flow S-sepharose). d1) 12.5% SDS-PAGE analysis of fraction from HiTrap SP cation exchange chromatography. d2) HiTrap SP elution profile shows p52:Bcl3 co-eluted together as a single peak which eluted at a higher salt concentration comparing to p52 dimer. e1) 12.5% SDS-PAGE analysis of fractions from Superdex-200 size exclusion chromatography. e2) Superdex-200 size exclusion chromatography elution profile shows a single peak, confirming that p52 and Bcl3 were eluted together as a complex.

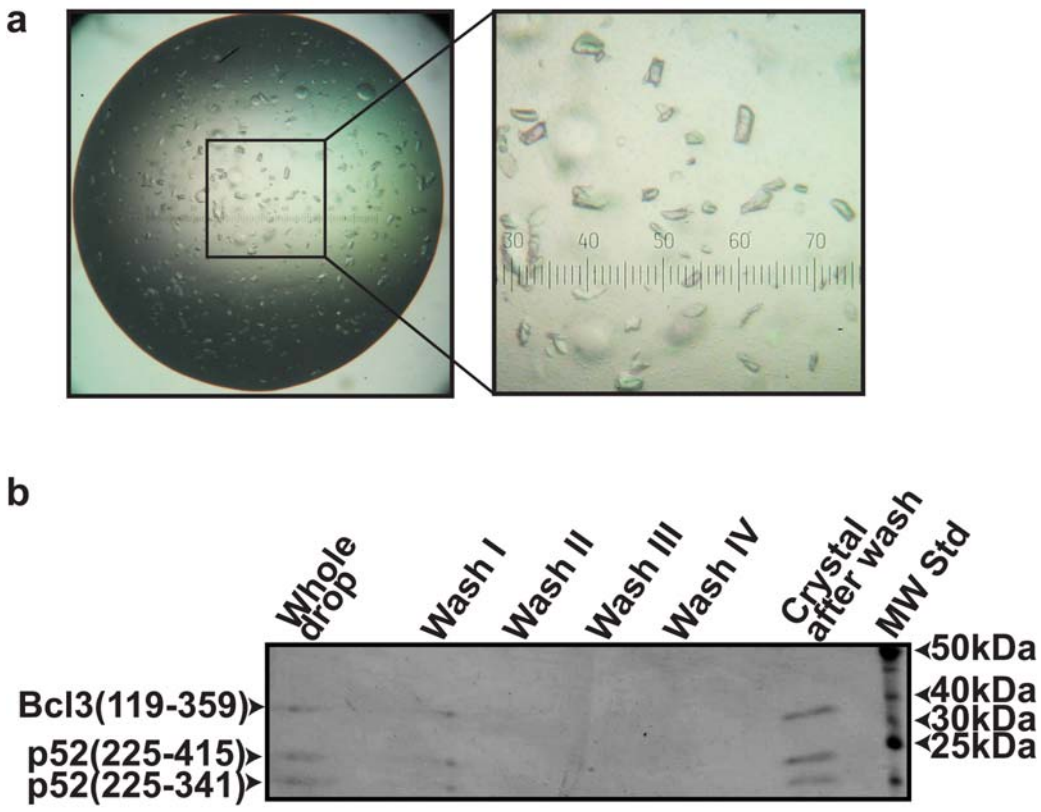

Figure 5.8 Crystallization of p52(225-341)/p52(225-415)D234N,Y247F:Bcl3(119-359) complex. a) Microcrystals from a crystallization trial condition contained the recombinant p52(225-341)/p52(225-415)D234N,Y247F:Bcl3(119-359) complex. b) SDS-PAGE analysis of the dissolved crystals in a).

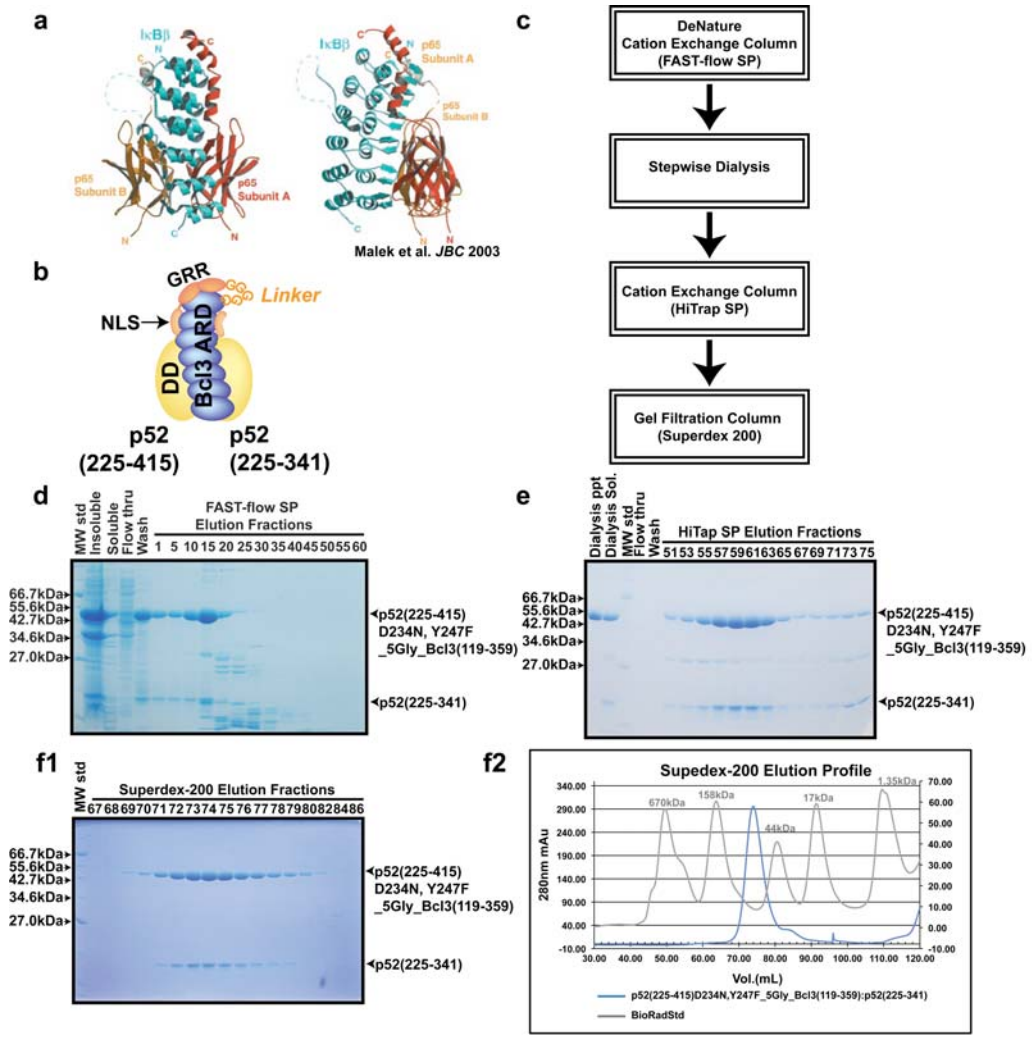

Figure 5.9 Purification of recombinant human p52:Bcl3 fusion protein complex. a) A ribbon diagram representation of the IκBβ:RelA(p65) complex crystal strucutre. b) Cartoon model of p52_5Gly_Bcl3 fusion protein. c) Purification scheme. d) 12.5% SDS-PAGE analysis of crude complex lysate purified by cation exchange chromatography (fast flow S-sepharose). e) 12.5% SDS-PAGE analysis of fraction from HiTrap SP cation exchange chromatography. f1) 12.5% SDS-PAGE analysis of fractions from Superdex-200 size exclusion chromatography. f2) Superdex-200 size exclusion chromatography elution profile shows a single peak, confirming that p52 and Bcl3 were eluted together as a complex. Overlaying with MW standards (BioRad) indicates the complex contains one molecule of p52:Bcl3 fusion protein and one molecule of p52 DD.

D. Discussion

As mentioned in the introduction, NF-κB p50 and p52 homodimers are called transcriptional repressors as they do not contain transcriptional activation domains. However, in association with a special class of transcriptional co-factors such as Bcl3 and IκBζ, these homodimers are able to act as transcriptional activators (Cogswell et al., 2000; Westerheide et al., 2001; Yamamoto et al., 2004). In essence, Bcl3 and IκBζ proteins provide the activation domain to p50 and p52 in trans. However, only from certain NF-κB target promoters the p50 or p52 complex with Bcl3 or IκBζ function as transcriptional activators. However, the promoter specificity is unclear. It is likely that signal-specific regulation of these coactivators, affinity of the ternary complex and the abundance of the homodimers in the nucleus contribute to the specificity of gene regulation by these coactivaotrs. Focus of this part is to study the binding interaction of the p52:Bcl3 complex by solving the x-ray structure of the complex.

In this chapter, we are investigating the role of Bcl3 as a co-factor. Structurally Bcl3 belongs to the IκB family (Michel et al., 2001; Na et al., 1999). However, functionally, Bcl3 is distinct from the prototypical inhibitor IκB proteins. As mentioned earlier, IκB proteins functions exclusively as inhibitors of NF-κB and reside primarily in the cytoplasm. In contrast, Bcl3 is a nuclear protein and can function to co-regulate NF-κB target gene transcription and primarily acts through the p50 and p52 homodimers.

We have co-expressed the non-tagged Bcl3 ARD and p52(225-415) in *E. coli* and the complex has been purified through multiple chromatographic steps. Employing traditional crystallization methods we have grown small crystals. For this core complex, we were facing difficulty in obtaining diffracting quality crystals. This might arise due to the involvement of one p52 GRR motif in contacting Bcl3 ARD whereas the other GRR remains flexible. Indeed, this is exactly what we have observed during our limited proteolysis experiments. Therefore, we have purified large amount of the proteolyzed complex which contains Bcl3 ARD and p52(225-415):p52(225-344) dimer; and we were able to grow small crystals of this proteolyzed complex also. However, this complex was crystallized in a condition containing 2M ammonium sulfate. The one p52 GRR portion might still remain flexible under such high salt condition and hindered the packing and the growth of the crystals. Obtaining well-ordered crystals is the first requirement in determining protein structure using X-ray crystallography. However, obtaining suitable and diffracting quality crystals is mostly a trial-and-error procedure due to the presence of many uncertainties. The heterogeneity of the proteins, the impurities present during crystallization, and the presence of flexible disordered regions within the proteins can all hinder the growth of protein crystals. Therefore, it is critical to find a suitable protein complex construct in which the important protein-protein interactions still remain intact, but the disordered regions are removed. In addition, the choices of precipitant, salt, buffer pH, additives, and even temperature for crystallization could all be

critical to promote crystal growth. Currently, we are still optimizing both the crystallization conditions and the complex constructs to see if any additional region is required for the p52:Bcl3 core complex formation in order to overcome the obstacles and improve the crystals for X-ray diffraction studies.

Chapter VI: Discussion

The NF-κB family of transcription factors plays a critical role in the immune system by regulating various physiological processes involving in both innate and adaptive immunity, inflammation, cell survival and cell proliferation. Due to the diverse regulation mechanism acting on NF-κB signaling, the signal dependent activation of NF-κB remains a challenging area of study. This thesis focuses on the mechanism of gene regulation of the NF-κB p52 homodimer and its specific transcriptional co-regulator, Bcl3. Numerous earlier studies indicated that p52 and Bcl3 function together: mice deficient in either *nfκb2/p100 (p52)* or *bcl3* alone had been generated by several groups in the late 1990s. The phenotypes of *nfκb2/p100 (p52)* null mice are largely overlapping with those observed in *bcl3* knockout mice, such as impaired in the ability to form the germinal center and to generate antibodies to T-dependent antigens (Caamano et al., 1998; Franzoso et al., 1998; Franzoso et al., 1997; Schwarz et al., 1997). These phenotypes are distinct from those of the *nfκb1/p105 (p50)* knockouts, supporting the notion that p52 homodimer and Bcl3 share common regulatory pathways. In addition, mice deficient in both *nfκb2* and *bcl3* genes, but not either one alone, led to a profound breakdown in central T cell tolerance resulting in rapid and fatal multiorgan inflammation (Zhang. et al., 2007). Authors suggested that this phenotype might be due to deficiencies in the non-overlapping functions of these two proteins. However, it is possible that in the case of single gene knockout mice, a close homolog might compensate the activity of the deleted gene product in T cell. For instance, p52 might compensate the function of

p50 in *nfκb1/p105 (p50)* knockout mice. These genetic studies were further supported by transfection studies which showed that p52 interacts with Bcl3 and that they could both activate and repress transcription. However, the detailed mechanism of their functional synergy remained unclear. Work reported in the thesis I showed that both proteins are activated in response to the same stimulus, and upon activation they work together to activate or repress gene transcription depending on the κB DNA sequence.

A. Activation of p52 and Bcl3

p52 is generated from its precursor protein, NF-κB2/p100. Having both NF-κB activation and IκB inhibition functions, NF-κB2/p100 poses a complex issue of maintaining both the processed p52 and the unprocessed p100 molecules in appropriate levels for their cellular functions. This study showed that the non-canonical NF-κB signaling pathway induces both processing and complete degradation of p100 in a biphasic event. In the first phase, translation independent complete degradation of p100 releases RelA containing dimers which lead to the transcription activation of target genes including the *nfκb2/p100* gene itself and the *relb* gene; and processing is the result of dynamic p100 assembly event in the second phase of the non-canonical signaling. There is a pool of p100 which is protected by RelB from being processed and degraded during signaling. This enables p100 to re-associated with RelA upon signal termination, thereby promoting the inhibitory activity of NF-κB2/p100. Therefore, the non-canonical signaling induces both

activation and suppression of NF-κB activity. The second pool undergoes processing and the processed product p52 can associate with either itself to form the p52 homodimer or associates with RelB to form the p52/RelB heterodimer. Although, this study has not addressed the issue, it is tempting to speculate that Bcl3 may induce the p52 homodimer formation. *In vitro* analytical ultracentrifugation (AUC) studies have found that the p52 homodimer is ~1000-fold weaker than the p50 homodimer. Moreover, cell extracts containing over expressed p52 homodimer bind κB DNA weakly. Purified p52 homodimer binds DNA only weakly compared to p50 and RelA homodimer. These properties of p52 homodimer might be due to weak dimerization affinity. I now showed that Bcl3 is also activated by the same stimulus that active p52 processing.

Bcl3 is a well-known specific transcriptional co-regulator for NF-κB p52 homodimer; however, the activation mechanism of Bcl3 and the mechanistic role of Bcl3 functions together with p52 homodimer dependent transcription in cells in not well understood. In this study I showed that like p100 expression, Bcl3 expression is also regulated by NF-κB. The mRNA expression levels of both genes are peaked around 8 to 12 after LPS treatment. Earlier studies suggested transient transfected Bcl3 is a constitutively nuclear protein in cells. Work presented here lends support to the notion that Bcl3 nuclear translocation is an inducible process. Also, Bcl3 phosphorylation is a stimulus-denpendent process. Two new Bcl3 phopshorylation sites had been identified, serines at positions 33 and 446. It is likely that phosphorylation of Ser33 is

responsible for nuclear translocation of Bcl3. A possible mechanism is that the nuclear localization signal (NLS) of Bcl3, located in its N-terminal region, is masked when Ser33 remains unphosphorylated. However, upon phosphorylation, alternative interactions mediated by pSer33 unmasked the NLS allowing it to interact with the nuclear import machinery. Phosphorylation-dephosphorylation dependent nuclear and cytoplasmic shuttling was described for other proteins such as NFAT family of transcription protein. In that case, however, signal-dependent dephosphorylation induces nuclear localization whereas steady state phopshoryaltion event conceal the NLS (Beals et al., 1997; Hogan et al., 2003; Okamura et al., 2004; Zhu et al., 1998). Phopshorylation of serine at position 446 is essential for Bcl3's stable interaction with the p52 homodimer. This observation is intriguing in the sense that LPS might induce phosphorylation of p100 leads to p52 generation while phosphorylation at Ser446 induced association between p52 and Bcl3. Earlier studies showed that baculovirus derived Bcl3 inhibits the complex formation between p52 and DNA (Nolan et al., 1993). In this case the result is opposite. It is possible that baculovirus derived protein remains unphosphorylated at Ser446 thus inhibits protein-DNA complex formation. An intriguing possibility is that the inhibitory activity of unphopshorylated Bcl3 is switched to a complex formation stimulatory activity through a single phosphorylation event. Future experiments will resolve this issue by isolating both forms of Bcl3 from baculovirus.

Two lines of evidence suggest that AKT is the kinase for Ser33 phosphorylation. Ser33 is located within the AKT consensus peptide and AKT inhibitor partially blocks Bcl3's transcription potential with p52 homodimer. More experiments are required to identify the cellular kinases for both Ser33 and Ser446 sites.

B. Transcriptional Regulation by the p52 Homodimer Complexed to Bcl3

Only three genes are thought to be regulated by the p52:Bcl3 complex under physiological conditions: P-Selectin, cyclin D1 and IP-10 (Cogswell et al., 2000; Leung et al., 2004; Pan and McEver, 1995). It was not clear why these promoters are not regulated by the classical NF-κB dimers such as the RelA homodimer or p50/RelA heterodimer. A careful inspection of κB sites that drives transcription of these genes reveal that they do not deviate from the consensus κB sequence in any significant manner than they differ from each other. For instance, Cyclin D1-κB site contains four contiguous thymines in the 3'- half sites. P-selectin-κB site, which is the only one studied extensively for p52 binding, has three nucleotide differences from the consensus site. Finally, IP-10 contains two κB sites of which one κB site (distal site) is common to the κB sites in many other promoters which have been shown to regulated by the p50/RelA heterodimer. Although it was shown that p50 or p52 and Bcl3 are required for its expression upon specific signaling conditions, it was not clear if both or only one of the two κB sites

were responding to Bcl3 and p52 or p50. The second κB site (proximal site) deviates from consensus from only position which is the central G/C bp. Incidentally, both Cyclin D1-κB and P-selectin κB site also contained a G/C bp at the central position. Based on the knowledge of X-ray crystal structures of several different NF-κB:κB DNA complexes one can deduce the binding strategy of NF-κB subunits for the consensus κB DNA (5' –GGGRN W YYCC-3') at the molecular level. The central base pair falls in the pseudo dyad axis; however, it barely makes any direct contact with NF-κB protein subunits. Therefore, NF-κB homodimer cannot bind even symmetric half sites identically. Moreover, many of the κB sites have AT-rich sequences in the form of AAATT or AATTT in the middle. These sequences are favored by RelA and cRel homodimers. κB DNAs containing these AT-rich sequences in the middle undergo approximately 20° bending towards the major groove. This bending might be essential for the RelA and cRel homodimer binding to DNA. In general, DNA dynamics alters with DNA sequences. Therefore, it is likely both DNA conformations and differential asymmetry introduced due to the sequence of the central bp may induce different overall conformations of the protein-DNA complex.

In combination of both *in vitro* and cellular approaches, this study showed for the first time how the transcriptional activity of NF-κB dimers is linked to the target different classes of κB DNA. There is a strong correlation between the sequence identity of the central base pair of a κB DNA and the

transcriptional activity of NF-κB dimers. The RelA homodimer prefers an A/T at the central position (A/T-centric), whereas the p52 homodimer prefers a G/C-centric κB site for the transcriptional activation. However, although the p52 homodimer is responsible for the nucleotide selectivity, being devoid of a transcriptional activation domain it requires Bcl3 for the transcriptional activity. Bcl3 knockdown experiments in primary macrophages have revealed the role of Bcl3 in the target gene transcription. The most striking observation is that the complex does not avoid A/T-centric κB sites as it also binds to these sites, perhaps even with higher affinity. However, upon binding to these A/T-centric sites, the p52:Bcl3 complex does not activate transcription. Although at this stage the mechanism is not clear, it appears that dynamic behavior of the complex changes as it forms ternary complexes with these two classes of κB sites. The p52:Bcl3:G/C-centric κB DNA complexes are more dynamic in the sense the complex does not form a recognizable ternary complex in gel-shift assays. It is possible that the faster off rate of binding which when resolved through electrophoresis forms a smear. However, the presence of the ternary complex is confirmed by antibody super-shift experiments. Antibody may stabilize the complex by reducing the off rate. The complex behave differently when binds to the A/T-centric κB sites. Whether or not binding behaviors different *in vivo* is only speculative so far. It is tempting to speculate that two distinct ternary complexes may recruit different proteins. For instance, repressor proteins might be recruited to the A/T-centric κB sites while co-activator complexes might be recruited to the G/C-centric κB sites. How that

might occur? We propose conformational variations of the p52:Bcl3 complex upon binding to two distinct classes of κB DNA sequences. While the relevant complex structures to discuss how conformations might vary are currently absent, some speculation can be made based on the differences observed in the p50 and p52 homodimers bound to near identical sites (Muller et al., 1995) (Figure 6.1). Conserved residues from p50 and p52 bind the identical sites differently as DNA non-contacting protein residues differ. Therefore, an argument can be made that when the central bp differs, they might transduce different contact networks resulting in different conformations in a distal site. Similarly, X-ray structures of RelA homodimer bound to related but distinct κB DNA, overall conformation of these complexes differ. Indeed, if all structures of NF-κB:DNA complexes are superposed, differential conformations of these complexes can be easily visualized. The extent of conformational change varies from marginal to significant levels. However, it is difficult to correlate a specific structural alteration to a specific cellular function. In other transcription factors such as glucocorticoid receptor (GR), nuclear hormone receptor and Drosophila Hox family transcription factors also show DNA sequence dependent transcriptional control (Joshi et al.; Meijsing et al., 2009; Ogawa et al., 2005).

For a deeper understanding of the mechanism of gene regulation by the p52:Bcl3 complex, it is necessary to determine the three-dimensional structures of the p52:Bcl3 complex bound both to G/C- vs. A/T-centric κB DNAs. Studying the precise molecular structures at the atomic level may

guide one to identify structural basis of the differences between NF-κB:IκB inhibition vs. activation complex. In this study, a p52:Bcl3 core complex has been identified and crystallized. Further study in optimizing both the crystallization conditions and the complex constructs needs to be done in order to overcome the obstacles and solve the structure of the p52:Bcl3 complex. If structural differences are observed, proteins will be mutated to abolish conformation-derived recruitment function using cellular experiments. It can be proposed that κB DNA sequence dependent function is not only displayed by the p52:Bcl3 complex, but also by other NF-κB dimers. Studying all dimers for their sequence-specific cellular function may lead one to reveal the functional code between a NF-κB dimer and a κB DNA. Using genome wide sequence information one can then propose a model of how each dimer can participate in eliciting a biological program.

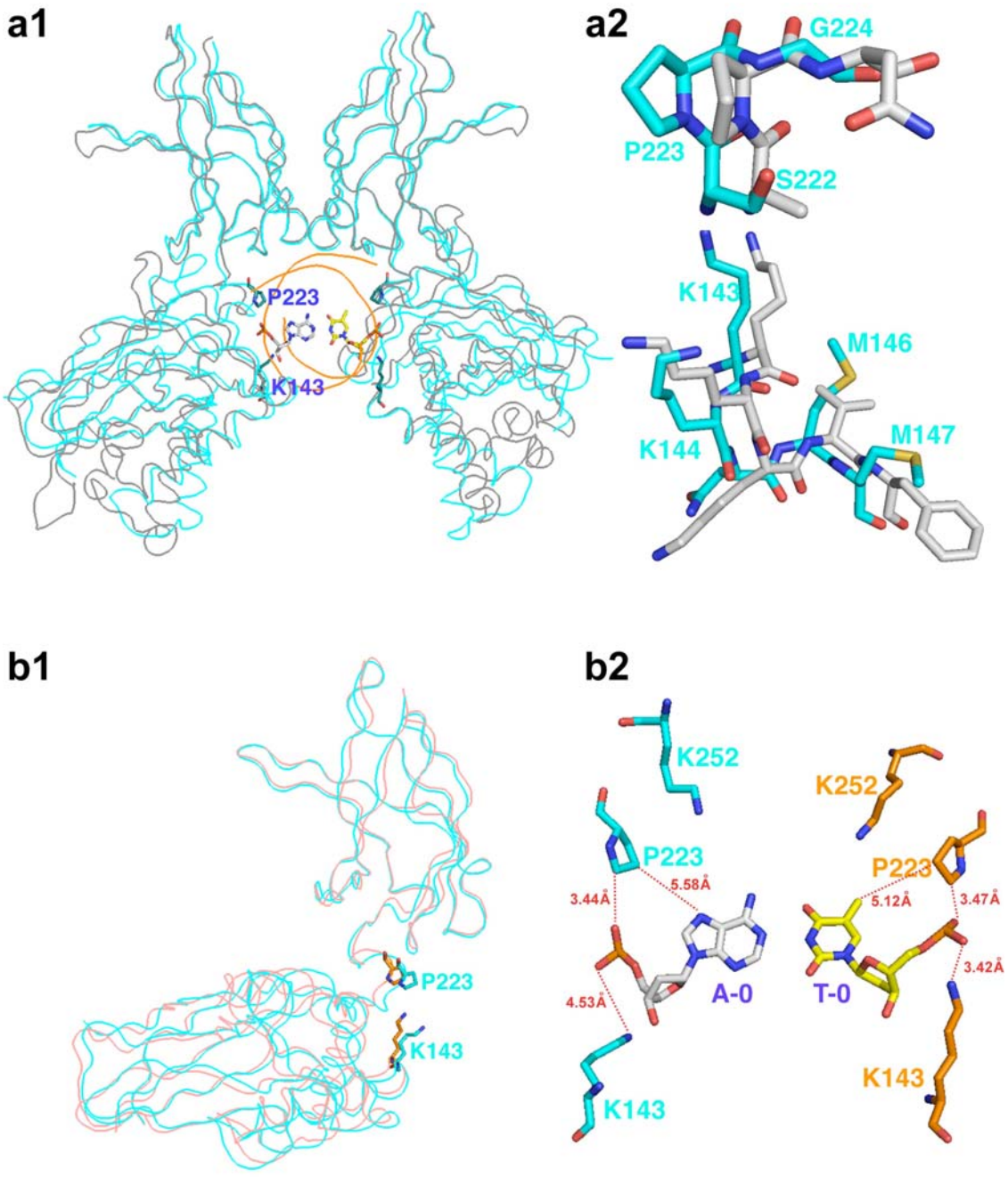

Figure 6.1 Comparison of X-ray crystal structures of p50 and p52 homodimer bound to κB DNAs. a1) and a2) Superposition of p50 (grey) (PDB 1SVC) and p52 (cyan) (PDB 1A3Q) in 11 base pair DNA complexes, P233 and K143 contact the backbone of the center A/T base pair. b1) and b2) Superposition of the two subunits (monomer 1 (cyan) and monomer2 (orange)) of p52:κB DNA complex. The residues asymmetrically contact the center A/T base pair are shown.

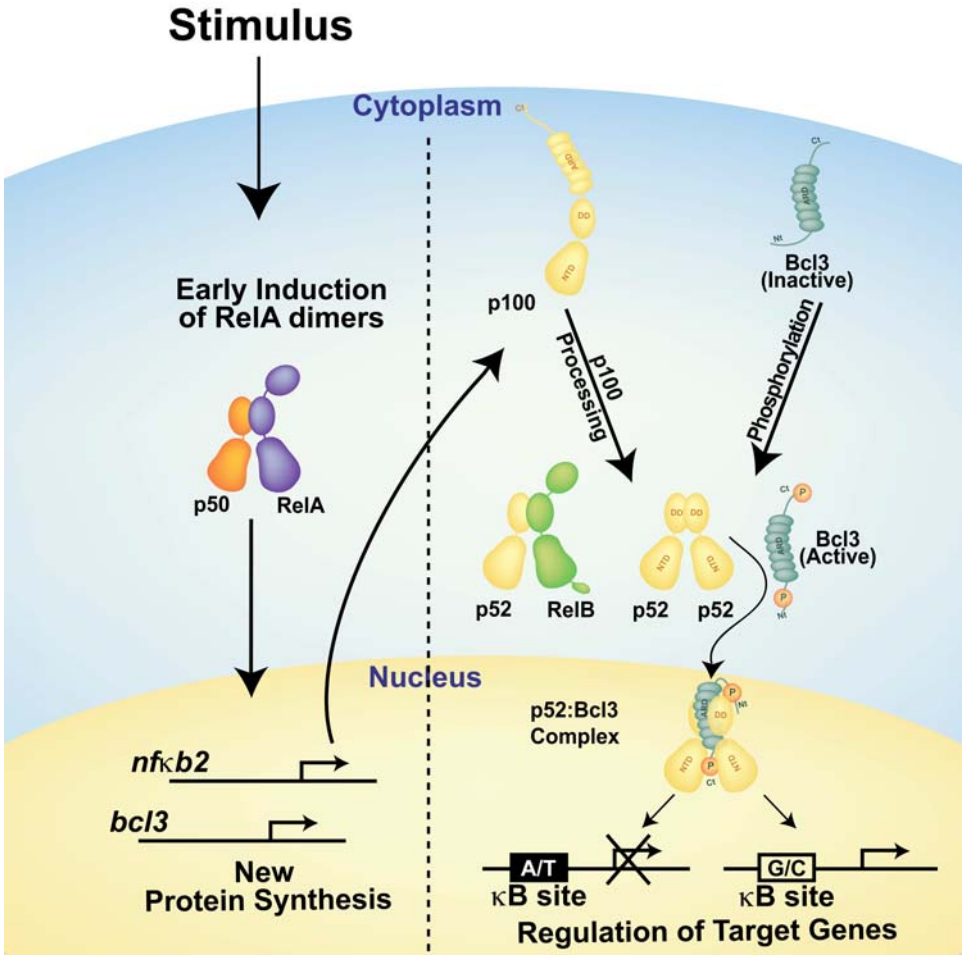

Figure 6.2 Model of stimulus-dependent activation of p52 and Bcl3, and gene regulation by the p52:Bcl3 complex. Upon stimulation, early activation of RelA dimers activates the expression of *nfκb2/p100* and *bcl3* genes. Newly synthesized p100 is processed to generate p52; and Bcl3 is regulated through phosphorylation events at multiple residues. The active Bcl3 complexes with p52 homodimer, translocate into nucleus, and regulate the target genes through binding to different sub-sets of κB sites.

References

Agalioti, T., Lomvardas, S., Parekh, B., Yie, J., Maniatis, T., and Thanos, D. (2000). Ordered recruitment of chromatin modifying and general transcription factors to the IFN-beta promoter. Cell *103*, 667-678.

Annunziata, C.M., Davis, R.E., Demchenko, Y., Bellamy, W., Gabrea, A., Zhan, F., Lenz, G., Hanamura, I., Wright, G., Xiao, W.*, et al.* (2007). Frequent engagement of the classical and alternative NF-kappaB pathways by diverse genetic abnormalities in multiple myeloma. Cancer Cell *12*, 115-130.

Arenzana-Seisdedos, F., Turpin, P., Rodriguez, M., Thomas, D., Hay, R.T., Virelizier, J.L., and Dargemont, C. (1997). Nuclear localization of I kappa B alpha promotes active transport of NF-kappa B from the nucleus to the cytoplasm. J Cell Sci *110 (Pt 3)*, 369-378.

Bain, J., Plater, L., Elliott, M., Shpiro, N., Hastie, C.J., McLauchlan, H., Klevernic, I., Arthur, J.S., Alessi, D.R., and Cohen, P. (2007). The selectivity of protein kinase inhibitors: a further update. Biochem J *408*, 297-315.

Baldwin, A.S., Jr. (1996). The NF-kappa B and I kappa B proteins: new discoveries and insights. Annu Rev Immunol *14*, 649-683.

Barre, B., and Perkins, N.D. The Skp2 promoter integrates signaling through the NF-kappaB, p53, and Akt/GSK3beta pathways to regulate autophagy and apoptosis. Mol Cell *38*, 524-538.

Basak, S., Kim, H., Kearns, J.D., Tergaonkar, V., O'Dea, E., Werner, S.L., Benedict, C.A., Ware, C.F., Ghosh, G., Verma, I.M., and Hoffmann, A. (2007). A fourth IkappaB protein within the NF-kappaB signaling module. Cell *128*, 369-381.

Beals, C.R., Sheridan, C.M., Turck, C.W., Gardner, P., and Crabtree, G.R. (1997). Nuclear export of NF-ATc enhanced by glycogen synthase kinase-3. Science *275*, 1930-1934.

Boeger, H., Bushnell, D.A., Davis, R., Griesenbeck, J., Lorch, Y., Strattan, J.S., Westover, K.D., and Kornberg, R.D. (2005). Structural basis of eukaryotic gene transcription. FEBS Lett *579*, 899-903.

Bonizzi, G., Bebien, M., Otero, D.C., Johnson-Vroom, K.E., Cao, Y., Vu, D., Jegga, A.G., Aronow, B.J., Ghosh, G., Rickert, R.C., and Karin, M. (2004).

Activation of IKKalpha target genes depends on recognition of specific kappaB binding sites by RelB:p52 dimers. Embo J *23*, 4202-4210.

Bork, P. (1993). Hundreds of ankyrin-like repeats in functionally diverse proteins: mobile modules that cross phyla horizontally? Proteins *17*, 363-374.

Bosisio, D., Marazzi, I., Agresti, A., Shimizu, N., Bianchi, M.E., and Natoli, G. (2006). A hyper-dynamic equilibrium between promoter-bound and nucleoplasmic dimers controls NF-kappaB-dependent gene activity. EMBO J *25*, 798-810.

Bours, V., Franzoso, G., Azarenko, V., Park, S., Kanno, T., Brown, K., and Siebenlist, U. (1993). The oncoprotein Bcl-3 directly transactivates through kappa B motifs via association with DNA-binding p50B homodimers. Cell *72*, 729-739.

Bours, V., Villalobos, J., Burd, P.R., Kelly, K., and Siebenlist, U. (1990). Cloning of a mitogen-inducible gene encoding a kappa B DNA-binding protein with homology to the rel oncogene and to cell-cycle motifs. Nature *348*, 76-80.

Brasier, A.R., Lu, M., Hai, T., Lu, Y., and Boldogh, I. (2001). NF-kappa B-inducible BCL-3 expression is an autoregulatory loop controlling nuclear p50/NF-kappa B1 residence. J Biol Chem *276*, 32080-32093.

Bundy, D.L., and McKeithan, T.W. (1997). Diverse effects of BCL3 phosphorylation on its modulation of NF-kappaB p52 homodimer binding to DNA. J Biol Chem *272*, 33132-33139.

Caamano, J.H., Rizzo, C.A., Durham, S.K., Barton, D.S., Raventos-Suarez, C., Snapper, C.M., and Bravo, R. (1998). Nuclear factor (NF)-kappa B2 (p100/p52) is required for normal splenic microarchitecture and B cell-mediated immune responses. J Exp Med *187*, 185-196.

Chen, F.E., Huang, D.B., Chen, Y.Q., and Ghosh, G. (1998a). Crystal structure of p50/p65 heterodimer of transcription factor NF-kappaB bound to DNA. Nature *391*, 410-413.

Chen, Y.Q., Ghosh, S., and Ghosh, G. (1998b). A novel DNA recognition mode by the NF-kappa B p65 homodimer. Nat Struct Biol *5*, 67-73.

Claudio, E., Brown, K., Park, S., Wang, H., and Siebenlist, U. (2002). BAFF-induced NEMO-independent processing of NF-kappa B2 in maturing B cells. Nat Immunol *3*, 958-965.

Cogswell, P.C., Guttridge, D.C., Funkhouser, W.K., and Baldwin, A.S., Jr. (2000). Selective activation of NF-kappa B subunits in human breast cancer: potential roles for NF-kappa B2/p52 and for Bcl-3. Oncogene *19*, 1123-1131.

Coope, H.J., Atkinson, P.G., Huhse, B., Belich, M., Janzen, J., Holman, M.J., Klaus, G.G., Johnston, L.H., and Ley, S.C. (2002). CD40 regulates the processing of NF-kappaB2 p100 to p52. Embo J *21*, 5375-5385.

Courtois, G., and Gilmore, T.D. (2006). Mutations in the NF-kappaB signaling pathway: implications for human disease. Oncogene *25*, 6831-6843.

Dechend, R., Hirano, F., Lehmann, K., Heissmeyer, V., Ansieau, S., Wulczyn, F.G., Scheidereit, C., and Leutz, A. (1999). The Bcl-3 oncoprotein acts as a bridging factor between NF-kappaB/Rel and nuclear co-regulators. Oncogene *18*, 3316-3323.

Dejardin, E., Droin, N.M., Delhase, M., Haas, E., Cao, Y., Makris, C., Li, Z.W., Karin, M., Ware, C.F., and Green, D.R. (2002). The lymphotoxin-beta receptor induces different patterns of gene expression via two NF-kappaB pathways. Immunity *17*, 525-535.

Dobrzanski, P., Ryseck, R.P., and Bravo, R. (1995). Specific inhibition of RelB/p52 transcriptional activity by the C-terminal domain of p100. Oncogene *10*, 1003-1007.

Franzoso, G., Bours, V., Azarenko, V., Park, S., Tomita-Yamaguchi, M., Kanno, T., Brown, K., and Siebenlist, U. (1993). The oncoprotein Bcl-3 can facilitate NF-kappa B-mediated transactivation by removing inhibiting p50 homodimers from select kappa B sites. EMBO J *12*, 3893-3901.

Franzoso, G., Carlson, L., Poljak, L., Shores, E.W., Epstein, S., Leonardi, A., Grinberg, A., Tran, T., Scharton-Kersten, T., Anver, M.*, et al.* (1998). Mice deficient in nuclear factor (NF)-kappa B/p52 present with defects in humoral responses, germinal center reactions, and splenic microarchitecture. J Exp Med *187*, 147-159.

Franzoso, G., Carlson, L., Scharton-Kersten, T., Shores, E.W., Epstein, S., Grinberg, A., Tran, T., Shacter, E., Leonardi, A., Anver, M.*, et al.* (1997).

Critical roles for the Bcl-3 oncoprotein in T cell-mediated immunity, splenic microarchitecture, and germinal center reactions. Immunity *6*, 479-490.

Fujita, T., Nolan, G.P., Liou, H.C., Scott, M.L., and Baltimore, D. (1993). The candidate proto-oncogene bcl-3 encodes a transcriptional coactivator that activates through NF-kappa B p50 homodimers. Genes Dev *7*, 1354-1363.

Fusco, A.J., Savinova, O.V., Talwar, R., Kearns, J.D., Hoffmann, A., and Ghosh, G. (2008). Stabilization of RelB requires multidomain interactions with p100/p52. J Biol Chem *283*, 12324-12332.

Ghisletti, S., Huang, W., Jepsen, K., Benner, C., Hardiman, G., Rosenfeld, M.G., and Glass, C.K. (2009). Cooperative NCoR/SMRT interactions establish a corepressor-based strategy for integration of inflammatory and anti-inflammatory signaling pathways. Genes Dev *23*, 681-693.

Ghosh, G., van Duyne, G., Ghosh, S., and Sigler, P.B. (1995). Structure of NF-kappa B p50 homodimer bound to a kappa B site. Nature *373*, 303-310.

Ghosh, S., Gifford, A.M., Riviere, L.R., Tempst, P., Nolan, G.P., and Baltimore, D. (1990). Cloning of the p50 DNA binding subunit of NF-kappa B: homology to rel and dorsal. Cell *62*, 1019-1029.

Ghosh, S., and Hayden, M.S. (2008). New regulators of NF-kappaB in inflammation. Nat Rev Immunol *8*, 837-848.

Ghosh, S., and Karin, M. (2002). Missing pieces in the NF-kappaB puzzle. Cell *109 Suppl*, S81-96.

Ghosh, S., May, M.J., and Kopp, E.B. (1998). NF-kappa B and Rel proteins: evolutionarily conserved mediators of immune responses. Annu Rev Immunol *16*, 225-260.

Gilmore, T.D., and Herscovitch, M. (2006). Inhibitors of NF-kappaB signaling: 785 and counting. Oncogene *25*, 6887-6899.

Gustin, J.A., Korgaonkar, C.K., Pincheira, R., Li, Q., and Donner, D.B. (2006). Akt regulates basal and induced processing of NF-kappaB2 (p100) to p52. J Biol Chem *281*, 16473-16481.

Hao, S., and Baltimore, D. (2009). The stability of mRNA influences the temporal order of the induction of genes encoding inflammatory molecules. Nat Immunol *10*, 281-288.

He, J.Q., Saha, S.K., Kang, J.R., Zarnegar, B., and Cheng, G. (2007). Specificity of TRAF3 in its negative regulation of the noncanonical NF-kappa B pathway. J Biol Chem *282*, 3688-3694.

Hoffmann, A., Levchenko, A., Scott, M.L., and Baltimore, D. (2002). The IkappaB-NF-kappaB signaling module: temporal control and selective gene activation. Science *298*, 1241-1245.

Hogan, P.G., Chen, L., Nardone, J., and Rao, A. (2003). Transcriptional regulation by calcium, calcineurin, and NFAT. Genes Dev *17*, 2205-2232.

Huang, D.B., Huxford, T., Chen, Y.Q., and Ghosh, G. (1997). The role of DNA in the mechanism of NFkappaB dimer formation: crystal structures of the dimerization domains of the p50 and p65 subunits. Structure *5*, 1427-1436.

Huxford, T., Huang, D.B., Malek, S., and Ghosh, G. (1998). The crystal structure of the IkappaBalpha/NF-kappaB complex reveals mechanisms of NF-kappaB inactivation. Cell *95*, 759-770.

Ishikawa, H., Carrasco, D., Claudio, E., Ryseck, R.P., and Bravo, R. (1997). Gastric hyperplasia and increased proliferative responses of lymphocytes in mice lacking the COOH-terminal ankyrin domain of NF-kappaB2. J Exp Med *186*, 999-1014.

Ishikawa, H., Claudio, E., Dambach, D., Raventos-Suarez, C., Ryan, C., and Bravo, R. (1998). Chronic inflammation and susceptibility to bacterial infections in mice lacking the polypeptide (p)105 precursor (NF-kappaB1) but expressing p50. J Exp Med *187*, 985-996.

Jacobs, M.D., and Harrison, S.C. (1998). Structure of an IkappaBalpha/NF-kappaB complex. Cell *95*, 749-758.

Joshi, R., Sun, L., and Mann, R. Dissecting the functional specificities of two Hox proteins. Genes Dev *24*, 1533-1545.

Kadonaga, J.T. (2004). Regulation of RNA polymerase II transcription by sequence-specific DNA binding factors. Cell *116*, 247-257.

Karin, M. (2006). Nuclear factor-kappaB in cancer development and progression. Nature *441*, 431-436.

Karin, M., and Ben-Neriah, Y. (2000). Phosphorylation meets ubiquitination: the control of NF-[kappa]B activity. Annu Rev Immunol *18*, 621-663.

Kashatus, D., Cogswell, P., and Baldwin, A.S. (2006). Expression of the Bcl-3 proto-oncogene suppresses p53 activation. Genes Dev *20*, 225-235.

Keats, J.J., Fonseca, R., Chesi, M., Schop, R., Baker, A., Chng, W.J., Van Wier, S., Tiedemann, R., Shi, C.X., Sebag, M.*, et al.* (2007). Promiscuous mutations activate the noncanonical NF-kappaB pathway in multiple myeloma. Cancer Cell *12*, 131-144.

Khorasanizadeh, S., and Rastinejad, F. (2001). Nuclear-receptor interactions on DNA-response elements. Trends Biochem Sci *26*, 384-390.

Kieran, M., Blank, V., Logeat, F., Vandekerckhove, J., Lottspeich, F., Le Bail, O., Urban, M.B., Kourilsky, P., Baeuerle, P.A., and Israel, A. (1990). The DNA binding subunit of NF-kappa B is identical to factor KBF1 and homologous to the rel oncogene product. Cell *62*, 1007-1018.

Kim, H.J., Hawke, N., and Baldwin, A.S. (2006). NF-kappaB and IKK as therapeutic targets in cancer. Cell Death Differ *13*, 738-747.

Kim, T.K., and Maniatis, T. (1997). The mechanism of transcriptional synergy of an in vitro assembled interferon-beta enhanceosome. Mol Cell *1*, 119-129.

Kunsch, C., Ruben, S.M., and Rosen, C.A. (1992). Selection of optimal kappa B/Rel DNA-binding motifs: interaction of both subunits of NF-kappa B with DNA is required for transcriptional activation. Mol Cell Biol *12*, 4412-4421.

Legarda-Addison, D., and Ting, A.T. (2007). Negative regulation of TCR signaling by NF-kappaB2/p100. J Immunol *178*, 7767-7778.

Leung, T.H., Hoffmann, A., and Baltimore, D. (2004). One nucleotide in a kappaB site can determine cofactor specificity for NF-kappaB dimers. Cell *118*, 453-464.

Liang, C., Zhang, M., and Sun, S.C. (2006). beta-TrCP binding and processing of NF-kappaB2/p100 involve its phosphorylation at serines 866 and 870. Cell Signal *18*, 1309-1317.

Liao, G., Zhang, M., Harhaj, E.W., and Sun, S.C. (2004). Regulation of the NF-kappaB-inducing kinase by tumor necrosis factor receptor-associated factor 3-induced degradation. J Biol Chem *279*, 26243-26250.

Liou, H.C., Nolan, G.P., Ghosh, S., Fujita, T., and Baltimore, D. (1992). The NF-kappa B p50 precursor, p105, contains an internal I kappa B-like inhibitor that preferentially inhibits p50. Embo J *11*, 3003-3009.

Livak, K.J., and Schmittgen, T.D. (2001). Analysis of relative gene expression data using real-time quantitative PCR and the 2(-Delta Delta C(T)) Method. Methods *25*, 402-408.

Malek, S., Huang, D.B., Huxford, T., Ghosh, S., and Ghosh, G. (2003). X-ray crystal structure of an IkappaBbeta x NF-kappaB p65 homodimer complex. J Biol Chem *278*, 23094-23100.

Maniatis, T., Falvo, J.V., Kim, T.H., Kim, T.K., Lin, C.H., Parekh, B.S., and Wathelet, M.G. (1998). Structure and function of the interferon-beta enhanceosome. Cold Spring Harb Symp Quant Biol *63*, 609-620.

Massoumi, R., Chmielarska, K., Hennecke, K., Pfeifer, A., and Fassler, R. (2006). Cyld inhibits tumor cell proliferation by blocking Bcl-3-dependent NF-kappaB signaling. Cell *125*, 665-677.

McNally, J.G., Muller, W.G., Walker, D., Wolford, R., and Hager, G.L. (2000). The glucocorticoid receptor: rapid exchange with regulatory sites in living cells. Science *287*, 1262-1265.

Meijsing, S.H., Pufall, M.A., So, A.Y., Bates, D.L., Chen, L., and Yamamoto, K.R. (2009). DNA binding site sequence directs glucocorticoid receptor structure and activity. Science *324*, 407-410.

Michaely, P., and Bennett, V. (1992). The ANK repeat: a ubiquitous motif involved in macromolecular recognition. Trends Cell Biol *2*, 127-129.

Michel, F., Soler-Lopez, M., Petosa, C., Cramer, P., Siebenlist, U., and Muller, C.W. (2001). Crystal structure of the ankyrin repeat domain of Bcl-3: a unique member of the IkappaB protein family. Embo J *20*, 6180-6190.

Moorthy, A.K., Savinova, O.V., Ho, J.Q., Wang, V.Y., Vu, D., and Ghosh, G. (2006). The 20S proteasome processes NF-kappaB1 p105 into p50 in a translation-independent manner. Embo J *25*, 1945-1956.

Mordmuller, B., Krappmann, D., Esen, M., Wegener, E., and Scheidereit, C. (2003). Lymphotoxin and lipopolysaccharide induce NF-kappaB-p52 generation by a co-translational mechanism. EMBO Rep *4*, 82-87.

Mueller, F., Wach, P., and McNally, J.G. (2008). Evidence for a common mode of transcription factor interaction with chromatin as revealed by improved quantitative fluorescence recovery after photobleaching. Biophys J *94*, 3323-3339.

Muller, C.W., Rey, F.A., Sodeoka, M., Verdine, G.L., and Harrison, S.C. (1995). Structure of the NF-kappa B p50 homodimer bound to DNA. Nature *373*, 311-317.

Na, S.Y., Choi, J.E., Kim, H.J., Jhun, B.H., Lee, Y.C., and Lee, J.W. (1999). Bcl3, an IkappaB protein, stimulates activating protein-1 transactivation and cellular proliferation. J Biol Chem *274*, 28491-28496.

Nishikori, M., Ohno, H., Haga, H., and Uchiyama, T. (2005). Stimulation of CD30 in anaplastic large cell lymphoma leads to production of nuclear factor-kappaB p52, which is associated with hyperphosphorylated Bcl-3. Cancer Sci *96*, 487-497.

Nolan, G.P., Fujita, T., Bhatia, K., Huppi, C., Liou, H.C., Scott, M.L., and Baltimore, D. (1993). The bcl-3 proto-oncogene encodes a nuclear I kappa B-like molecule that preferentially interacts with NF-kappa B p50 and p52 in a phosphorylation-dependent manner. Mol Cell Biol *13*, 3557-3566.

Novack, D.V., Yin, L., Hagen-Stapleton, A., Schreiber, R.D., Goeddel, D.V., Ross, F.P., and Teitelbaum, S.L. (2003). The IkappaB function of NF-kappaB2 p100 controls stimulated osteoclastogenesis. J Exp Med *198*, 771-781.

Ogawa, S., Lozach, J., Benner, C., Pascual, G., Tangirala, R.K., Westin, S., Hoffmann, A., Subramaniam, S., David, M., Rosenfeld, M.G., and Glass, C.K. (2005). Molecular determinants of crosstalk between nuclear receptors and toll-like receptors. Cell *122*, 707-721.

Ohno, H., Takimoto, G., and McKeithan, T.W. (1990). The candidate proto-oncogene bcl-3 is related to genes implicated in cell lineage determination and cell cycle control. Cell *60*, 991-997.

Okamura, H., Garcia-Rodriguez, C., Martinson, H., Qin, J., Virshup, D.M., and Rao, A. (2004). A conserved docking motif for CK1 binding controls the nuclear localization of NFAT1. Mol Cell Biol *24*, 4184-4195.

Pan, J., and McEver, R.P. (1995). Regulation of the human P-selectin promoter by Bcl-3 and specific homodimeric members of the NF-kappa B/Rel family. J Biol Chem *270*, 23077-23083.

Panne, D., Maniatis, T., and Harrison, S.C. (2007). An atomic model of the interferon-beta enhanceosome. Cell *129*, 1111-1123.

Park, S.G., Chung, C., Kang, H., Kim, J.Y., and Jung, G. (2006). Up-regulation of cyclin D1 by HBx is mediated by NF-kappaB2/BCL3 complex through kappaB site of cyclin D1 promoter. J Biol Chem *281*, 31770-31777.

Parker, S.F., Perkins, N.D., Gitlin, S.D., and Nabel, G.J. (1996). A cooperative interaction of human T-cell leukemia virus type 1 Tax with the p21 cyclin-dependent kinase inhibitor activates the human immunodeficiency virus type 1 enhancer. J Virol *70*, 5731-5734.

Perkins, N.D., Felzien, L.K., Betts, J.C., Leung, K., Beach, D.H., and Nabel, G.J. (1997). Regulation of NF-kappaB by cyclin-dependent kinases associated with the p300 coactivator. Science *275*, 523-527.

Perkins, N.D., and Gilmore, T.D. (2006). Good cop, bad cop: the different faces of NF-kappaB. Cell Death Differ *13*, 759-772.

Phair, R.D., Scaffidi, P., Elbi, C., Vecerova, J., Dey, A., Ozato, K., Brown, D.T., Hager, G., Bustin, M., and Misteli, T. (2004). Global nature of dynamic protein-chromatin interactions in vivo: three-dimensional genome scanning and dynamic interaction networks of chromatin proteins. Mol Cell Biol *24*, 6393-6402.

Rao, P., Hayden, M.S., Long, M., Scott, M.L., West, A.P., Zhang, D., Oeckinghaus, A., Lynch, C., Hoffmann, A., Baltimore, D., and Ghosh, S. IkappaBbeta acts to inhibit and activate gene expression during the inflammatory response. Nature *466*, 1115-1119.

Rayasam, G.V., Elbi, C., Walker, D.A., Wolford, R., Fletcher, T.M., Edwards, D.P., and Hager, G.L. (2005). Ligand-specific dynamics of the progesterone receptor in living cells and during chromatin remodeling in vitro. Mol Cell Biol *25*, 2406-2418.

Rocha, S., Martin, A.M., Meek, D.W., and Perkins, N.D. (2003). p53 represses cyclin D1 transcription through down regulation of Bcl-3 and inducing increased association of the p52 NF-kappaB subunit with histone deacetylase 1. Mol Cell Biol *23*, 4713-4727.

Roeder, R.G. (2005). Transcriptional regulation and the role of diverse coactivators in animal cells. FEBS Lett *579*, 909-915.

Rosenfeld, M.G., Lunyak, V.V., and Glass, C.K. (2006). Sensors and signals: a coactivator/corepressor/epigenetic code for integrating signal-dependent programs of transcriptional response. Genes Dev *20*, 1405-1428.

Sanjo, H., Zajonc, D.M., Braden, R., Norris, P.S., and Ware, C.F. Allosteric regulation of the ubiquitin:NIK and TRAF3 E3 ligases by the lymphotoxin-{beta} receptor. J Biol Chem.

Savinova, O.V., Hoffmann, A., and Ghosh, G. (2009). The Nfkb1 and Nfkb2 proteins p105 and p100 function as the core of high-molecular-weight heterogeneous complexes. Mol Cell *34*, 591-602.

Sawka-Verhelle, D., Escoubet-Lozach, L., Fong, A.L., Hester, K.D., Herzig, S., Lebrun, P., and Glass, C.K. (2004). PE-1/METS, an antiproliferative Ets repressor factor, is induced by CREB-1/CREM-1 during macrophage differentiation. J Biol Chem *279*, 17772-17784.

Schmid, R.M., Perkins, N.D., Duckett, C.S., Andrews, P.C., and Nabel, G.J. (1991). Cloning of an NF-kappa B subunit which stimulates HIV transcription in synergy with p65. Nature *352*, 733-736.

Schwarz, E.M., Krimpenfort, P., Berns, A., and Verma, I.M. (1997). Immunological defects in mice with a targeted disruption in Bcl-3. Genes Dev *11*, 187-197.

Sedgwick, S.G., and Smerdon, S.J. (1999). The ankyrin repeat: a diversity of interactions on a common structural framework. Trends Biochem Sci *24*, 311-316.

Sen, R., and Baltimore, D. (1986a). Inducibility of kappa immunoglobulin enhancer-binding protein Nf-kappa B by a posttranslational mechanism. Cell *47*, 921-928.

Sen, R., and Baltimore, D. (1986b). Multiple nuclear factors interact with the immunoglobulin enhancer sequences. Cell *46*, 705-716.

Senftleben, U., Cao, Y., Xiao, G., Greten, F.R., Krahn, G., Bonizzi, G., Chen, Y., Hu, Y., Fong, A., Sun, S.C., and Karin, M. (2001). Activation by IKKalpha of a second, evolutionary conserved, NF-kappa B signaling pathway. Science *293*, 1495-1499.

Sengchanthalangsy, L.L., Datta, S., Huang, D.B., Anderson, E., Braswell, E.H., and Ghosh, G. (1999). Characterization of the dimer interface of transcription factor NFkappaB p50 homodimer. J Mol Biol *289*, 1029-1040.

Sheridan, P.L., Sheline, C.T., Cannon, K., Voz, M.L., Pazin, M.J., Kadonaga, J.T., and Jones, K.A. (1995). Activation of the HIV-1 enhancer by the LEF-1 HMG protein on nucleosome-assembled DNA in vitro. Genes Dev *9*, 2090-2104.

Shih, V.F., Kearns, J.D., Basak, S., Savinova, O.V., Ghosh, G., and Hoffmann, A. (2009). Kinetic control of negative feedback regulators of NF-kappaB/RelA determines their pathogen- and cytokine-receptor signaling specificity. Proc Natl Acad Sci U S A *106*, 9619-9624.

Solan, N.J., Miyoshi, H., Carmona, E.M., Bren, G.D., and Paya, C.V. (2002). RelB cellular regulation and transcriptional activity are regulated by p100. J Biol Chem *277*, 1405-1418.

Sprague, B.L., Pego, R.L., Stavreva, D.A., and McNally, J.G. (2004). Analysis of binding reactions by fluorescence recovery after photobleaching. Biophys J *86*, 3473-3495.

Sun, S.C., and Ley, S.C. (2008). New insights into NF-kappaB regulation and function. Trends Immunol *29*, 469-478.

Sun, S.C., and Xiao, G. (2003). Deregulation of NF-kappaB and its upstream kinases in cancer. Cancer Metastasis Rev *22*, 405-422.

Vallabhapurapu, S., and Karin, M. (2009). Regulation and function of NF-kappaB transcription factors in the immune system. Annu Rev Immunol *27*, 693-733.

Vallabhapurapu, S., Matsuzawa, A., Zhang, W., Tseng, P.H., Keats, J.J., Wang, H., Vignali, D.A., Bergsagel, P.L., and Karin, M. (2008). Nonredundant

and complementary functions of TRAF2 and TRAF3 in a ubiquitination cascade that activates NIK-dependent alternative NF-kappaB signaling. Nat Immunol *9*, 1364-1370.

Varfolomeev, E., Blankenship, J.W., Wayson, S.M., Fedorova, A.V., Kayagaki, N., Garg, P., Zobel, K., Dynek, J.N., Elliott, L.O., Wallweber, H.J.*, et al.* (2007). IAP antagonists induce autoubiquitination of c-IAPs, NF-kappaB activation, and TNFalpha-dependent apoptosis. Cell *131*, 669-681.

Viatour P, D.E., Warnier M, Lair F, Claudio E, Bureau F, Marine JC, Merville MP, Maurer U, Green D, Piette J, Siebenlist U, Bours V, Chariot A. (2004). GSK3-mediated BCL-3 phosphorylation modulates its degradation and its oncogenicity. Mol Cell. *16*, 35-45.

Viatour, P., Dejardin, E., Warnier, M., Lair, F., Claudio, E., Bureau, F., Marine, J.C., Merville, M.P., Maurer, U., Green, D.*, et al.* (2004a). GSK3-mediated BCL-3 phosphorylation modulates its degradation and its oncogenicity. Mol Cell *16*, 35-45.

Viatour, P., Merville, M.P., Bours, V., and Chariot, A. (2004b). Protein phosphorylation as a key mechanism for the regulation of BCL-3 activity. Cell Cycle *3*, 1498-1501.

Viatour, P., Merville, M.P., Bours, V., and Chariot, A. (2005). Phosphorylation of NF-kappaB and IkappaB proteins: implications in cancer and inflammation. Trends Biochem Sci *30*, 43-52.

Viatour P, M.M., Bours V, Chariot A. (2005). Protein phosphorylation as a key mechanism for the regulation of BCL-3 activity. Cell Cycle. *3*, 1498-1501.

Westerheide, S.D., Mayo, M.W., Anest, V., Hanson, J.L., and Baldwin, A.S., Jr. (2001). The putative oncoprotein Bcl-3 induces cyclin D1 to stimulate G(1) transition. Mol Cell Biol *21*, 8428-8436.

Xiao, G., Cvijic, M.E., Fong, A., Harhaj, E.W., Uhlik, M.T., Waterfield, M., and Sun, S.C. (2001a). Retroviral oncoprotein Tax induces processing of NF-kappaB2/p100 in T cells: evidence for the involvement of IKKalpha. EMBO J *20*, 6805-6815.

Xiao, G., Fong, A., and Sun, S.C. (2004). Induction of p100 processing by NF-kappaB-inducing kinase involves docking IkappaB kinase alpha (IKKalpha) to

p100 and IKKalpha-mediated phosphorylation. J Biol Chem *279*, 30099-30105.

Xiao, G., Harhaj, E.W., and Sun, S.C. (2001b). NF-kappaB-inducing kinase regulates the processing of NF-kappaB2 p100. Mol Cell *7*, 401-409.

Xue, Y., Ren, J., Gao, X., Jin, C., Wen, L., and Yao, X. (2008). GPS 2.0, a tool to predict kinase-specific phosphorylation sites in hierarchy. Mol Cell Proteomics *7*, 1598-1608.

Yamamoto, M., Yamazaki, S., Uematsu, S., Sato, S., Hemmi, H., Hoshino, K., Kaisho, T., Kuwata, H., Takeuchi, O., Takeshige, K.*, et al.* (2004). Regulation of Toll/IL-1-receptor-mediated gene expression by the inducible nuclear protein IkappaBzeta. Nature *430*, 218-222.

Zarnegar, B.J., Wang, Y., Mahoney, D.J., Dempsey, P.W., Cheung, H.H., He, J., Shiba, T., Yang, X., Yeh, W.C., Mak, T.W.*, et al.* (2008). Noncanonical NF-kappaB activation requires coordinated assembly of a regulatory complex of the adaptors cIAP1, cIAP2, TRAF2 and TRAF3 and the kinase NIK. Nat Immunol *9*, 1371-1378.

Zhang, M.Y., Harhaj, E.W., Bell, L., Sun, S.C., and Miller, B.A. (1998). Bcl-3 expression and nuclear translocation are induced by granulocyte-macrophage colony-stimulating factor and erythropoietin in proliferating human erythroid precursors. Blood *92*, 1225-1234.

Zhang, Q., Didonato, J.A., Karin, M., and McKeithan, T.W. (1994). BCL3 encodes a nuclear protein which can alter the subcellular location of NF-kappa B proteins. Mol Cell Biol *14*, 3915-3926.

Zhang., X., Wong., H., Claudio., E., Brown., K., and Siebenlist., U. (2007). A role for the IkappaB family member Bcl-3 in the control of central immunologic tolerance. Immunity *27(3)*, 438-452.

Zhu, J., Shibasaki, F., Price, R., Guillemot, J.C., Yano, T., Dotsch, V., Wagner, G., Ferrara, P., and McKeon, F. (1998). Intramolecular masking of nuclear import signal on NF-AT4 by casein kinase I and MEKK1. Cell *93*, 851-861.